"The effect of Polyhydroxyalkanoates (PHAs) in Microbial Fuel Cells (MFCs)"

Master's thesis

Maria Makridou

Supervisor: Dr. Argyro Tsipa
Assistant Professor, Department of Civil and Environmental Engineering, University of Cyprus

Examiner: Dr. Dimitris Stagonas
Lecturer, Department of Civil and Environmental Engineering, University of Cyprus

June 2024

1

Abbreviations

BES	Bio-electrochemical systems
BSF	Biosurfactant
CCV	Closed Circuit Voltage
CCV	Closed-circuit voltage
COD	Chemical Oxygen Demand
EET	Extracellular Electron Transfer
EET	Extracellular Electron Transfer
ET	Electron transfer
FAMEs	Fatty Acid Methyl Esters
FAs	Fatty Acids
GC/MS	Gas Chromatography/Mass Spectrometry
MAs	Mycolic acids
MET	Microbial Electrochemical Technology
MFC	Microbial Fuel Cell
OCV	Open Circuit Voltage
OW	Oily Wastewater
PAHs	Polycyclic aromatic hydrocarbons
PHAs	Polyhydroxy alkanoates
TPHs	Total petroleum hydrocarbons

Abstract

Bioremediation technologies are eco-friendly and usually nature-based solutions to combat environmental pollution. Among them, bioelectrochemical systems (BES), such as microbial fuel cells (MFCs), can be used to accelerate the process. In MFCs, the degradation of pollutants can result in generation of electricity and/or other added-value products contributing to a circular economy concept while producing non-toxic, biodegradable compounds and renewable energy. Waste cooking oil (WCO) is an agro-industrial wastewater stream of severe environmental concern. MFCs could be an effective treatment way to manage WCO with concurrent production of electricity and added-value products. Furthermore, the effect of added-value products, such as polyhydroxyalkanoates (PHAs) which are considered as biopolymers to replace the petrochemical based polymers used in plastics, on electricity generation is examined.

Firstly, enrichment experiments, with activated sludge (AS) as inoculum and acetate, which is known to be favorable for PHAs production, as carbon source was used. Six samples were isolated fed with different initial sodium acetate concentration. Next generation sequencing was performed to identify the microorganisms in the six mixed cultures. It was realized that as sodium acetate concentration was increased, an increased abundance of microorganisms belonging Actinobacteria was observed in the samples. Considerable amounts of the genus Corynebacterium of the family Corynebacteriaceae were found in S4 (6 g/L acetate) (18.90%), S5 (8g/L acetate) (49.75%) and S6 (10g/L acetate) (65.82%). The species *Corynebacterium sputi* was found in S5 (63.24%) and S6 (63.24%) in high concentrations. 24h cultures were performed for all samples. Gas Chromatography-Mass spectrometry (GC/MS) intracellular analysis revealed that all samples had the same PHAs, at different abundance. In particular, 3-hydroxydecanoate, 3-hydroxydodecanoate and 3-hydroxytetradecanoate. Many fatty acids (FAs) were also observed indicating microbial lipids production. As Corynebacterium seems to be correlated with PHA production and is electroactive, the mixed culture with high abundance of this genus was chosen for further studies (10g/L acetate). So MFCs were set up using this microorganism and WCO in the anode to check the effect of PHAs. MFCs using AS and WCO in the anode and were also set up, for comparison.

In the MFCs with AS and WCO which operated for 183 days, the highest % COD removal was noted at day 80, an average of 49%. Extracellular production of a white compound was obvious.

The product formed was a mixture of biosurfactants produced by the mixed microbial community of AS. Biosurfactants are amphiphilic molecules with hydrophobic and hydrophilic portions that reduces the surface and interfacial tensions between fluids of different polarities, enhancing the solubility, bioavailability and biodegradation of hydrophobic substrates. In total, 12 FAMEs were detected. The specific biosurfactants' lipid profile indicates an enhanced degradation of hydrophobic substances, such as hydrocarbons and fats of WCO due to the many fatty acids detected in it.

The MFCs operation of mixed cultures as inoculum and WCO as fuel lasted 97 days. The initial resistance was 4.5 kΩ and gradually decreased to 3 kΩ. On the 97th day of operation and 7 days after the last feed replacement of the anode with WCO, several analyses were performed. Intracellularly, twenty-two FAs ranging from C_5-C_{25}, were detected in all MFCs at similar concentrations. In total, 6 medium chain length PHAs were observed which are the double amount compared to 24h-aerobic cultures. Comparing the MFCs found here and under 24h-aerobic conditions, the culture here shows itself to be in survival mode. On average 56% COD removal was observed. Extracellularly, total petroleum hydrocarbons (TPHs) and FAs of WCO before and after treatment were measured. The mean hydrocarbons removal rate was 75.4%, with some of them, especially the n-alkanes, reaching removal rates > 60%. Both aromatic and aliphatic hydrocarbons were biodegraded. In total, 7 FAs were detected in WCO. Mixed cultures in MFCs appear to have effectively diminished the unsaturated FAs of methyl elaidate and methyl linoleate, as well as methyl behenate. However, the concentrations of saturated ones to MFCs were significantly higher. This outcome may be explained by the gradual growth of intra- and extracellular metabolites, such as polyhydroxyalkanoates (PHAs) and biosurfactants, in the anodic compartment. In addition, the Emulsification Index test was performed indicating that this mixed culture possibly produces biosurfactants.

Comparing the best MFCs from each condition (AS and mixed cultures), the MFC with AS and WCO reached maximum current at 0.145 mA and power was measured at 0.105 mW, while in the MFC with mixed culture and WCO power was measured as high as 0.163 mW and current reached 0.233 mA. In the latter MFC, when the fuel is depleted, microorganisms can then use PHAs as electron donors to continue the process of electron transfer which was also observed in this thesis. After 7 days with no feed, where the WCO's components were significantly removed, PHAs were

accumulated while electricity generation remained at high levels. On top, comparing PHAs accumulation at aerobic conditions (after enrichment) and PHAs under MFCs conditions, more PHAs, in terms of variety, were produced showing the capability of the microorganisms to survive and perform under adverse conditions (i.e. no WCO-fuel feed). This is a novel and promising circular-based approach for wastewater treatment with concurrent added-value products and renewable energy generation.

Table of Contents

Table of Figures

Table of Tables

Introduction

Environmental pollution is a huge threat of the planet. Nowadays there are several thermo-, chemical and physical remediation processes using advanced technologies. However, these technologies are cost and energy-intensive, as well as time consuming. On the contrary, bioremediation technologies are eco-friendly and usually nature-based solutions to combat environmental pollution.

Among them, bioelectrochemical systems (BES), such as microbial fuel cells (MFCs), can be used to accelerate the process of bioremediation. In BES, the degradation of pollutants can result in generation of electricity and/or other added-value products contributing to a circular economy concept while producing non-toxic, biodegradable compounds and renewable energy.

Agro-industrial wastewater management is an environmental issue concerning European Union and the nations. Waste cooking oil (WCO) is an agro-industrial wastewater which also derives from households. Its improper disposal has resulted in environmental concerns while it severely affects the soil, water and groundwater ecosystems.

BES could be an effective treatment way to manage WCO. Therefore, in this thesis the use of BES to remediate WCO is assessed with concurrent production of electricity and added-value products. Furthermore, the effect of added-value products on electricity generation is examined. Among the added-value products assessed are the polyhydroxyalkanoates (PHAs) which as considered as biopolymers to replace the petrochemical based polymers used in plastics. PHAs are considered biodegradable; thus, their use can minimize the negative effects of plastics in the environment.

1. **Environmental Pollution and traditional remediation technologies**

For a long time, there has been grounds for concern regarding the release of potentially dangerous chemicals into the environment (X. Wang et al., 2020). Widespread chemical pollution of the environment poses a substantial threat to human health and harms delicate ecosystems, making it a global issue. Governments are devoting significant resources to the remediation of various contaminants from soil, sediment, groundwater, and the atmosphere (H. Wang et al., 2015). According to estimates from the industry, the worldwide market for environmental remediation

was worth USD 110.68 billion in 2022 and is projected to grow to USD 198.11 billion by 2030 (Varnava et al., 2024).

The traditional methods of remediation have involved either excavating contaminated soil and disposing of it in a landfill or capping and enclosing the affected parts of a site. The techniques have a few shortcomings. The first approach merely shifts the pollution to a different location and could pose serious risks while handling, excavating, and transporting hazardous materials. Additionally, finding new landfill sites for the material's final disposal is becoming more and more difficult and expensive. The pollution remains on site, necessitating long-term monitoring and upkeep of the isolation barriers—along with all the related expenses and possible liability—so the cap and contain approach is really a stopgap measure (Kensa, 2011).

Landfilling is the least desirable option and should only be used when absolutely required, according to the EU's waste hierarchy. In the EU, landfilling accounted for 24% of all municipal garbage produced during 2018. The environment and human health may suffer as a result of this. Leachate production can contaminate groundwater and produce methane, a powerful greenhouse gas. In addition to providing for measures, procedures, and guidance to prevent or reduce negative effects on the environment as much as possible, the Directive (EU) 2018/850 of the European Parliament and of the Council of May 30, 2018, amending Directive 1999/31/EC on the landfill of waste, aims to ensure a progressive reduction of waste landfilling, particularly of waste that is suitable for recycling or other recovery. Furthermore, resources from Europe's economy are needlessly misused when recyclable waste is landfilled (UNION, 2018).

If at all possible, destroying the pollutants entirely or at the very least turning them into harmless chemicals is a better strategy than the conventional ones. Because there are typically not enough appropriate electron donors or acceptors, the transformation of pollutants in nature proceeds slowly. Eventually, a proper driving force is required to propel the biotic or abiotic reductions or oxidations of the pollutants, respectively. Artificially introduced technologies included phytoremediation, adsorption, electrodialysis, ion exchange, precipitation, membrane filtration, microbiological techniques, and nanotechnology to expedite the transformation of pollutants through natural processes. However, these traditional technologies are typically labor-and/or energy-intensive, chemically and energy-intensive, and difficult to manage. Furthermore, the uses

of such technologies have been further limited by the limited availability of electron donors and acceptors, the absence of interaction between pollutants and amendments, the interference of other co-existing pollutants, and the production of harmful by-products.

One alternative is bioremediation, which uses natural biological activity to either remove or render harmless certain toxins. By definition, bioremediation is the process of breaking down environmental pollutants into less hazardous forms by using living organisms, mainly microbes. Utilizing naturally occurring fungus, bacteria, and plants, it breaks down or detoxifies chemicals that pose a risk to the environment or public health (Kensa, 2011).

The main reasons for the challenges are that each area is different, most of the methods in use today demand a lot of energy and chemical supplies, and the remediation procedure may require years or even decades. In contrast to energy- and chemical-intensive physical excavation or chemical oxidation/reduction, bioremediation is thought to be more cost-effective and environmentally benign. Common challenges for bioremediation include lack of contact between the contaminants and amendments due to the heterogeneous matrix, limited availability of electron donors and acceptors, and slow kinetics. However, the effectiveness of bioremediation is primarily determined by the interplay between the abundance of electron donor and acceptor, as well as carbon sources for the functional microorganisms (H. Wang et al., 2015).

2.   Microbial electrochemistry as an alternative to traditional remediation technologies

It is safe to say, without going too far, that most contaminants in the environment are not broken down or removed very quickly because there isn't an appropriate electron source or acceptor present. Sometimes there isn't a good (bio)catalyst available either. Therefore, the main focus of current bioremediation efforts is on providing this donor/acceptor, which frequently entails adding chemicals to the contaminated matrix. This problem is addressed by microbial electrochemical processes, which directly supply or remove electrons using an electrode or a solid state electron donor/acceptor (X. Wang et al., 2020).

Microbial electrochemistry-based techniques have been proposed as a substitute for traditional remediation technologies in the past decade due to the drawbacks of the latter. Within the field of bioelectrochemistry, microbial electrochemistry examines and applies electron transfer reactions that occur between living microbial cells and solid-state electrodes or naturally occurring minerals; thus accelerating bioremediation of pollutants. This field of technological development, known as microbial electrochemical technology (MET) suggests that the microbial metabolism is purposefully connected to a solid-state electron donor or acceptor, which could be an electrode or a mineral particle. It is essentially an anode when the electrode accepts electrons opposed to a cathode when the electrode provides electrons (Fig.1).
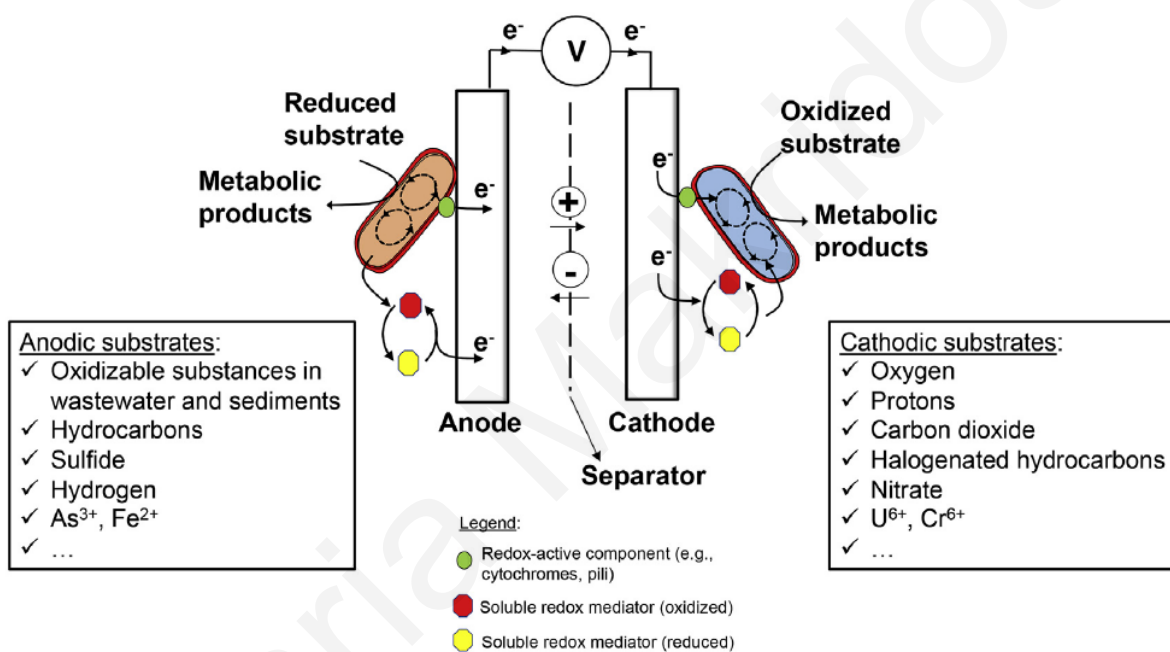
Figure 1. Schematic overview of microbially-catalyzed reactions taking place at the anode and at the cathode of a microbial electrochemical systems (X. Wang et al., 2020)

Microbial fuel cell (MFC) is the archetype of MET and the most common device for bioremediation using microbial electrochemistry (Fig.2). Microbial fuel cells (MFCs) can be described as energy transducers (Ieropoulos et al., 2017), since is an innovative renewable technology, which uses microbial metabolism to generate electricity (You et al., 2021). The suitability of several substrates for power generation in MFCs has been investigated, with differing degrees of success. Simple low carbon compounds like acetate, as well as rapidly fermentable ones like glucose and complex ones like those present in urine and wastewater, are some of the

substrates (Obata et al., 2020). With the ability to use organic materials as fuel, the MFC technology has expanded quickly as a promising sustainable power supply system (Mohd Yusoff et al., 2013).

The positive cathode and the negative anode, each with an electrode, are the two chambers that constitute a MFC. A semipermeable membrane (sometimes referred to as an electrolyte in certain situations) divides the two half-cells and permits protons produced in the anode as a result of bacterial oxidation of organic molecules to pass through to the cathode. Current flow is facilitated by electrons passing through an external connecting wire or circuit (Ieropoulos et al., 2017). The electrons are produced by the microbial metabolic pathways that are digesting biomass into protons, electrons and CO_2 (Gajda et al., 2014). At the cathode, dissolved oxygen reacts with incoming electrons and protons to produce H_2O as a byproduct (Ieropoulos et al., 2017).
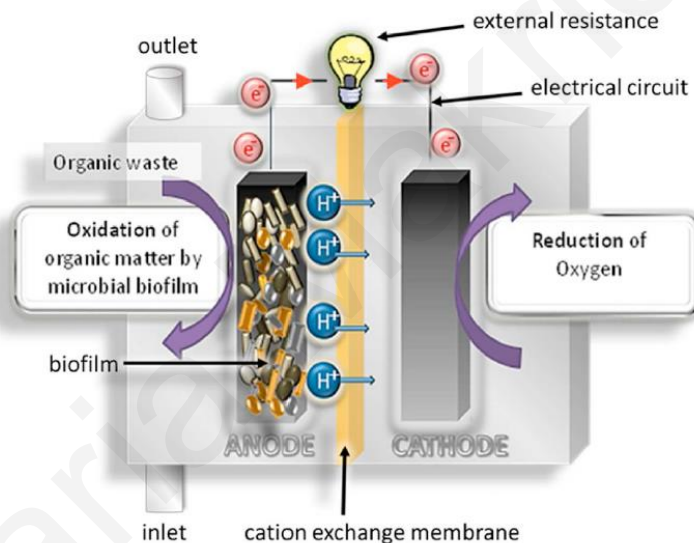
Figure 2. Diagram of a Microbial Fuel Cell with microbial anode operated under continuous supply of organic substrate (Greenman et al., 2022)

With a few exceptions that require the use of extremophilic bacteria, this biological fuel cell can function at room temperature (15–30 °C), in contrast to other "classic" chemical fuel cells. While the majority of chemical fuel cells function using refined and processed fuels including methanol and hydrogen, the mixed microbial communities found in the electroactive biofilms of MFCs can utilize an extensive array of substrates, including different types of solid and liquid organic wastes/pollutants and laboratory bacterial growth mediums. When organic wastes/pollutants are

used as MFC feedstock, the organic matter contained therein is consumed by bacteria, which removes the waste (treatment) (You et al., 2021). The utilization of biomass found in wastewater can be an invaluable instrument in securing a sustainable future, as it includes an important amount of energy (Gajda et al., 2014). One of the technology's competitive benefits is its dual-utility feature, which allows for the simultaneous generation of electricity and the treatment of waste/pollutants (You et al., 2021). Owing to these unique qualities, MFCs are frequently referred to as biological batteries or bio-batteries in the literature; however, this is only accurate in situations where the fuel supply is fixed and will eventually run out (Ieropoulos et al., 2017).

3. Waste cooking oil: an environmental pollution factor

Oily wastewater constitutes just one of the billions of contaminants that pose a serious risk to the environment contributing to environmental pollution. Oils, fats, greases, and a variety of dissolved organic and/or inorganic materials make up the oily wastewater. Many different businesses, including the petrochemical, edible oil refinery, drilling operation, metal processing, poultry processing, restaurant, dairy, butcher, and tannery industries, can produce this kind of wastewater. High quantities of harmful substances, fatty acids, and hydrocarbons like polycyclic aromatic and total petroleum hydrocarbons are what define it. Treatment of oily wastewater is therefore crucial (Varnava et al., 2024).

In particular, one of the common oils streams that can be found in oily wastewater is the oil residue that remains after cooking that is known as Waste Cooking Oil (WCO). The main source of cooking oil is edible oil-producing plants. With the growing worldwide population and rising food consumption, the WCO disposal problem is becoming more and more of a concern. On top of that, economic considerations frequently lead to the repeated use of the same oil during continuous frying. The process of frying food repeatedly releases oxygen into the oil, which reacts with unsaturated acylglycerols to produce a variety of compounds including polymeric and dimeric acids, polymeric acylglycerols, and polyglycerols that raise the viscosity of the frying fat. Therefore, reusing WCO makes the oil more acidic and releases an offensive odor due to lipid browning, which makes the oil unfit for human consumption (Goh et al., 2020). In addition to that, WCO's large volume makes final disposal difficult, and improper discharge into drains or sewers can result in obstructions, unpleasant smells, and rodent issues. Furthermore, long-lasting substances included in WCO raise the organic load on water sources and create a thin layer on the

surface of the water that lowers the dissolved oxygen content needed for subaquatic species, altering the ecology (M. Lopes et al., 2020).

4. Waste Cooking oil and bioremediation and bioelectrochemistry approaches

With the proper processing and disposal of WCO as a feedstock, this critical environmental situation can be transformed into a profitable and environmentally beneficial opportunity (S. Sharma et al., 2019). Specifically, the accumulated free fatty acids that it contains, make it a technically feasible feedstock for biofuel production. WCO belongs in the second generation of biofuels which are based on the principle of the utilization of excess biomass and waste. Moreover, because it is obtained from a number of different sources, including fast food restaurants, food processing companies, our households, and restaurants, it is also widely accessible and reasonably priced. In addition to that, the degraded used cooking oil has a low economic value because it features a high water content and free fatty acid content for effective biofuel conversion (Goh et al., 2020).

Sources of carbon and nitrogen in culture medium, especially those used for industrial applications, should try to meet the following requirements: (a) arise from inexpensive substrates, (b) be readily available throughout the year, (c) be easily disinfected (d) allow for the highest possible yield of biomass and product formation, (e) be adaptable to various cultivation techniques (batch, fed-batch, or continuous), (f) produce no hazardous wastes and in greater quantities than the initial residue, and (g) be simple to work with at every stage of the cultivation process (production, extraction, purification, and waste treatment). WCO currently meets the above requirements and has the potential to be a readily accessible substrate for microbial growth and metabolite synthesis.

Several researchers have developed ways which employ microorganisms to simultaneously degrade oily wastes and produce high-value products. Since WCO is regarded as hazardous to the environment and has highly energy-demanding degradation processes, using it directly as feedstock for microbial processes is a great way to increase the economic value of these wastes and lower the production costs of valuable compounds. Certain species of bacteria, fungi, and yeast can use WCO as a source of energy and carbon to produce added-value compounds.

One of the primary metabolites produced by the microbial conversion of WCO, especially by bacterial species, is polyhydroxyalkanoates (PHAs), an eco-friendly substitute for synthetic

polymers. Numerous bacterial species, including *Pseudomonas sp., Cupriavidus necator, Klebsiella pneumonia, Bacillus sp., and Burkholderia thailandensis*, are able to obtain PHAs intracellularly from WCO.

Biosurfactants (BSFs) is another instance of metabolites produced by the microbial conversion of WCO. In order to improve the solubility, bioavailability, and biodegradation of hydrophobic substrates, biosurfactants—amphiphilic compounds containing hydrophobic and hydrophilic portions—reduce the surface (air-water) and interfacial (water-oil) tensions between fluids of opposite polarity. Although the opportunistic pathogen Pseudomonas aeruginosa is strongly connected to the synthesis of biosurfactants from WCO, other bacterial species, including Bacillus and Streptomyces, are also known to create surface-active compounds. Though other species were investigated, Candida species—especially Candida tropicalis—have received the greatest attention when it comes to yeast strains and their ability to produce biosurfactants from WCO (M. Lopes et al., 2020). Specifically, S. Sharma et al., 2019 proved the capacity of Pseudomonas aeruginosa MTCC7815, a strain that produces biosurfactant, to use WCO as the only carbon source for biosurfactant synthesis. This was an important study because it showed how waste may be turned into profit by investigating the possibility of employing inexpensive substrate to produce biosurfactants.

In their study, for the first time, Pasternak et al., 2023 proposed the horizontal MFC system, capable of producing biosurfactants, where their quantity is directly associated with the power output and waste rapeseed oil was used as a sustainable fuel to drive both processes. The use of waste products can help solve the challenge of excessive production expenses. Therefore, the purpose of this work was to establish the net positive energy process of bioelectrochemical synthesis of biosurfactants from waste rapeseed oil, examine the effects of MFC design on biosurfactant and electricity production, and determine the role of electricity generation in the synthesis as a possible, real-time monitoring method. All of the examined MFCs operated as vertical systems at first, producing very little electricity. Consequently, the MFCs were redesigned to function as passive, horizontally aligned systems, and the possibility of vertically agitated control was also explored. The horizontal arrangement enhanced the oil substrate's distribution within the anode chamber, boosting the oil's bioavailability to microorganisms. This had a direct impact on the growth of biofilms and the subsequent breakdown of the oil. Furthermore, only in the horizontal MFC was a decrease in

surface tension, a sign of the presence of biosurfactants, observed. As a result, it has been demonstrated that altering the electrode's orientation can greatly boost the efficiency of the degradation of waste vegetable oil. Most importantly, they have shown that the presence of biosurfactants is directly correlated with power generation and that biosurfactant production was only observed in horizontal MFCs. This may further allow for easy and inexpensive monitoring of biosurfactant synthesis in well-established bioelectrochemical synthesis setups.

5. Mixed cultures *vs* pure cultures in MFCs

In MFCs, both pure and mixed cultures have been employed in the literature. Due to their ease of preparation, affordability, and potential for self-mediation, mixed cultures—particularly wastewater cultures—have been advocated by some researchers as having greater efficacy (Mohamed et al., 2018). This outcome is consistent with prior research explaining that interspecies interaction and their aggregate development are the cause of high current production.

Pure cultures can generate electricity from a limited number of substrates. Different substrates can be used as food by bacterial species in mixed cultures, and metabolites produced by one strain of bacteria may be consumed by a different one, increasing substrate usage and, as a result, increasing the amount of electrons flowing to the anode. Redox mediators generated by one strain can help other low-efficient exoelectrogens with electron transfer, which is another likely explanation for the strain's ability to produce more electricity (S. C. D. Sharma et al., 2021). On the other hand, other researchers support that pure cultures have been found to perform better due to fewer adverse interactions between the different types of microorganisms (Mohamed et al., 2018).

6. Activated Sludge (AS)

In order to remove pollutants, biological wastewater treatment procedures usually rely on microorganisms in activated sludge (AS). These bacteria frequently group together to create activated sludge flocs, granules, and biofilm. The key to treating wastewater and identifying the cause of issues is the form and functionality of activated sludge. Extracellular polymeric substances (EPS) composition, sedimentation, morphology, structure, microbiological structure, hydrophobicity, and sedimentation may all have an impact on how well the activated sludge process treats wastewater (X. Wang et al., 2024).

Municipal wastewater treatment plants (WWTP) are beginning to take a more serious look at waste activated sludge (WAS) treatment, and the expense of this treatment makes up more than half of the WWTP's overall operating costs (Geng et al., 2020). Many approaches have been developed to recover energy and resources (e.g., biogas, H_2, syngas, bio-oil, and biodiesel) from WAS. These technologies include incineration/co-incineration, wet air oxidation, supercritical water oxidation, gasification, pyrolysis, hydrothermal treatment, etc. (Geng et al., 2021).

Processes used in municipal wastewater treatment result in high energy consumption and carbon emissions. Nonetheless, organic materials found in municipal wastewater have the potential to serve as a significant source of carbon (Lu et al., 2024). WAS is an inevitable byproduct of the wastewater treatment process which is produced during the activated sludge process (Geng et al., 2020). WAS was once thought of as waste, but in recent years, it has come to be seen as a resource. It appears possible to address both the energy problem and environmental problems at the same time using energy recovery from WAS (Geng et al., 2021).

MFC is an environmentally beneficial technology since it can directly recover electricity from a variety of bio-wastes (e.g., wastewater, WAS, kitchen waste, manure, etc.) under mild operating conditions (Geng et al., 2020). A wide range of bacteria that produce electricity have been reported to be present in activated sludge. Consequently, at the anode, activated sludge is used as an inoculum (Rashid et al., 2013).

MFC as a wastewater and WAS treatment solution has proven to have potential financial benefits (Geng et al., 2020). However, in typical MFCs, limited WAS hydrolysis restricts energy production and WAS reduction. Numerous pretreatment techniques, including sonication, ozonation, sterilization, heat/alkaline pretreatment, and alkaline pretreatment, have been used to speed up WAS hydrolysis for improved energy generation and sludge reduction in MFCs (Geng et al., 2021).

7. Polyhydroxyalkanoates (PHAs) as added-value bioproducts

Polyhydroxyalkanoates (PHAs) are microbial, linear polyesters composed of 3-hydroxy acid monomers (Pagliano et al., 2021) and they are produced by Gram-negative and Gram-positive eubacteria in both aerobic and anaerobic conditions, as well as several archaea that live in environmentally extreme habitats, to help them survive and compete in environments where carbon and energy sources are scarce (Licciardello et al., 2019). Numerous microbes can store

organic and/or inorganic inclusions surrounded by phospholipids within their cells. PHAs have a core of polyester that is surrounded by phospholipids or proteins. PHAs are stored as granules ranging in size from 0.2 to 0.5 μm in the cytoplasm of various bacteria (Raza et al., 2018) (Fig. 3).

Because of the multiple production conditions of the PHAs, the length and composition of their side chains might vary, affecting the macromolecule's ultimate thermomechanical qualities (Tomietto et al., 2020). According to the quantity of carbons in the side chains, PHAs are divided into three categories: short, medium, and long chain length (scl, mcl, and lcl). The repeat units in short chain length (scl) PHAs are hydroxy fatty acids (HFAs) with a 3–5 carbon chain length (C_3–C_5), while repeat units in medium chain length (mcl) PHAs are C_6–C_{14}. Generally, scl-PHAs are crystalline polymers with a fragile and rigid structure, whilst mcl-PHAs are amorphous thermoplastics, with varying degrees of crystallinity as well as elastomeric and adhesive capabilities. Long chain length (lcl) PHAs, which are composed of monomers with more than 14 carbon atoms, are less prevalent and less researched (Licciardello et al., 2019).

Various types of PHAs can be produced by both prokaryotic and eukaryotic microorganisms. In terms of PHA production, bacteria can be split into two categories. Bacteria in the first category accumulate PHAs only when a nutrient, such as phosphorous, nitrogen, oxygen, or magnesium is limited, and they do not accumulate PHAs during the phase of growth. The second category accumulates PHAs while growing and does not require any nutritional restriction (Raza et al., 2018).

Regularly, PHAs show similar characteristics to conventional, petroleum-based polymers. Some physiochemical properties of PHAs are their insolubility in water, resistance to UV, high degree of polymerization, stiffness, high volume to surface ratio and thermoplasticity (V. Sharma et al., 2021). PHAs are soluble in chloroform, as well as in other chlorinated solvents, resistant to hydrolytic attack and they sink in water which enables anaerobic biodegradation in sediments.
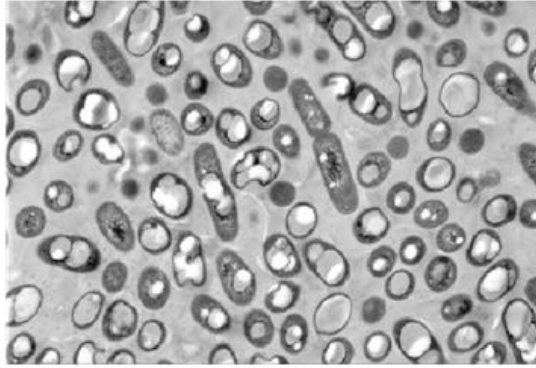
Figure 3. Microscopic image of PHA granules (V. Sharma et al., 2021)

PHAs also exhibit general properties like high processability, non-toxicity, and structural diversity (Behera et al., 2022). Additionally, they are fully biocompatible and biodegradable (e.g., degrades in soils) as well as acting as piezoelectric materials. The type and composition of the polymer, environmental conditions, and the microorganisms that degrade PHAs all have an impact on their biodegradation (Raza et al., 2018). Importantly, PHAs are differentiated from other polymers because of their ability to biodegrade in a variety of environments, including soil, sea, and lake water (Behera et al., 2022).

Bacterial PHA biopolymers are renewable and environmentally friendly biomaterials that could be used to replace plastics in a variety of industries, including packaging, food services, biomedicine, and agriculture (Nicolò et al., 2014). As packaging films paper, they can be used to manufacture coatings, shopping bags, diapers, cups, and carpets, among other things (V. Sharma et al., 2021). On the other hand, PHAs can be used for applications that are more common, such as cosmetics and toys (Tomietto et al., 2020).

Chaijak et al., 2024, first reported on PHA recovery from MFC. Their study specifically looked into *Enterobacter sp*.'s capacity to produce PHA and bioelectrics in a dual chamber MFC. Two of the study's main benefits are that it reduces textile wastewater treatment by utilizing the bioelectricity produced by MFC and it produces PHA with added value, making it both highly significant and economically viable.

Aim of the study

The aim of this thesis is to evaluate the biodegradation of WCO using the innovative technology of MFCs while exploring the effect of PHAs storage.

To achieve this goal,

A. Mixed cultures able to store PHAs were enriched with AS using sodium acetate as carbon source

B. MFCs using AS as inoculum and WCO as fuel were tested

C. MFCs using mixed cultures able to store PHAs and use WCO as fuel were also assessed.

Materials & Methods

1. Microbial Enrichment experiments

Sodium Acetate (50 g L^{-1}) was subjected to the process of enrichment which endorsed the growth of desired microorganisms. For each enrichment experiment, in the beginning, 5% (w/v) activated sludge coming from the municipal wastewater treatment plant of Anthoupoli (Cyprus) was used as an inoculum with 2% (1 g L^{-1}), 4% (2 g L^{-1}), 8% (4 g L^{-1}), 12% (6 g L^{-1}), 16% (8 g L^{-1}) and 20% (10 g L^{-1}) (v/v) Sodium Acetate (50 g L^{-1}), respectively. In all six enrichment experiments, 10% (v/v) of 10 times concentrated (10 ×) M9 minimal medium (i.e., 33.91 g Na$_2$HPO$_4$, 15 g KH$_2$PO$_4$, 15 g NaCl, 5 g NH$_4$Cl in 0.5 L dH$_2$O) and 0,2% (v/v) of 500 times concentrated (500 ×) MgSO$_4$ (12.0372 g in 100 mL dH$_2$O) was added. Microbial enrichment experiments were performed in a total volume of 100 mL in a 500 mL Erlenmeyer flask. The incubation period of the first enrichment process lasted for 7 days at a temperature of 30 ◦C and 100 rpm (Shaking Orbital Incubator SI50, Stuart). On the first day (after 24h), 2 mL of liquid Trace Element Solution (i.e. 3.43 g MnSO$_4$, 3.80 g CaCl$_2$, 1.57 g CuSO$_4$, 5 g FeSO$_4$ in 1 L dH$_2$O) was added in each culture, to boost the microorganisms' growth. On the fourth day (4d), the enrichment experiments were moved to anaerobic conditions until the last (7d) of their incubation. The intention of this procedure was to increase the growth of microbial populations that are able to tolerate anaerobic conditions, since these are the most common conditions used in MFCs. At the end of the incubation period, 10% (v/v) of the first culture was transferred into a freshly prepared media, which contained Sodium Acetate, M9 and MgSO$_4$ at the concentration and conditions mentioned above. Each subculture lasted 7 days and was conducted 1 more time. Again, this time, 10% (v/v) of the previous culture was used as inoculum for the new culture. Microbial growth was measured by optical density (OD) at 600 nm (UV-Visible Spectrophotometer, JASCO V-530 PC, Nicosia, Cyprus). The enrichment period was followed by streaking of the bacterial culture in plates with agar medium. Six agar mediums with different Sodium Acetate concentrations were prepared (1,5 % agar, 10% M9, 0.2 % MgSO$_4$, 2% Trace Element Solution, 2% (1 g L^{-1}), 4% (2 g L^{-1}), 8% (4 g L^{-1}), 12% (6 g L^{-1}), 16% (8 g L^{-1}) and 20% (10 g L^{-1}) Sodium Acetate respectively, and the rest of the volume was filled with DH$_2$O). Three hundred (300) μL of the liquid cultures were spread to a Petri dish containing nutrient broth agar. The solid cultures were incubated at 30 ◦C for until colonies were formed. Six colony mixtures, one from each culture, were collected from the nutrient agar. Then, each mixture was re-grown in liquid media which contained Sodium Acetate, M9 and

MgSO$_4$ at the concentration and conditions mentioned above with a total volume of 100 mL in a 500 mL Erlenmeyer flask at 30 ∘C and 100 rpm (Shaking Orbital Incubator SI50, Stuart) for 24 hours. Each culture was centrifuged at 4ºC, 10000rpm for 20 min to separate biomass and supernatant. The latter was discarded, and biomass was stored at -20ºC until further use. Also, microbial culture aliquots of the six cultures were separated and stored in 25% (v/v) glycerol at -80 ∘C.

2. DNA extraction

For total genomic DNA (gDNA) extraction, microbial culture aliquots by each of the six cultures were grown in liquid media which contained Sodium Acetate, M9 and MgSO$_4$ at the concentration and conditions mentioned above with a total volume of 100 mL in a 500 mL Erlenmeyer flask at 30 ∘C and 100 rpm (Shaking Orbital Incubator SI50, Stuart) for 13 days. Following that, each culture was centrifuged at 4ºC, 10000rpm for 20 min to separate biomass and supernatant. The latter was discarded, and biomass was stored at -20ºC. Total DNA of each microbial sample was extracted using the DNeasy Powersoil Kit, Microbial genomic DNA (Qiagen, Düsseldorf, Germany), following instructions of the manufacturer. The extracted gDNA was used for 16S rRNA amplicon sequencing (Macrogen Ltd., Amsterdam, the Netherlands).

3. Next-generation sequencing

Total extracted gDNA of the six cultures were sent for Next generation sequencing which was performed by Macrogen Ltd. (Amsterdam, the Netherlands). The region used for the method was 16S V3-V4 and the full length of the primer sequences targeting this region for 16S PCR amplification were:

Forward primer:

5' TCGTCGGCAGCGTCAGATGTGTATAAGAGACAGCCTACGGGNG GCWGCG 3'.

Reverse primer:

5'GTCTCGTGGGCTCGGAGATGTGTATAAGAGACAGGACTACHVGGGTATCTAATCC3'.

The Library Kit used was Herculase II Fusion DNA Polymerase Nextera XT Index Kit V2 and the type of sequencer was Illumina platform. Briefly, the total extracted gDNA of each sample underwent quality control (QC) to proceed to library construction. Library is prepared by random

fragmentation of the gDNA of each sample, followed by 5' and 3' adapter ligation. Adapter-ligated fragments were then PCR amplified and purified using gel electrophoresis. For cluster generation, the library was loaded into a flow cell where fragments were captured on a lawn of surface-bound oligos complementary to the library adapters. Each fragment was then amplified into distinct, clonal clusters through bridge amplification. When cluster generation was complete, the templates were ready for sequencing. Illumina SBS technology utilizes a proprietary reversible terminator-based method that detects single bases as they were incorporated into DNA template strands. As all 4 reversible, terminator-bound dNTPs were present during each sequencing cycle, natural competition minimizes incorporation bias and greatly reduces raw error rates compared to other technologies. The result for each microbial culture was highly accurate base-by-base sequencing that virtually eliminates sequence-context-specific errors, even within repetitive sequence regions and homopolymers. The Illumina sequencer generated raw images utilizing sequencing control software for system control and base calling through an integrated primary analysis software called RTA (Real Time Analysis). The BCL (base calls) binary was converted into FASTQ utilizing illumina package bcl2fastq. Adapters were not trimmed away from the reads.

4. Microbial fuel cell construction and operation

4.1 Microbial fuel cell construction and operation with mixed cultures and WCO

A triplet of medium-sized 5.4 cm × 4.4 cm × 1.4 cm (h, w, d) double chamber microbial fuel cells (MFCs), with a working volume of 33 mL for both the anode and cathode compartments (50 mL in total), was fabricated using polyacrylic material. The anode and cathode chambers were internally separated by a 6 × 5 cm cation exchange membrane (CEM, 125 × 125 mm, VWR Chemicals, UK). The anode and cathode electrodes used in this study were constructed from pieces of 9 cm × 30 cm plain carbon veil, folded down to 3 cm × 4 cm to fit inside the MFC framework. The anolyte was filled with 22,5 mL medium (2,5 mL Sodium Acetate, 20 mL dH$_2$O) and 2,5 mL of the Culture 6 (10 g L^{-1} Sodium Acetate concentration). The catholyte was potassium ferricyanide, [K3Fe(CN)6], 0.5M in potassium phosphate buffer, pH 7. The MFC was operated in both open circuit voltage (OCV) and closed-circuit voltage (CCV) operating conditions; for the latter, the anode and cathode electrodes were connected with a resistor, whose value was determined depending on experiment. The initial resistor value was 4.5 kΩ. Both the anode and cathode were set at a pH of 7. The MFC was operated in fed-batch mode, whereby the feeding

with minimal medium (10% M9 medium, 0.2% MgSO4, 89.8% dH2O) was carried out when the output voltage decreased below baseline, under sterile semi-anaerobic conditions. Also, additions of waste cooking oil (0.120 mL) started after 48h and kept going every 7 days. On the other hand, the catholyte from the 15th operation day onwards was regularly changed every 14 days upon intense darkening observation. After the system demonstrated stable performance for an extended duration (68 days), the resistance was reduced from 4.5 kΩ to 4 kΩ and then to 3 kΩ on the 84th day. All MFC components were sterilized before use. No external electron mediators were used during the study.

4.2 Microbial fuel cell construction and operation with AS and WCO

Another triplet of medium-sized 4 cm × 3 cm × 1 cm (h, w, d) double chamber microbial fuel cells (MFCs), with a working volume of 12 mL for both the anode and cathode compartments (48 mL in total), was fabricated using polyacrylic material. The anode and cathode chambers were internally separated by a 6 × 5 cm cation exchange membrane (CEM, 125 × 125 mm, VWR Chemicals, UK). The anode and cathode electrodes used in this study were constructed from pieces of 9 cm × 30 cm plain carbon veil, folded down to 2.6 cm × 3.8 cm to fit inside the MFC framework. The anolyte was filled with 5 mL medium (1.4 mL Sodium Acetate, 3.6 mL DH2O) and 6 mL of Activated Sludge Solution. In order to activate the included microorganisms, the activated sludge Solution was prepared beforehand in a duran bottle, containing 100 mL activated sludge provided from Anthoupoli wastewater treatment plant and a small amount of pure glucose. The catholyte was potassium ferricyanide, $[K_3Fe(CN)_6]$, 0.5 M in potassium phosphate buffer, pH 7. The MFC was operated in both open circuit voltage (OCV) and closed-circuit voltage (CCV) operating conditions; for the latter, the anode and cathode electrodes were connected with a resistor, whose value was determined depending on experiment and from polarization studies. The initial resistor value was 4.5 kΩ. Both the anode and cathode were set at a pH of 7. The MFC was operated in fed-batch mode, whereby the feeding with minimal medium (10% M9 medium, 0.2% MgSO4, 89.8% DH2O) was carried out when the output voltage decreased below baseline, under sterile semi-anaerobic conditions. Also, additions of waste cooking oil (0.120 mL) started after 48h and kept going every 7 days. On the other hand, the catholyte from the 15th operation day onwards was regularly changed every 14 days upon intense darkening observation. Following the first polarization study, on the 28th day, the resistor values were set to 10 kΩ, 8 kΩ and 8 kΩ for

each MFC, respectively. On the 44th day, another polarization study was performed, resulting in resistance values of 4.5 kΩ, 3.5 kΩ and 5 kΩ. Subsequently, on the 50th day, after third polarization study, the resistance values were set to 7 kΩ, 8 kΩ and 5 kΩ. All MFC components were sterilised before use. No external electron mediators were used during the study. An assembly of a microbial fuel cell is presented in Figure 4.
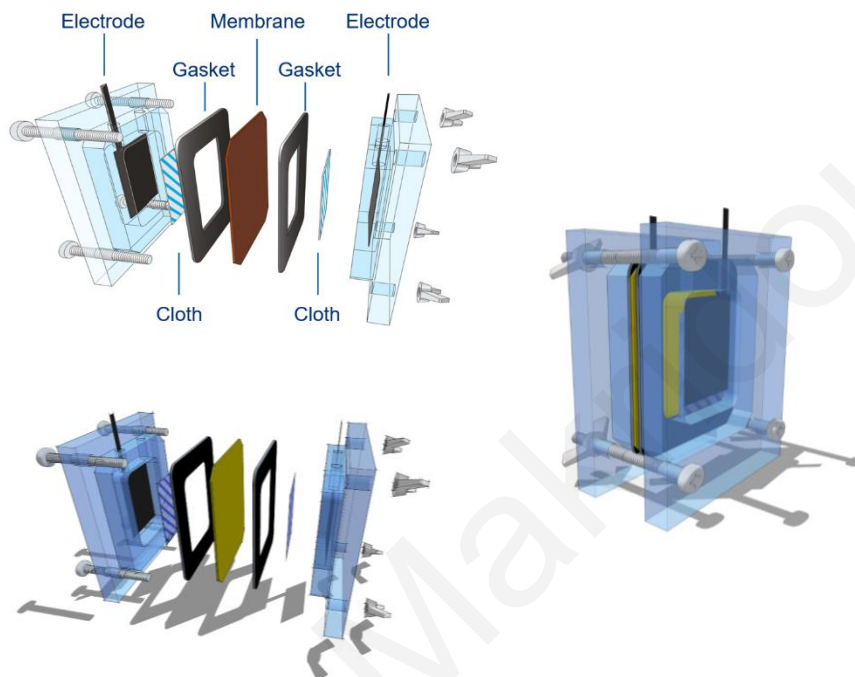
Figure 4. The assembly of the microbial fuel cell

5. Analytical techniques: chemical oxygen demand (COD)

Two dilutions of waste cooking oil 1:10 (1.5 mL waste cooking oil, 1.5 mL M9 medium, 0.03 mL MgSO$_4$, 11.97 mL dH$_2$O) and 1:100 (0.5 mL waste cooking oil, 5 mL M9 medium, 0.1 mL MgSO$_4$, 44.40 mL DH$_2$O) were prepared for COD measurement. Samples were taken from both MFCs triplets for COD analysis. For each sample, a total of 1 mL of supernatant was collected. The method for the determination of COD was done based on the guidelines of a commercial kit (Supelco, Inc, Sigma-Aldrich, St. Louis, MI, USA) with COD range between 500 and 10,000 mg/L. The control for the COD measurement contained the medium and 1 mL dH$_2$O.

6. Biosurfactant extraction and isolation

To isolate the BSF, after each experiment was complete, the cultures were centrifuged for 25 min at 4500 rpm to precipitate and remove the biomass which was saved at 4 ∘C for later use. The first

step of the BSF recovery process was to adjust the cell-free supernatants to a pH of 2 by adding 1M H2SO4. Then, the samples were left in the refrigerator at 4 ∘C overnight. The day after, the supernatant was centrifuged for 30 min at 8000 rpm, leading to the precipitation of the BSF, and the supernatant was disposed. Following, 5 mL of a mixture of chloroform: methanol (2:1 v/v) was added to the precipitated BSF. The liquid was forcefully mixed by the vortex, resulting in the dissolving of the BSF. The mixture was incubated for 15 min at 30 ∘C. After that, the BSF solution was centrifuged at 8000 rpm for 30 minutes, resulting in the precipitation of partially purified BSF. The supernatant was removed, and the precipitate was allowed to dry before being stored at -20°C.

7. Emulsification Index (E24)

The emulsification index (E24) was determined by adding 2 mL of DCF to the same amount of two different aqueous solutions (5% (w/v) and 1% (w/v)) of biosurfactant extracted as above. The DCF-biosurfactant solution was vortexed at maximum speed for 2 min and left to stand for 24 h. After that time period, the E24 was calculated as the percentage of height of emulsified layer (mm) divided by the total height of the liquid column (mm) (Equation (1)). The emulsification percentage was determined based in triplicates.

E24 = (Height of emulsion layer/Total height of solution) x 100 **(1)**

8. Gas Chromatography and Mass Spectrometry (GC-MS) analysis
8.1 Fatty acids methyl esters, FAMEs (Biomass) for PHAs analysis

For each experiment, 2- 7 mg of biomass (Dry Cell Weight) were weighed and placed into the reaction vial. Into the reaction vial was also added 0.8 mL of methanol, 0.2 mL of Sulfuric Acid. It was closed tightly and shaken (vortex), in order to breakdown the PHA granules and the cell membrane and the PHAs got released. Then, the reaction vial was placed in the heating block at 100 °C for 4 hours. After the reaction, the reaction vial was left to cool down to room temperature. The solution from the reaction vial was transferred into a tube and extracted three times with water. The aqueous layer (upper layer) was discarded, and a small amount of MgSO4 was added to the organic phase as a drying agent. The organic phase was filtered and transferred into new a new tube. Following that, the organic phases were collected and combined, and then the solvent was evaporated at room temperature. Lastly, the sample was dissolved in 1.0 mL hexane and transferred to a GC-MS vial having a capacity of 2 mL and GC-MS analysis was performed.

To detect fatty acid methyl esters (FAMEs), GC-MS analysis was performed on a 6890GC-7895MS (Agilent, USA) equipped with a HP-5MS capillary column, 30 m 0.25 mm 0.25 mm (Agilent, USA). The temperature of EI ion13 source was set at 230°C with 70 eV of ionization energy. The carrier gas was helium (99.999%), the flow rate was 1.0 mL/min, the injector temperature was 250°C, the injection volume was 1.0 mL, and the split ratio was 10:1. The oven temperature was held initially at 60°C for 3 min, then increased to 250°C at 10°C/min and finally kept at 250°C for 10 min (You et al., 2014). Qualitative and quantitative analysis of fatty acids methyl esters were conducted, using the Calibration curves of FAMEs (Appendix).

8.2 Fatty acids methyl esters, FAMEs (Supernatant)

A total of 100 μL anolyte sample was methylated and converted to FAMEs following the procedure below: One milliliter of n-hexane was added to 100 μL of anolyte sample. Thereafter, 1 mL of sodium methoxide 1 M (2 g of NaOH in 50 mL methanol) solution was added and the mixture was vortexed for 30 s. The solution was, then, centrifuged at 1200 rpm and incubated at room temperature for 10 min to separate out the clear layer solution containing FAMEs from the turbid aqueous layer. Finally, a small amount of a desiccant, anhydrous MgSO4, was added to the obtained sample to ensure its dehydration. Prior to GC/MS analysis, the final solution was filtered and then transferred into a 2 mL GC vial.

The FAMEs were analyzed by a 8060 GC/5977B MSD equipped with an Agilent HP-5MS Ultra Inert capillary column. The temperature of EI ion source was set at 230 °C with 70 eV of ionization energy. Helium (99.999%) was used as carrier gas at a flow rate of 1.0 mL/min. The injector temperature was maintained at 250 °C with the following oven conditions: 50 °C kept constant for 1 min; increased up to 200 °C with 10 °C/min rate and 1 min hold; further increased up to 230 °C with 3 °C/min rate; followed by 23 min hold at 230 °C (50 min total run time). The injection was splitless with a volume of 1.0 μL. MS was performed at scan and SIM positive ion mode over the 46–500 m/z range. The MS spectra obtained for the FAMEs was first matched to the US NIST mass spectral library database and, then identified and quantified using established calibration curves.

8.3 Total petroleum hydrocarbons, TPHs

A total of 1 mL of the anolyte was transferred into a test tube and extracted with 5 mL n-hexane. Following extraction, the organic (upper) phase was collected and a small amount of desiccant, anhydrous MgSO4, was added to ensure dehydration. Prior to GC/MS analysis, the final solution was filtered and transferred into a 2 mL GC vial. The TPHs were analyzed by a 8060 GC/5977B MSD (Agilent Technologies, Inc., Santa Clara, CA, USA) equipped with an Agilent HP-5MS Ultra Inert capillary column (30 m long. 0.25 mm ID. 0.25 μm film thickness). The temperature of the ion source was set at 230 °C with 70 eV of ionization energy. Helium (99.999%) was used as carrier gas at a flow rate of 1.0 mL/min. The injector temperature was maintained at 250 °C with the following ramp-up conditions: 50 °C kept constant for 1 min; increased up to 110 °C with 10 °C/min rate and 1 min hold; further increased up to 270 °C with 3 °C/min rate and 1 min hold; followed by a final increase at 300 °C with 15 °C/min rate and 10 min hold (74 min total run time). The injection was splitless with a volume of 1.0 μL. MS was performed at scan mode over the 46–800 m/z range. The MS spectra obtained for the TPHs was matched to the US National Institute of Standards and Technology (NIST) mass spectral library database.

8.4 Polycyclic aromatic hydrocarbons, PAHs

The extraction of polycyclic aromatic hydrocarbons (PAHs) was carried out with the method mentioned in TPHs analysis section. The extracted sample was analyzed on the 8060 GC/5977B MSD equipped with the Agilent HP-5MS Ultra Inert capillary column. The temperature of EI ion source was set at 230 °C with 70 °eV of ionization energy. Helium (99.999%) was used as carrier gas at a flow rate of 1.0 mL/min. The injector temperature was maintained at 320 °C with the following oven conditions: 80 °C kept constant for 1 min; increased up to 200 °C with 25 °C/min rate; further increased up to 335 °C with 8 °C/min rate and 6.325 min hold (29 min total run time). The injection was splitless with a volume of 1.0 μL. MS was performed at scan and SIM positive ion mode over the 75–300 m/z range. The MS spectra obtained for the PAHs was matched to the US NIST mass spectral library database.

8.5 Fatty acid methyl esters, FAMEs for BSF

From each experiment, up to 10.0 mg of extracted BSF were weighed and dispersed in 1.0 mL of 6M HCl solution in a reaction vial. The reaction vial was then placed in the heating block at 90 °

C for 24 hours to carry out the acid hydrolysis reaction. After that, the entire product solution was placed into a tube and extracted three times with diethyl ether. The aqueous layer was discarded, and a small amount of MgSO4 was added to the organic phase as a drying agent. The organic phases were filtered, gathered, mixed, and evaporated at room temperature. The residues were then treated with 1.0 mL of a 10% (v/v) H_2SO_4-methanol solution and left to esterify at 55°C for 6 hours. Water and diethyl ether were added after esterification and extracted three times. As in the former case, the aqueous layer was discarded, and a small amount of MgSO4 was added to the organic phase as a drying agent. The fatty acid methyl esters-containing organic phases were filtered, collected and combined, and then the solvent was evaporated at room temperature. Lastly, the esterified sample was dissolved in 1.0 mL hexane and transferred to a GC-MS vial having a capacity of 2 mL and GC-MS analysis was performed.

Results

1. Microbial enrichment process

A fundamental method for growing mixed cultures and eliminating organic and salinized materials from various wastewater types is the enrichment process. In the experiments, bacterial growth was noted on the nutrient broth agar plate after the enrichment period as well as during that time. This indicates the organic content which is necessary for microorganisms' growth existed in the experiments. Consequently, the initial enrichment procedure using activated sludge encouraged and accelerated the development of bacteria that could use sodium acetate as a substrate. Using nutrient broth agars, six distinct mixed bacterial samples were recovered from each enrichment culture. The mixed bacterial cultures were labeled as S1, S2, S3, S4, S5, S6.

2. 16S amplicon sequencing

16S amplicon sequencing was used to characterize each mixed culture's DNA. Specifically, Figure 5 showed that the phylum Actinomycetota (Actinobacteria) can be detected in all six samples with gradual increase at its concentration in each sample and S6 reaching the highest abundance (66.69%). On the other hand, phylum Bacteroidota showed gradual concentration decrease through

Figure 5. Relative abundance of bacterial phylum recovered from each of the six mixed bacterial cultures (S1, S2, S3, S4, S5, S6) using 16S amplicon sequencing.

each sample, with the highest abundance in S1 (65.81%). Phylum Pseudomonadota was also found in all samples at significant concentrations, with highest concentration in S4 (58.98%), S3 (52.67%) and S5 (44.59%).

Figure 6 showed that the class Actinomycetes can be detected in all six samples with gradual increase at its concentration in each sample, respectively. The dominant class for S1 (59.53%) is Flavobacteriia, for S2 (20.00%) is Betaproteobacteria and for S3 (31.39%), S4 (39.82%) is Alphaproteobacteria. The class Actinomycetes of the phylum Actinomycetota prevaled in S5 (50.49%) and S6 (66.45%). All cultures contained lower concentrations of Gammaproteobacteria.

Figure 6. Relative abundance of bacterial class recovered from each of the six mixed bacterial cultures (S1, S2, S3, S4, S5, S6) using 16S amplicon sequencing.

In more detail, Figure 7 showed the orders found in the samples, after the analysis. In S1 (59.53%) and S2 (17.86%) the dominant order was Flavobacteriales. In S4 (28.78%), S5 (50.14%), S6 (66.25%) high abundancies of the order Mycobacteriales were observed. The order Hyphomicrobiales was detected in all six samples, with higher concentration in S3 (18.91%).
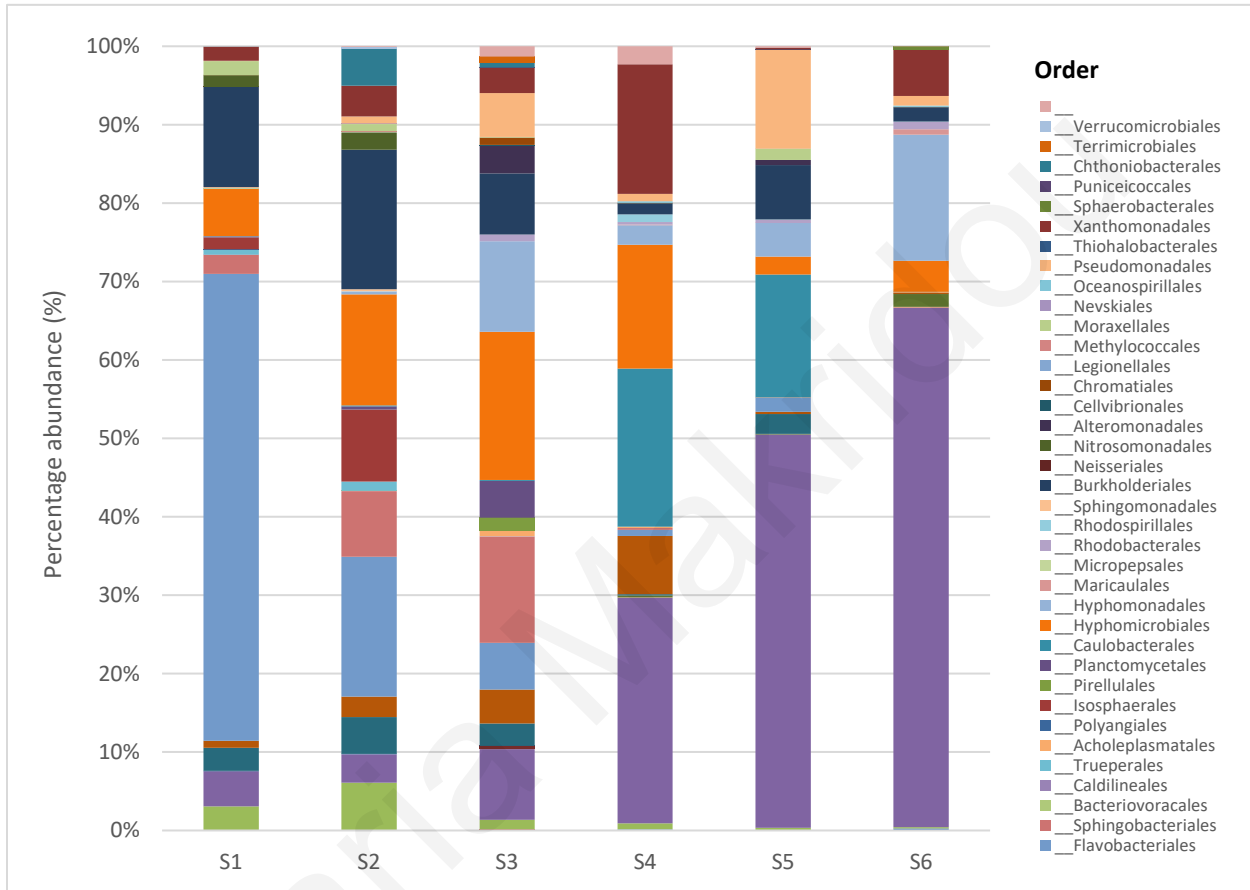
Figure 7. Relative abundance of bacterial order recovered from each of the six mixed bacterial cultures (S1, S2, S3, S4, S5, S6) using 16S amplicon sequencing.

Particularly, Figure 8 showed that the family of Weeksellaceae is detected in high abundance in S1 (51.03%) and in lower concentrations in S2 (15.54%) and S3 (1.31%). Alcaligenaceae family is also found in every culture, but in S2 (16.91%) in higher concentration. S2, S3 and S4 contain microorganisms from various families. In S3 families like Sphingobacteriaceae (13.52%), Hyphomonadaceae (11.53%) and Brucellaceae (10.66%) are detected. Caulobacteraceae can be

found in S4 (20.15%) and S5 (15.67%). However, high percentage abundance of the family Corynebacteriaceae was noted, especially in S5 (49.75%) and S6 (65.82%).
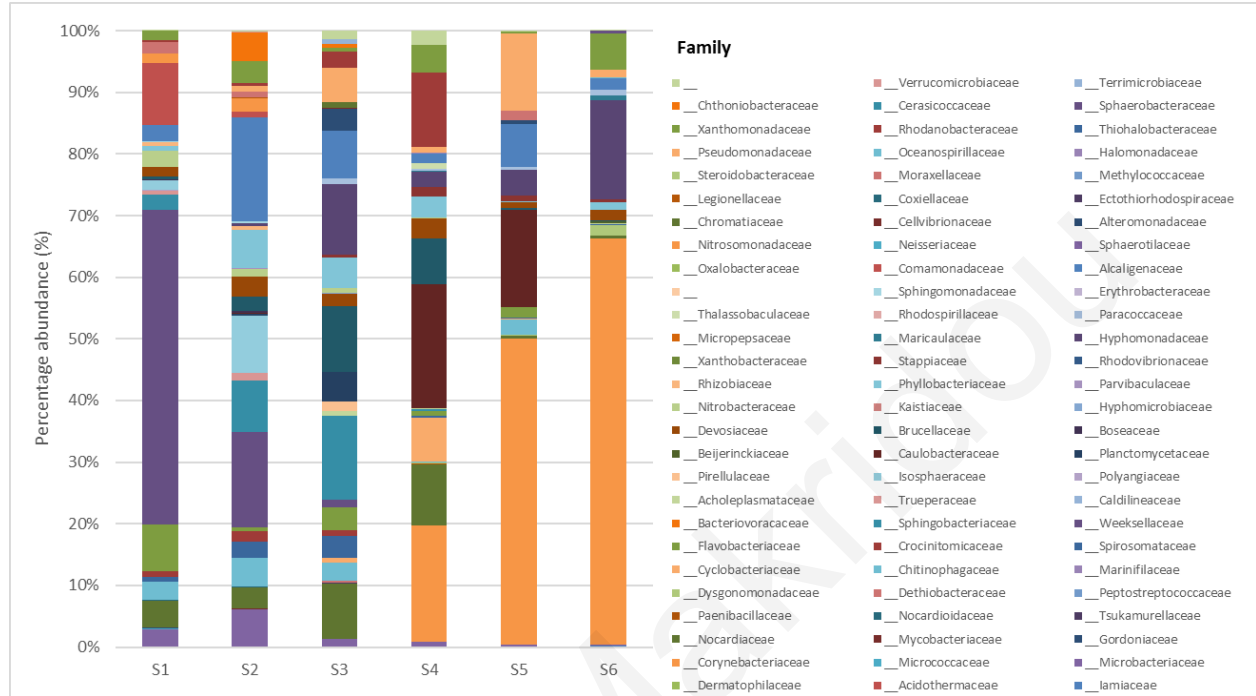
Figure 8. Relative abundance of bacterial family recovered from each of the six mixed bacterial cultures (S1, S2, S3, S4, S5, S6) using 16S amplicon sequencing.

Going into more analytics of the families mentioned previously, Figure 9 indicates the genera found in the samples. High percentage abundance of the genus Moheibacter was noticed in S1 (51.00%). Considerable amounts of the genus Corynebacterium of the family Corynebacteriaceae were found in S4 (18.90%), S5 (49.75%) and S6 (65.82%). In S2, S3, S4 a larger variety of different genera was observed. However, the percentage abundance of these genera was low.
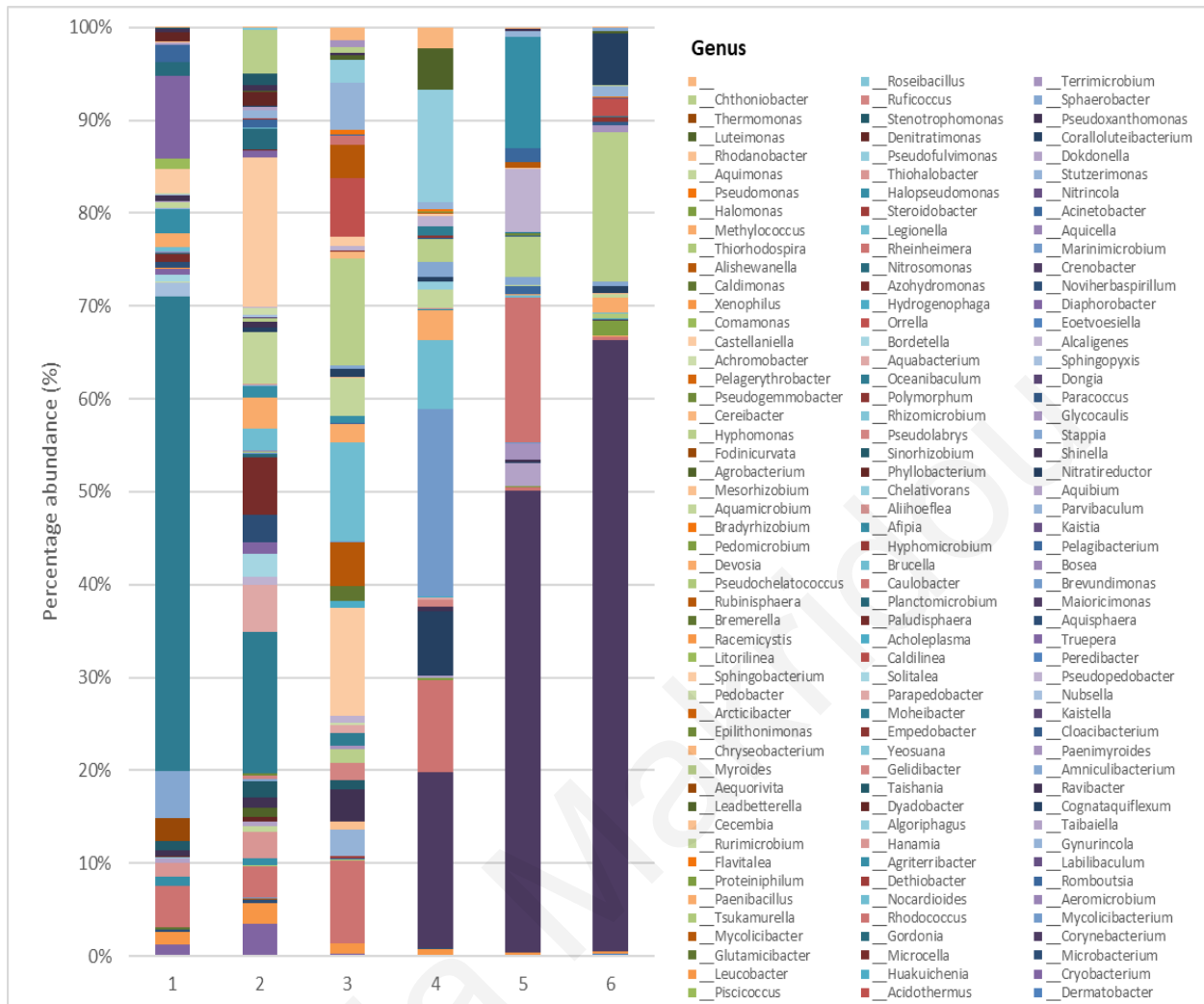
Figure 9. Relative abundance of bacterial genus recovered from each of the six mixed bacterial cultures (S1, S2, S3, S4, S5, S6) using 16S amplicon sequencing.

Lastly, as it is shown in Figure 10, in S1 the species *Moheibacter lacus* was detected in relatively high percentage abundance (50.98%). The species *Corynebacterium sputi* was located in S5 (63.24%) and S6 (63.24%) in high concentrations. On the other hand, S2, S3 and S4 presented a great variety of microorganisms, without any species predominating in quantity.
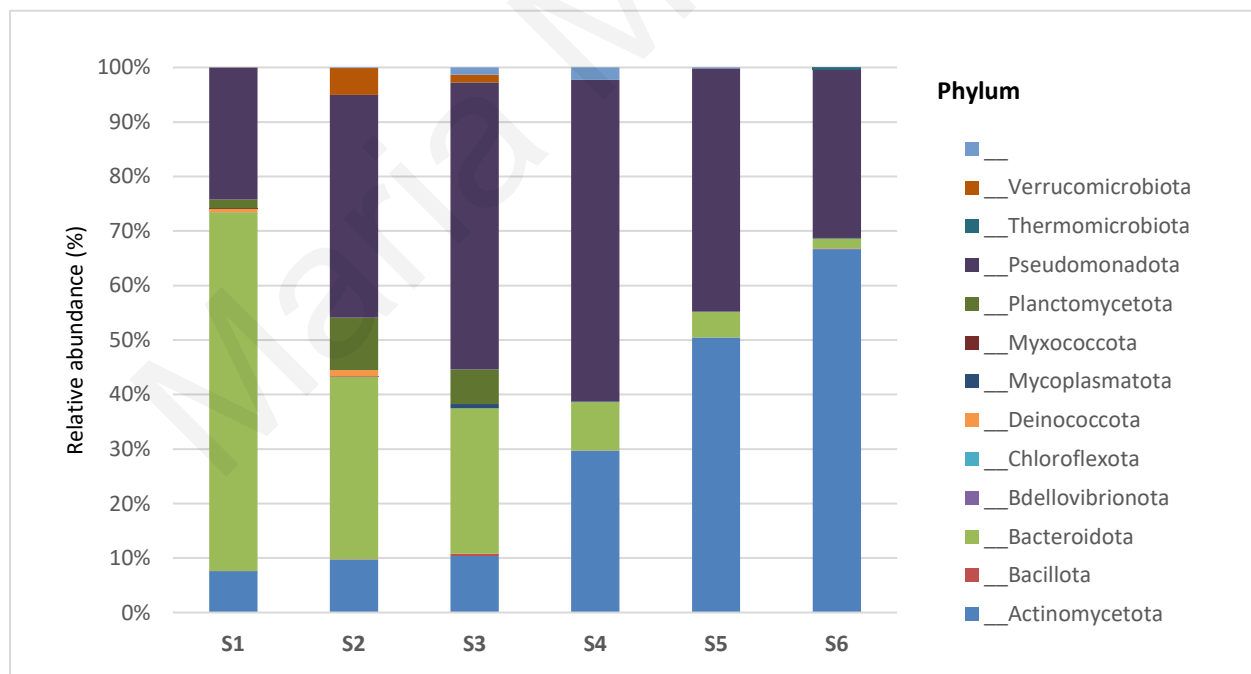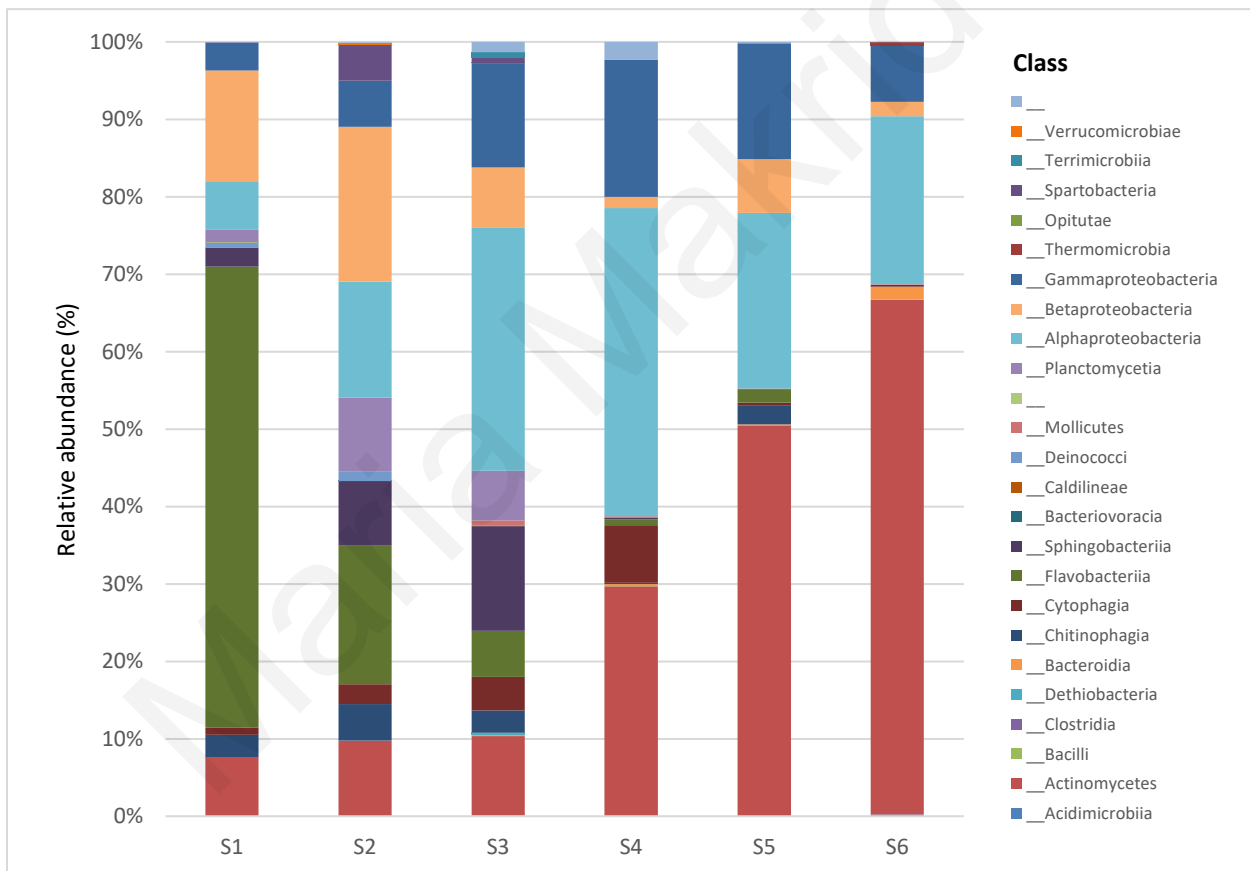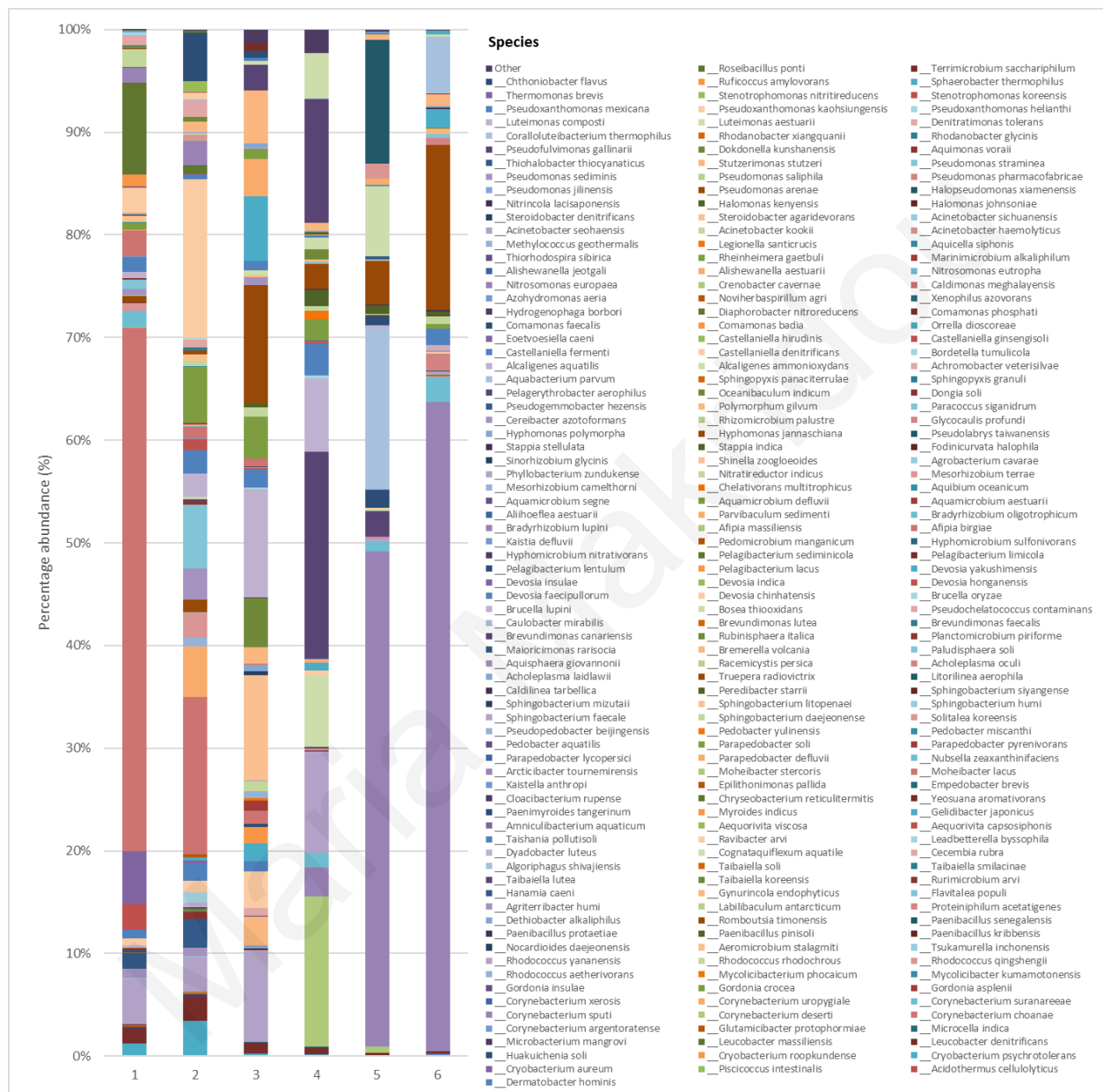
Figure 10. Relative abundance of bacterial species recovered from each of the six mixed bacterial cultures (S1, S2, S3, S4, S5, S6) using 16S amplicon sequencing.

3. Production and accumulation of FAMEs and PHAs in mixed cultures of enrichment process

3. 1 Production and accumulation of FAMEs in mixed cultures of enrichment process

Fatty acids (FAs) were calculated from the extracted and isolated biomass from each enrichment experiment. FAs were subjected to methyl-esterification and the obtained FAMEs were analyzed by GC/MS. In Table 1, the FAMEs that were detected in mixed culture 1 with 1 g/L sodium acetate concentration are presented. In total, seven FAMEs were observed. Quantitative analysis revealed that the major FAMEs in this culture are methyl palmitate (170.78 ppm) and methyl stearate (123.20 ppm), whereas methyl dodecanoate (26.28 ppm), methyl elaidate (17.50 ppm), methyl myristate (13.12 ppm), methyl decanoate (12.14 ppm) and methyl pentadecanoate (8.56 ppm) were identified in significantly lower concentrations.

In mixed culture 2, where the sodium acetate concentration was 2 g/L, methyl palmitate (332.46 ppm) and methyl stearate (208.87 ppm) were found in even greater abundance (Table 2). However, methyl dodecanoate (47.62 ppm), methyl pentadecanoate (38.43 ppm) and methyl myristate (13.02 ppm) were found in significantly lower concentrations.

Mixed culture 3 (4 g/L sodium acetate concentration), did not present any significant differences from mixed culture 2 (Table 3). The major FAMEs in this culture are methyl stearate (173.33 ppm) and methyl palmitate (148.34 ppm). In this mixed culture, unlike the previous, methyl palmitoleate (34.89 ppm) was produced. Furthermore, methyl pentadecanoate was not detected in this case.

In Table 4, the FAMEs detected in mixed culture 4 (6 g/L sodium acetate) are presented. Relatively, lower concentration of FAMEs was found in this culture, with methyl stearate being the only one surpassing 50 ppm. Also, it is important to note that methyl decanoate was observed, in contrast to the previous two concentrations.

Lastly, the FAMEs detected in mixed culture 6, where the sodium acetate concentration was 10 g/L, are presented in Table 5. Quantitative analysis showed that the major FAMEs were methyl stearate (1400.33 ppm) and methyl elaidate (619.82 ppm) with significant difference. To sum up,

the analysis of FAMES in mixed cultures that the FAMEs produced intracellularly are similar qualitatively and quantitatively with small differences.

Table 1. Quantitative analysis of FAMES in mixed culture 1 (1 g/L Sodium Acetate Concentration)

FAMEs (1 g/L)

No.	Chemical (Empirical) Name	Molecular Formula	Molecular weight	Retention time (min)	Concentration (ppm)
1	Decanoic acid, methyl ester – Methyl decanoate	$C_{11}H_{22}O_2$	186.29	11.042	12.14
2	Dodecanoic acid, methyl ester – Methyl dodecanoate	$C_{13}H_{26}O_2$	214.34	13.621	26.28
3	Tetradecanoic acid, methyl ester – Methyl tetradecanoate (myristate)	$C_{15}H_{30}O_2$	242.4	16.035	13.12
4	Pentadecanoic acid, methyl ester – Methyl pentadecanoate	$C_{16}H_{32}O_2$	256.42	17.253	8.56
5	Hexadecanoic acid, methyl ester – Methyl palmitate	$C_{17}H_{34}O_2$	270.45	18.581	170.78
6	9-Octadecenoic acid (E), methyl ester – Methyl elaidate	$C_{19}H_{36}O_2$	296.49	21.803	17.50
7	Octadecanoic acid, methyl ester – Methyl stearate	$C_{19}H_{38}O_2$	298.5	21.964	123.20

Table 2. Quantitative analysis of FAMES in mixed culture 2 (2 g/L Sodium Acetate Concentration)

FAMEs (2 g/L)

No.	Chemical (Empirical) Name	Molecular Formula	Molecular weight	Retention time (min)	Concentration (ppm)
1	Dodecanoic acid, methyl ester – Methyl dodecanoate	$C_{13}H_{26}O_2$	214.34	13.621	47.62
2	Tetradecanoic acid, methyl ester – Methyl tetradecanoate (myristate)	$C_{15}H_{30}O_2$	242.4	15.92	13.02
3	Pentadecanoic acid, methyl ester – Methyl pentadecanoate	$C_{16}H_{32}O_2$	256.42	17.253	38.43
4	Hexadecanoic acid, methyl ester – Methyl palmitate	$C_{17}H_{34}O_2$	270.45	18.581	332.46
5	Octadecanoic acid, methyl ester – Methyl stearate	$C_{19}H_{38}O_2$	298.5	21.964	208.87

Table 3. Quantitative analysis of FAMES in mixed culture 3 (4 g/L Sodium Acetate Concentration)

	FAMEs (4 g/L)				
No.	*Chemical (Empirical) Name*	*Molecular Formula*	*Molecular weight*	*Retention time (min)*	*Concentration (ppm)*
1	Dodecanoic acid, methyl ester – Methyl dodecanoate	$C_{13}H_{26}O_2$	214.34	13.621	86.05
2	Tetradecanoic acid, methyl ester – Methyl tetradecanoate (myristate)	$C_{15}H_{30}O_2$	242.4	15.92	22.11
3	9-Hexadecenoic acid, methyl ester – Methyl palmitoleate	$C_{17}H_{32}O_2$	268.43	18.4	34.89
4	Hexadecanoic acid, methyl ester – Methyl palmitate	$C_{17}H_{34}O_2$	270.45	18.581	148.34
5	Octadecanoic acid, methyl ester – Methyl stearate	$C_{19}H_{38}O_2$	298.5	21.964	173.33

Table 4. Quantitative analysis of FAMES in mixed culture 4 (6 g/L Sodium Acetate Concentration)

	FAMEs (6 g/L)				
No.	*Chemical (Empirical) Name*	*Molecular Formula*	*Molecular weight*	*Retention time (min)*	*Concentration (ppm)*
1	Decanoic acid, methyl ester – Methyl decanoate	$C_{11}H_{22}O_2$	186.29	11.042	14.93
2	Dodecanoic acid, methyl ester – Methyl dodecanoate	$C_{13}H_{26}O_2$	214.34	13.621	13.54
3	Tetradecanoic acid, methyl ester – Methyl tetradecanoate (myristate)	$C_{15}H_{30}O_2$	242.4	15.92	31.87
4	Hexadecanoic acid, methyl ester – Methyl palmitate	$C_{17}H_{34}O_2$	270.45	18.581	19.24
5	Octadecanoic acid, methyl ester – Methyl stearate	$C_{19}H_{38}O_2$	298.5	21.964	69.13

Table 5. Quantitative analysis of FAMES in mixed culture 6 (10 g/L Sodium Acetate Concentration)

No.	Chemical (Empirical) Name	Molecular Formula	Molecular weight	Retention time (min)	Concentration (ppm)
FAMEs (10 g/L)					
1	Dodecanoic acid, methyl ester – Methyl dodecanoate	$C_{13}H_{26}O_2$	214.34	13.621	17.85
2	Tetradecanoic acid, methyl ester – Methyl tetradecanoate (myristate)	$C_{15}H_{30}O_2$	242.4	16.035	12.74
3	Hexadecanoic acid, methyl ester – Methyl palmitate	$C_{17}H_{34}O_2$	270.45	18.581	31.33
4	9-Octadecenoic acid (E), methyl ester – Methyl elaidate	$C_{19}H_{36}O_2$	296.49	21.803	619.82
5	Octadecanoic acid, methyl ester – Methyl stearate	$C_{19}H_{38}O_2$	298.5	21.964	1400.33

3.2 Production and accumulation of PHAs in mixed cultures

A detailed analysis has been performed to identify and quantify the composition of PHAs at the different sodium acetate concentrations used as substrate to the isolated mixed cultures coming from the enrichment process, tested in this study. PHAs were calculated from the biomass stored from the six cultures after the enrichment process. PHAs were subjected to methyl-esterification and the obtained PHAs were analyzed by GC/MS.

The detailed PHAs composition is presented in Table 6 where a set of three PHAs was found which is discernible in the total ion chromatogram illustrated in Figure 11. These are methyl 3-hydroxydecanoate ($C_{11}H_{22}O_3$), methyl 3-hydroxydodecanoate ($C_{13}H_{26}O_3$) and Methyl 3-hydroxytetradecanoate ($C_{15}H_{30}O_3$). It was observed that the identified PHAs were the same at different sodium acetate concentrations. In total, three PHAs were detected in all cultures. Furthermore, it is observed that the PHAs produced as mcl being C10, C12 and C14, respectively. No data were available for the concentration at 8 g/L. Therefore, in future work it is necessary to repeat this analysis. The accumulation of PHAs at each sample when different concentrations of sodium acetate were used is presented below.

Quantitative analysis (Figure 12) revealed that methyl 3-hydroxydecanoate was detected in high percentages in the mixed cultures with 10 g/L and 6 g/L sodium acetate concentrations. Furthermore, at concentrations 1 g/L, 2 g/L and 4 g/L considerable amounts (>50%) were found as well. The results of the quantitative analysis for methyl 3-hydroxydodecanoate in the different mixed cultures with different sodium acetate concentrations are shown in Figure 13. The highest abundance of this PHA was noted at 6 g/L, followed by 1 g/L, 2 g/L, 4 g/L and 10 g/L.

Table 6. Results of qualitative PHAs analysis in mixed cultures with different sodium acetate concentrations as substrate.

No.	Chemical – Empirical Name	Molecular Formula	HA methyl ester	Molecular weight (g/mol)	Retention time (min)	Sodium acetate concentration				
						1g / L	2g / L	4g / L	6g/L	10g/L
1	Methyl 3-hydroxydecanoate	$C_{11}H_{22}O_3$	3HD	202.29	12.87	√	√	√	√	√
2	Methyl 3-hydroxydodecanoate	$C_{13}H_{26}O_3$	3HDD	230.34	15.03	√	√	√	√	√
3	Methyl 3-hydroxytetradecanoate	$C_{15}H_{30}O_3$	3HTD	258.40	17.78	√	√	√	√	√

Polyhydroxyalkanoates - GC chromatogram
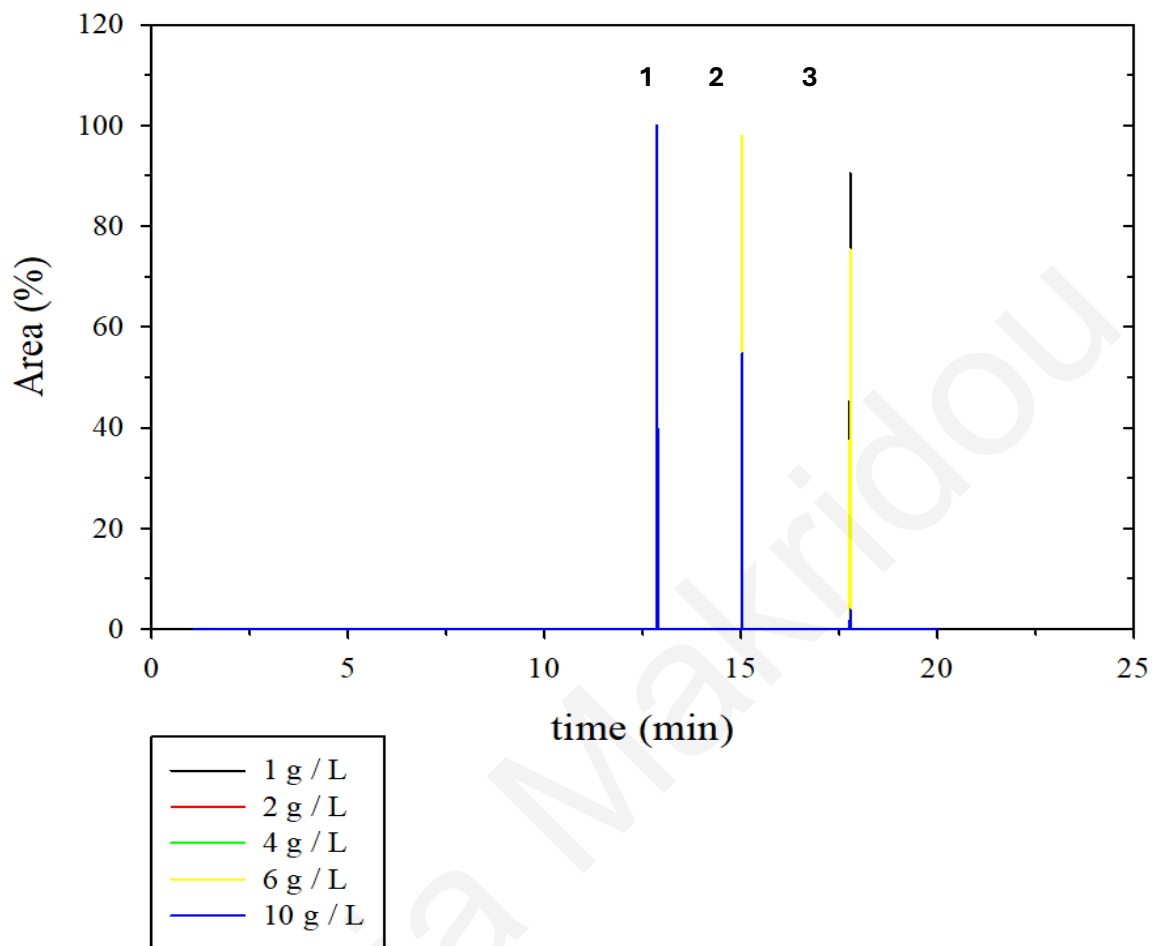
Figure 11. Polyhydroxyalkanoates (PHAs) analysis; Ion chromatograms at $m/z = 74$ where three hydroxy acids were detected in six mixed cultures with varying sodium acetate concentrations. Peaks 1–3 correspond to methyl 3-hydroxydecanoate ($C_{11}H_{22}O_3$), methyl 3-hydroxydodecanoate ($C_{13}H_{26}O_3$) and Methyl 3-hydroxytetradecanoate ($C_{15}H_{30}O_3$), respectively.
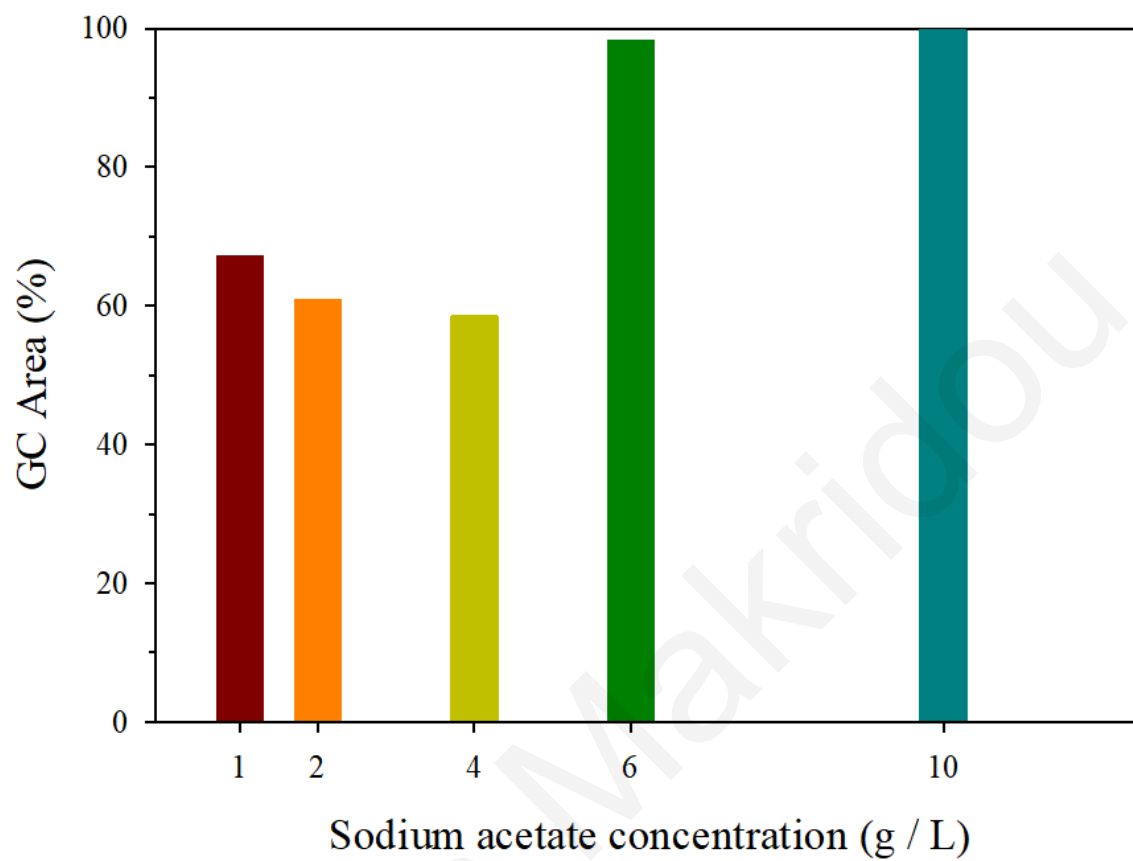
Figure 12. Quantitative results of methyl 3-hydroxydecanoate in the six mixed cultures with different sodium acetate concentrations.

Methyl 3-hydroxydodecanoate
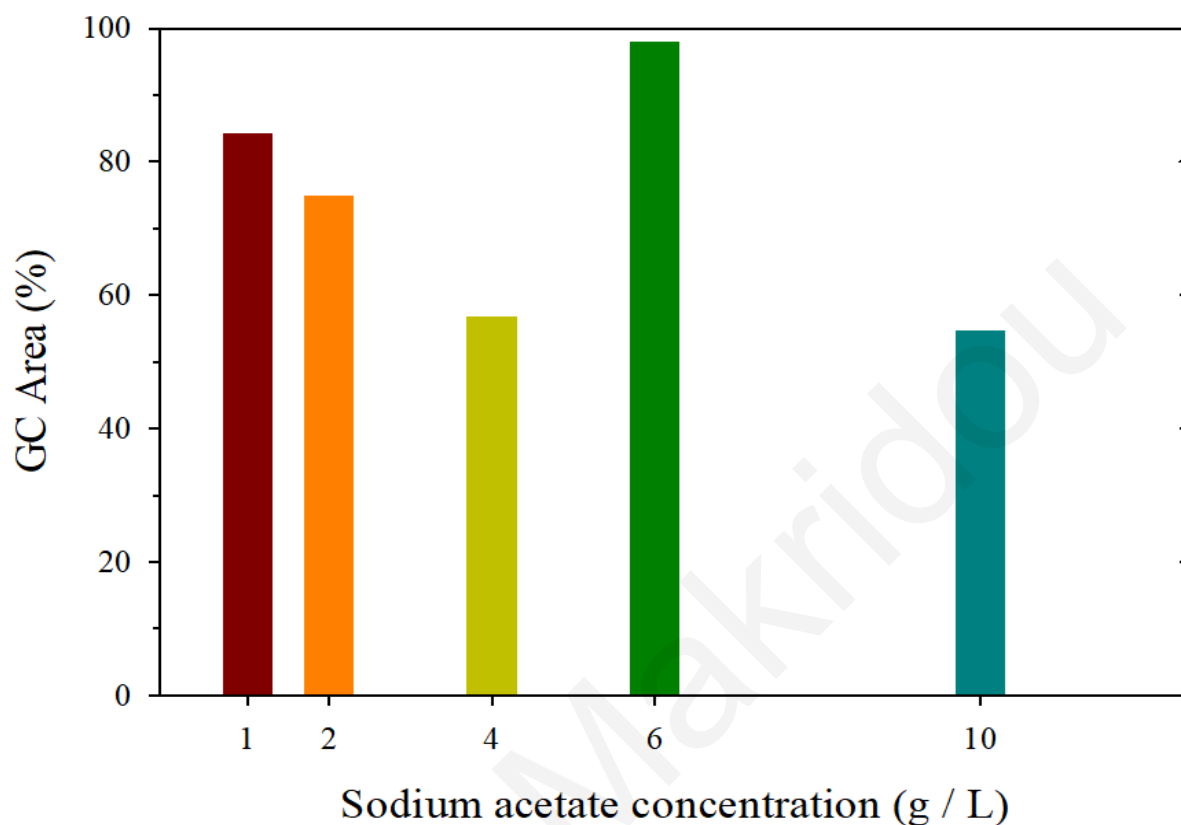
Figure 13. Quantitative results of methyl 3-hydroxydodecanoate in the six mixed cultures with different sodium acetate concentrations.

In Figure 14, quantitative results of methyl 3-hydroxytetradecanoate in the different mixed cultures with different sodium acetate concentrations are presented. In contrast with the previous PHAs found, methyl 3-hydroxytetradecanoate is mostly found in 1 g/L concentration followed by 6 g/L. At concentrations 2 g/L and 4 g/L lower abundances were noticed. Lastly, a relatively insignificant amount was detected in the culture with 10g/L concentration of sodium acetate.

Methyl 3-hydroxytetradecanoate
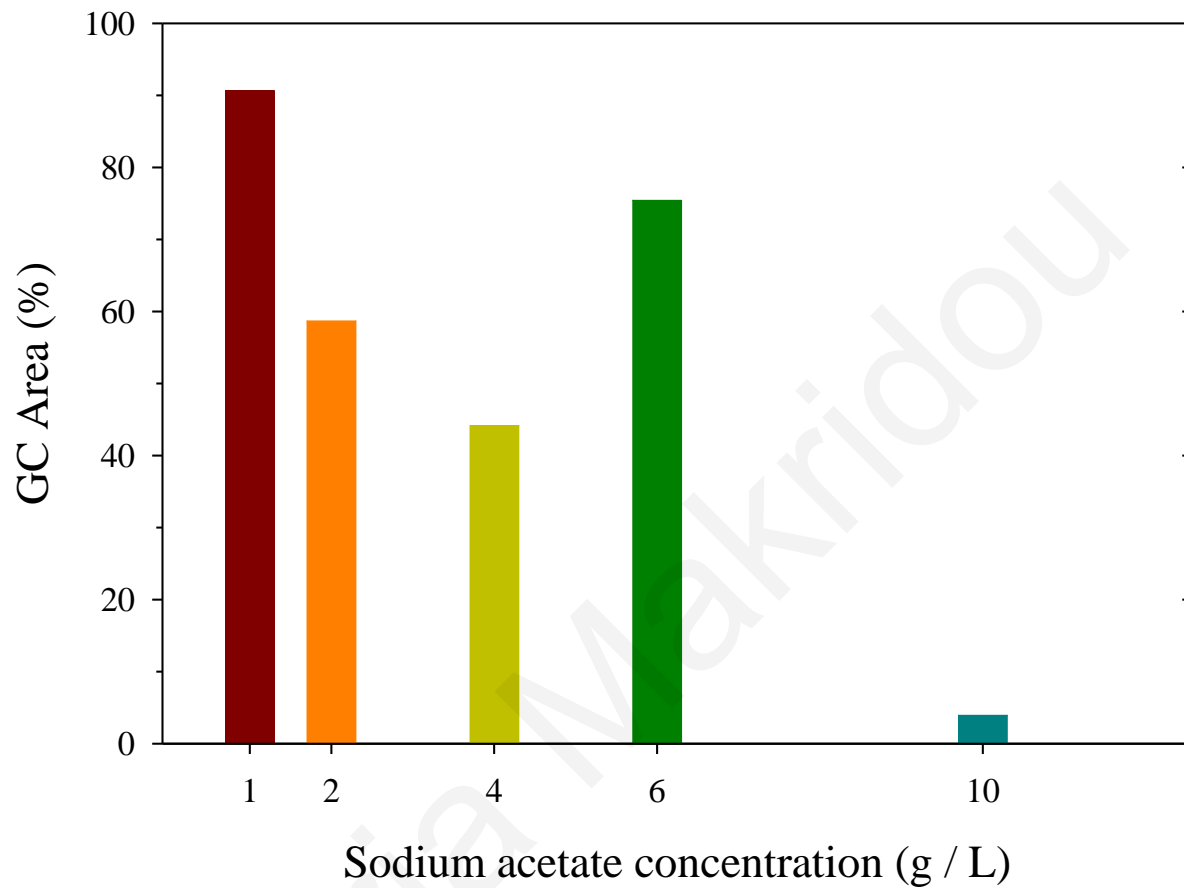
Figure 14. Quantitative results of methyl 3-hydroxytetradecanoate in the six mixed cultures with different sodium acetate concentrations.

4. Performance of the MFCs with AS and WCO

This MFC experimental set up was based on addition of AS as inoculum and WCO as fuel. The experiment lasted 221 days. Three MFCs were set up with identical experimental conditions. The results of each MFC performance based on voltage (mV), current (mA) and power (mW) production are presented below.

4.1 Energy generation of MFC 1 set up with AS and WCO

Data over the full 221-day duration of the experiment are shown in Figure 10, regarding MFC 1. Electricity generation was observed from the beginning of the experiment up to the first 50 days. Following the polarization studies, an almost stable MFC performance was observed, in terms of CCV (Closed-circuit voltage) and electricity generation. Specifically, three polarization studies were carried out. Following the first polarization study carried out on day 27, where the resistance was increased from 4.5 kΩ to 10 kΩ, an increase in output voltage data (from 116 mV to 556 mV) was observed. The next two polarization studies were carried out on 43rd day where the resistance was set back to 4.5 kΩ and on 49th day where the resistance was increased to 7 kΩ. The highest CCV was observed on day 11 at 811 mV (R= 10 kΩ) (Fig.15-1A). Current reached 0.129 mA on day 15 when resistance was 4.5 kΩ. It is observed that there is a decrease over the period of time (Fig.15-1B). Power reached 0.075 mW on day 15 when resistance was 4.5 kΩ. Similarly to current generation, it is observed that there is a decrease over the period of time (Fig.15-1C).
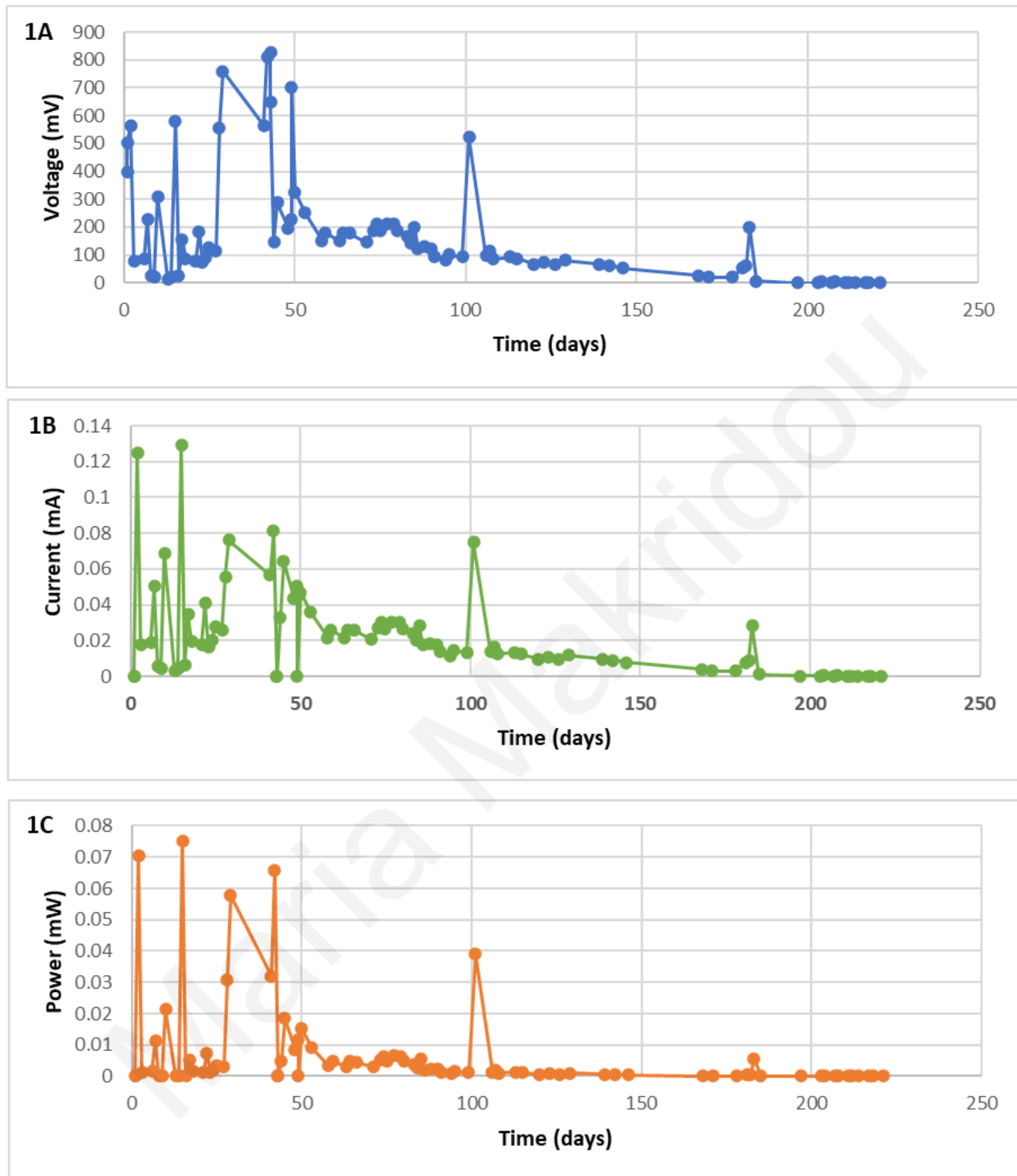
Figure 15. Voltage (mV), current (mA) and power (mW) of the double chambered MFC 1 with AS and WCO.

4.2 Energy generation of MFC 2 set up with AS and WCO

Simultaneously, the same experiment was performed for the other MFCs triplet. The polarization studies were carried out on the same days. However, the electricity production was not the same for each MFC. For MFC 2, after the first polarization study the resistance was increased from 4.5 kΩ to 8 kΩ. Following that, it decreased to 3.5 kΩ and eventually it was set back to 8 kΩ. Specifically, as it is shown in Figure 16, electricity generation of MFC 2 was significantly reduced after 75 days. The maximum voltage production at closed circuit conditions was noted at day 24 at 771 mV (Fig. 16-2A), when the resistance was at 4.5 kΩ. Current at this point was at 0.17 mA (Fig. 16-2B) and power at 0.13 mW (Fig. 16-2C).

4.3 Energy generation of MFC 3 set up with AS and WCO

On the contrary, MFC 3 performed better than the other two in terms of electricity production. High and steady amounts of electricity were generated during the whole period that the experiment lasted (Figure 17). Following the first polarization study, the resistance was increased from 4.5 kΩ to 8 kΩ. The resistance was set to 5 kΩ after the second polarization study and it remained the same after the last one. The maximum CCV were observed at days 73 (725 mV), 115 (710 mV), 129 (726 mV) and 208 (713 mV), while the resistance was at 8 kΩ (Fig.17-3A). Current at these points were 0.145 mA, 0.142 mA, 0.145 mA and 0.142 mA, respectively (Fig.17-3B). Power was measured as high as 0.105 mW, 0.101 mW, 0.105 mW and 0.102 mW at the same points mentioned before (Fig.17-3C). Moreover, high current production was observed at days 22 and 23, reaching 0.168 mA and 0.171 mA, respectively. On these days, the power generation was 0.126 mW and 0.131 mW, respectively. The higher power production can perhaps be attributed to healthy biofilm formation over time on the anode electrode.
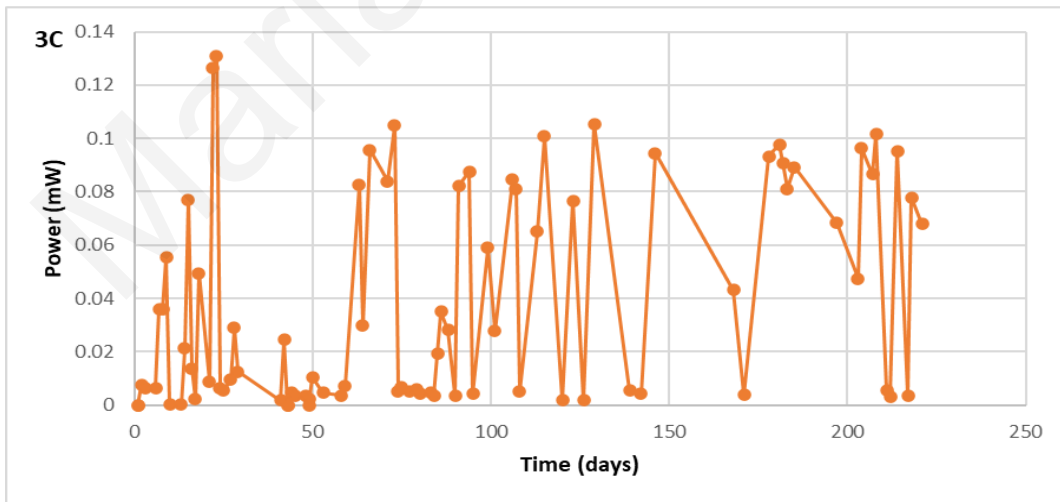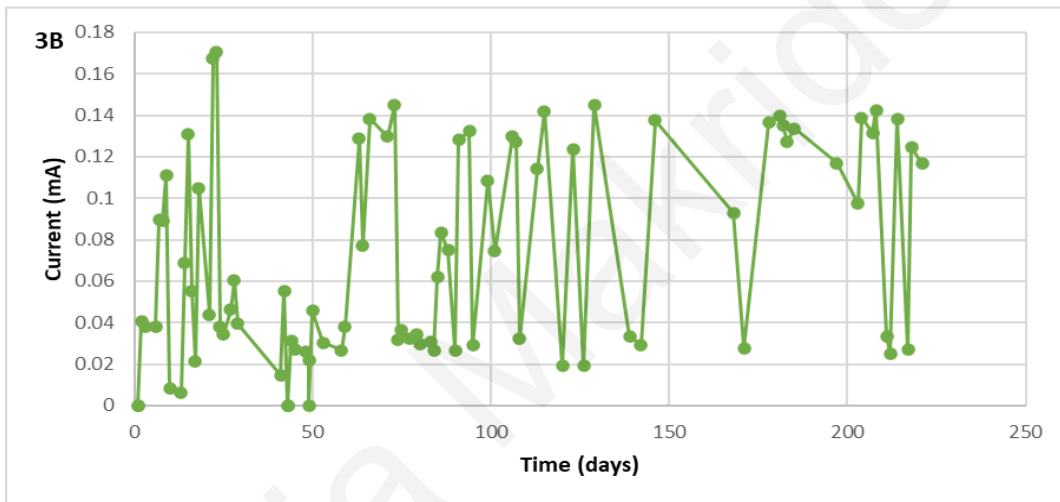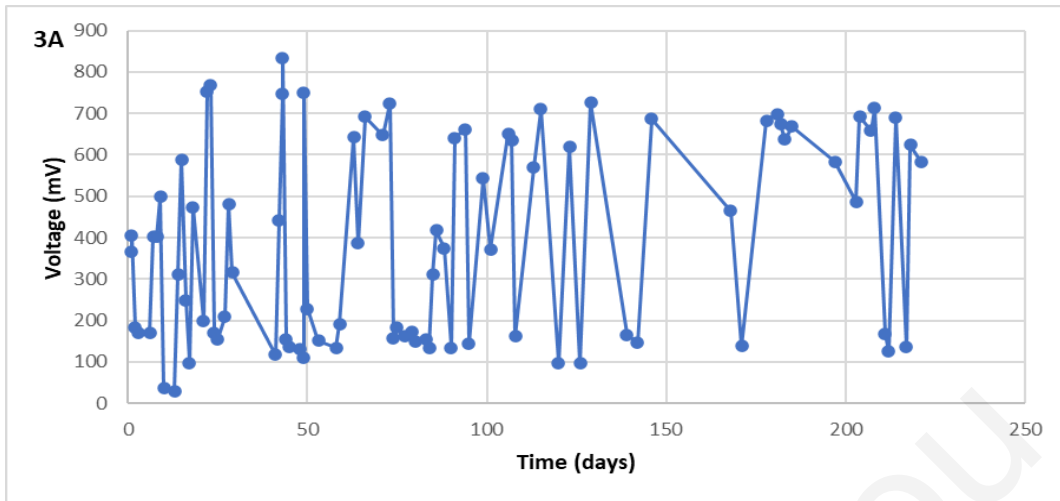
Figure 16. Voltage (mV), current (mA) and power (mW) of the double chambered MFC 3 with AS and WCO.

54

4.4 COD removal of MFCs with AS and WCO

To evaluate the biodegradation potential of each MFC with AS and WCO, the COD removal for each MFC was measured at different time points (80th, 94th, 101st day), right before the weekly feed with WCO (Fig. 18). The highest % COD removal was noted at day 80, reaching 54.82% (MFC 1), 47.71% (MFC2) and 47.94% (MFC3). After 14 days (day 94), the values decreased to 15.83%, 30.73% and 27.29% respectively. The % COD removal measurements a week later (day 101) were 32.11%, 41.06% and 27.75%. Based on these performances, MFC 3 was chosen for further studies. On day 183, another % COD removal measurement for MFC 3 was taken, at 29.17%. A decrease in COD removal performance is observed over time which is constant at lower levels after 183 days of operation.
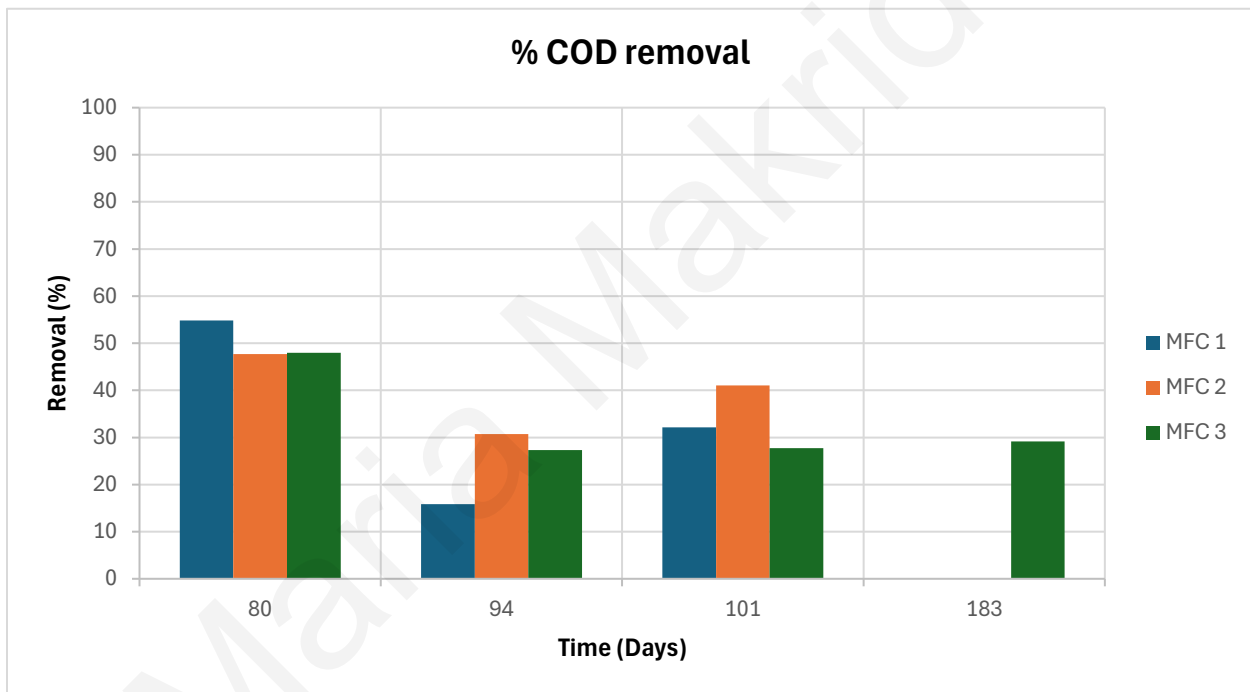
Figure 17.Indicative % COD removal from the three MFCs with AS and WCO.

4.5 Identification and quantification of FAMEs in biosurfactant of MFCs with AS and WCO

In the MFCs which performed with AS and WCO, extracellular production of a white compound was obvious. As it is shown, in Figure 19 there was biofilm and product formation in all MFCs, especially in MFC 3. It is expected that the product formed is a mixture of biosurfactants produced by the mixed microbial community of AS. Biosurfactants are amphiphilic molecules with hydrophobic and hydrophilic portions that reduces the surface (air-water) and interfacial (water-oil) tensions between fluids of different polarities, enhancing the solubility, bioavailability and biodegradation of hydrophobic substrates (M. Lopes et al., 2020). The specific biosurfactant's lipid profile indicates an enhanced degradation of hydrophobic substances, such as hydrocarbons and fats of WCO due to the many fatty acids detected in it.

Fatty acids (FAs) were calculated on the last day of operation and 7 days after the last feed replacement of the anode with WCO. FAs were subjected to methyl-esterification and the obtained FAMEs were analyzed. Therefore, herein a detailed analysis by GC/MS has been performed to identify and quantify the composition of lipids (i.e FAMEs) of the biosurfactant potentially produced in MFCs with AS and WCO. The detailed FAMEs composition is presented in Table 7. In total, 12 FAMEs were detected where half of them were quantified based on the FAMEs calibration curve (Appendix). There was no significant difference in the quantities of FAMEs produced among the three MFCs. Methyl stearate, methyl linoneate, methyl elaidate and methyl palmitate were the major FAMEs observed, respectively.
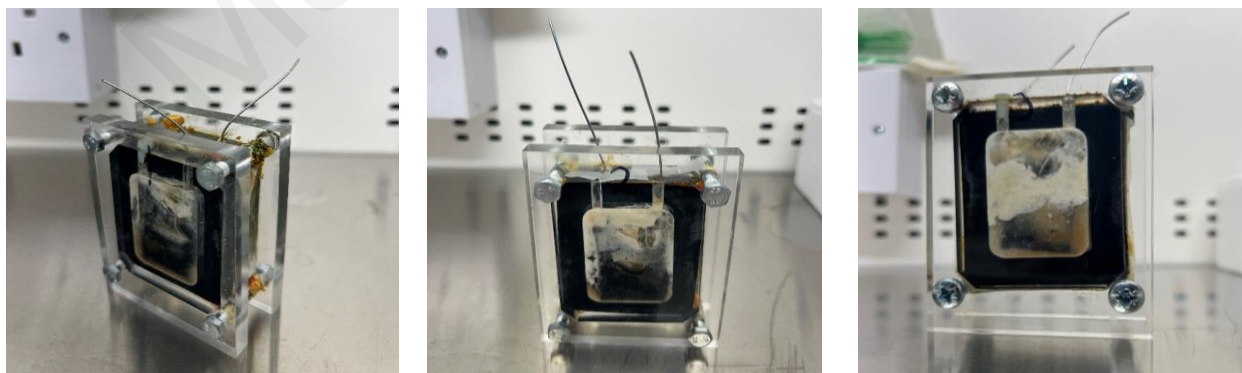
Figure 18. MFCs 1,2,3 with AS and WCO.

Table 7. Qualitative and quantitative analysis of FAMES in biosurfactant of MFCs with AS and WCO

No.	Chemical (Empirical) Name	Molecular Formula	Molecular weight (g/mol)	Retention time (min)	R^2	y_0	a	MFC 1	MFC 2	MFC 3
1	4-Oxo-pentanoic acid methyl ester	$C_6H_{10}O_3$	130.14	6.213				√	√	√
2	Benzoic acid, 3,4-dimethyl-, methyl ester	$C_{10}H_{12}O_2$	164.201	11.6				√	√	√
3	9-Oxononanoic acid methyl ester	$C_{10}H_{18}O_3$	186.248	12.635				√	√	√
4	Tridecanoic acid, 12-methyl-, methyl ester	$C_{15}H_{30}O_2$	242.397	16.051				√	√	√
5	9-Hexadecenoic acid, methyl ester – Methyl palmitoleate	$C_{17}H_{32}O_2$	268.43	18.482	0.9996	-11918.6	1195.029	282.19	316.30	588.05
6	Hexadecanoic acid, methyl ester – Methyl palmitate	$C_{17}H_{34}O_2$	270.45	18.729	0.9997	-10505.5	3400.087	1476.54	1561.82	1549.50
7	Hexadecanoic acid, 10-hydroxy-, methyl ester	$C_{17}H_{34}O_3$	286.4	26.333				√	√	√
8	9,12-Octadecadienoic acid (Z,Z), methyl ester – Methyl linoneate	$C_{19}H_{34}O_2$	294.47	21.652	0.9995	-8389.24	985.7395	3896.01	6398.48	6566.36
9	9-Octadecenoic acid (E), methyl ester – Methyl elaidate	$C_{19}H_{36}O_2$	296.49	21.767	0.9987	-9173.93	1100.179	2112.85	4133.87	4952.88
10	9-Octadecenoic acid (Z), methyl ester – Methyl oleate	$C_{19}H_{36}O_2$	296.49	21.915	0.9999	-14946	3094.297	111.30	254.80	344.15
11	Octadecanoic acid, methyl ester – Methyl stearate	$C_{19}H_{38}O_2$	298.5	22.244	0.9963	-2720.08	668.06	9699.34	10100.29	10502.37
12	Octadecanoic acid, 10-oxo-, methyl ester	$C_{19}H_{36}O_3$	312.5	25.939				√	√	√
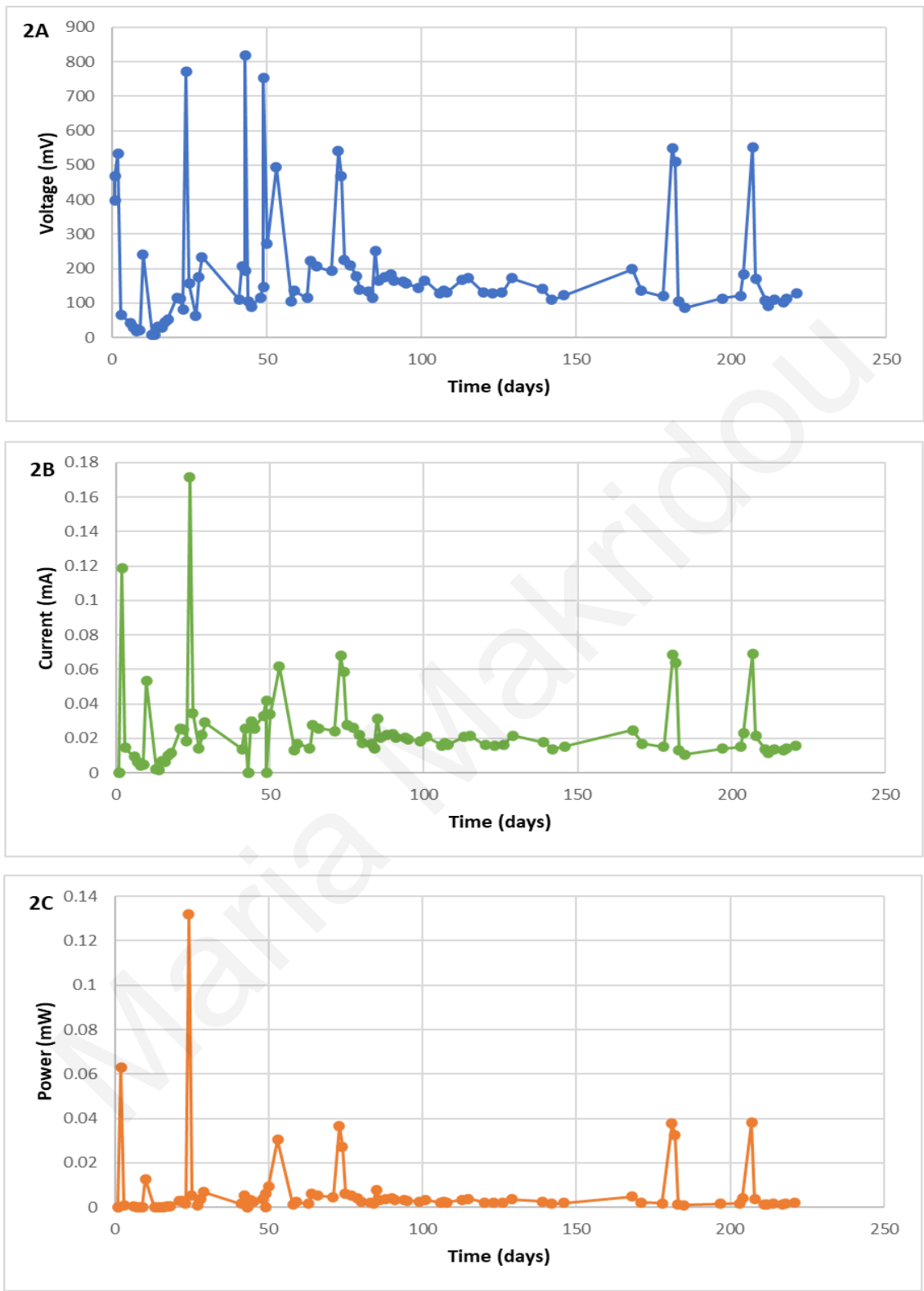
Figure 19. Voltage (mV), current (mA) and power (mW) of the double chambered
MFC 2 with AS and WCO.

58

5. Performance of the MFCs with mixed cultures and WCO

This MFC experimental set up was based on addition of mixed cultures as inoculum and WCO as fuel. The experiment lasted 97 days. Three MFCs were set up with identical experimental conditions. The results of each MFC performance based on voltage (mV), current (mA) and power (mW) production are presented below. Unlike the other triplet, polarization studies were not conducted for this one. The initial resistance was 4.5 kΩ for the three MFCs. The resistance value was decreased gradually to 4 kΩ on the 68th day and then to 3 kΩ on the 84th day.

5.1 Energy generation of MFC 1 set up with mixed cultures and WCO

Data over the full 97-day duration of the experiment are shown in Figure 20. Electricity generation was relatively high and steady throughout the whole period for MFC 1. Following the first resistance change carried out on day 68, where the resistance was decreased from 4.5 kΩ to 4 kΩ, an increase in output voltage data was observed. The next change was carried out on 84th day where the resistance was set to 3 kΩ resulting in a decrease in output voltage, The highest CCV was observed at 607 mV on day 51 (R= 4.5 kΩ) (Fig.20-1A). Current reached 0.141 mA on day 82 when resistance was 4 kΩ (Fig.20-1B). Power reached 0.08 mW on day 51 when resistance was 4.5 kΩ (Fig.20-1C).
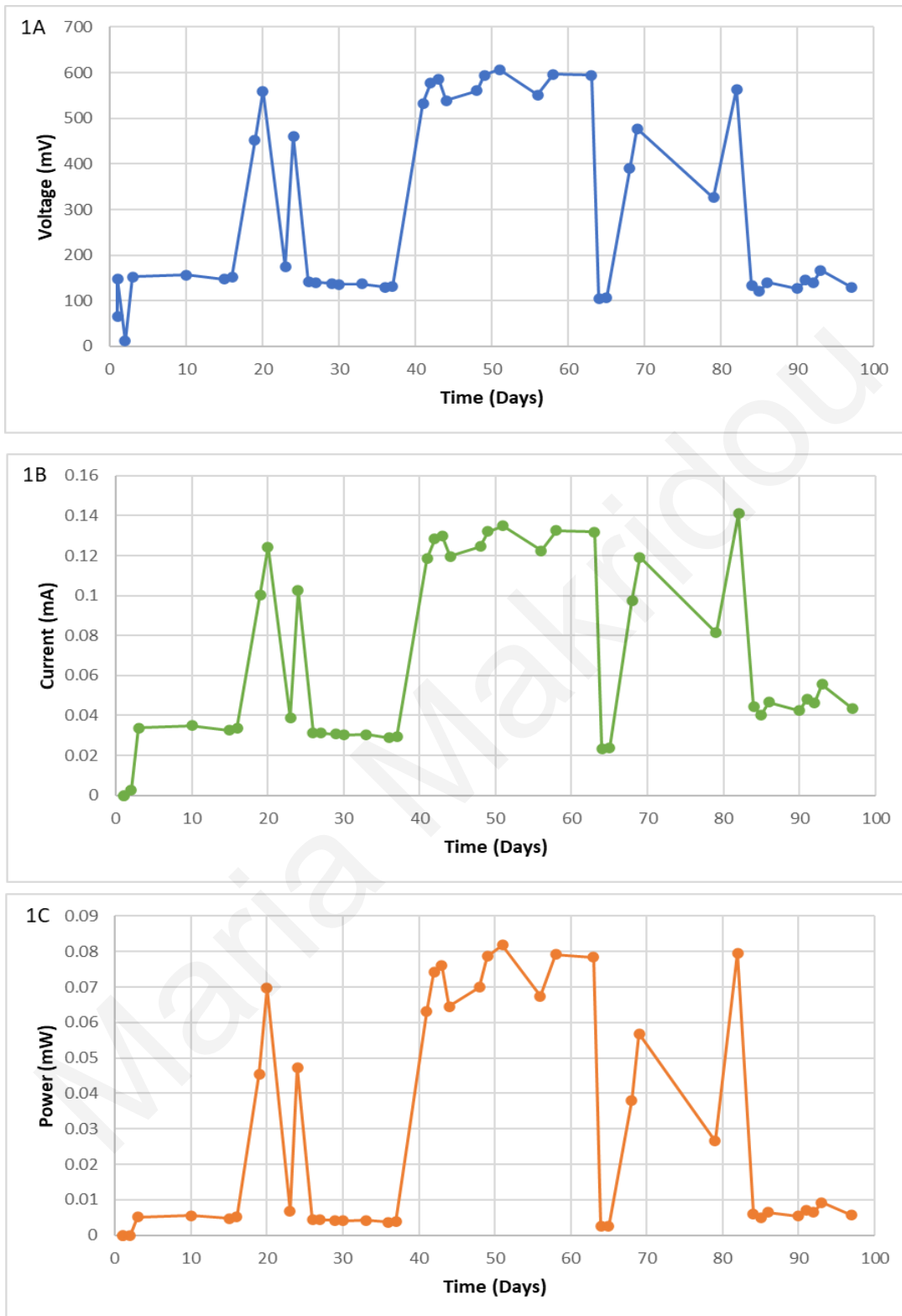
Figure 20. Voltage (mV), current (mA) and power (mW) of the double chambered MFC 1 with mixed cultures and WCO.

5.2 Energy generation of MFC 2 set up with mixed cultures and WCO

On the other hand, MFC 2 performed worse than the other two in terms of electricity production. Electricity generation was observed from the beginning of the experiment up to the first 37 days, then it was significantly reduced. The resistances changes that followed did not affect the output in any way. The maximum voltage production at closed circuit conditions was noted at day 27 at 608 mV (Fig. 21-2A), when the resistance was at 4.5 kΩ. Current at this point was at 0.135 mA (Fig. 21-2B) and power at 0.08 mW (Fig. 21-2C).
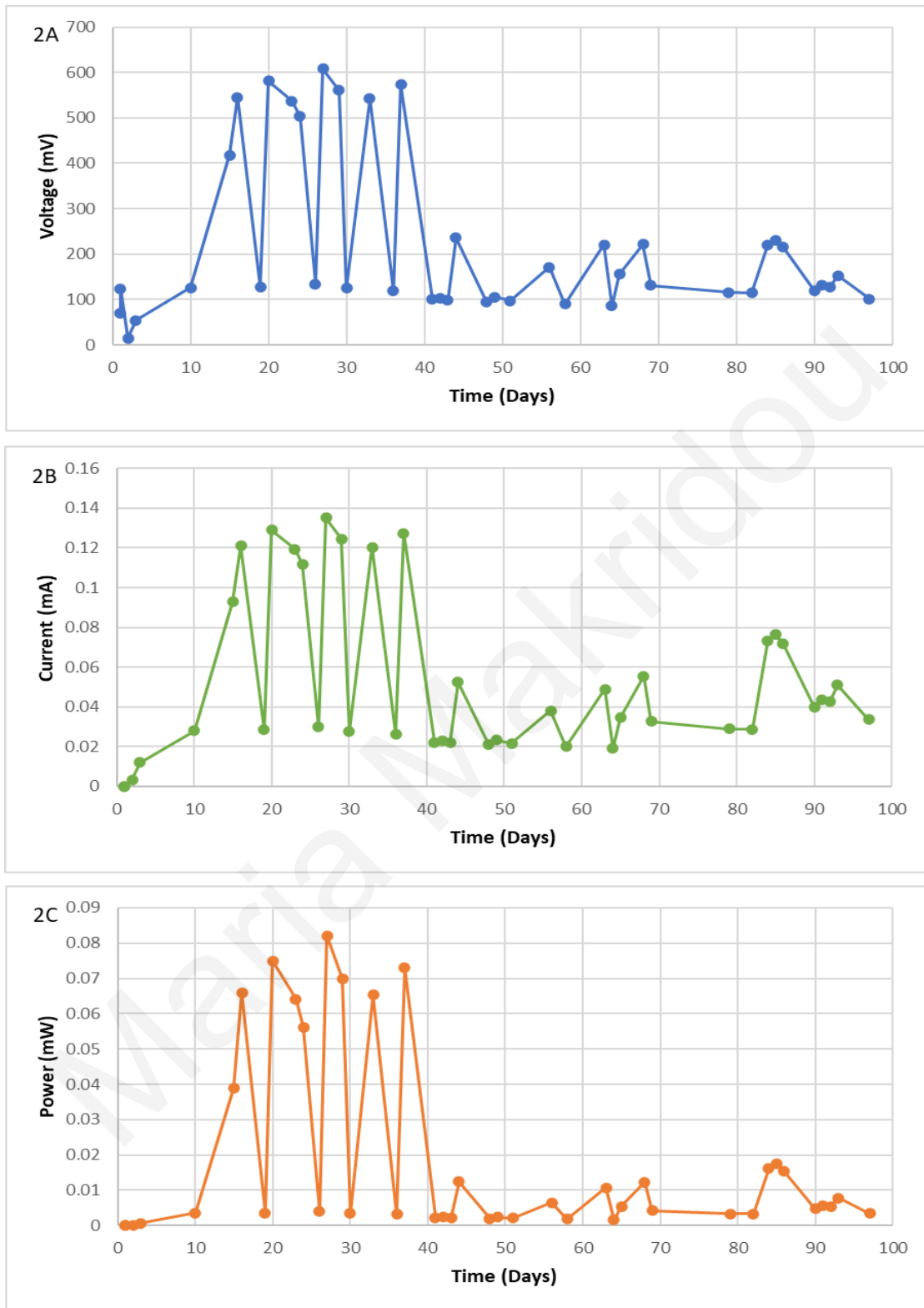
Figure 21. Voltage (mV), current (mA) and power (mW) of the double chambered MFC 2 with mixed cultures and WCO.

5.3 Energy generation of MFC 3 set up with mixed cultures and WCO

At the same time, the same experiment was performed for the third MFC of the triplet. The resistance changes were carried out on the same days. MFC 3 performed very well in terms of electricity production. High and steady amounts of electricity were generated during the whole period that the experiment lasted (Figure 22). In Figure 22-3A, the maximum CCV at day 91 (700 mV), while the resistance was at the lowest (3 kΩ) is shown. Current reached 0.233 mA at this point (Fig.22-3B) and power was measured as high as 0.163 mW (Fig.22-3C).
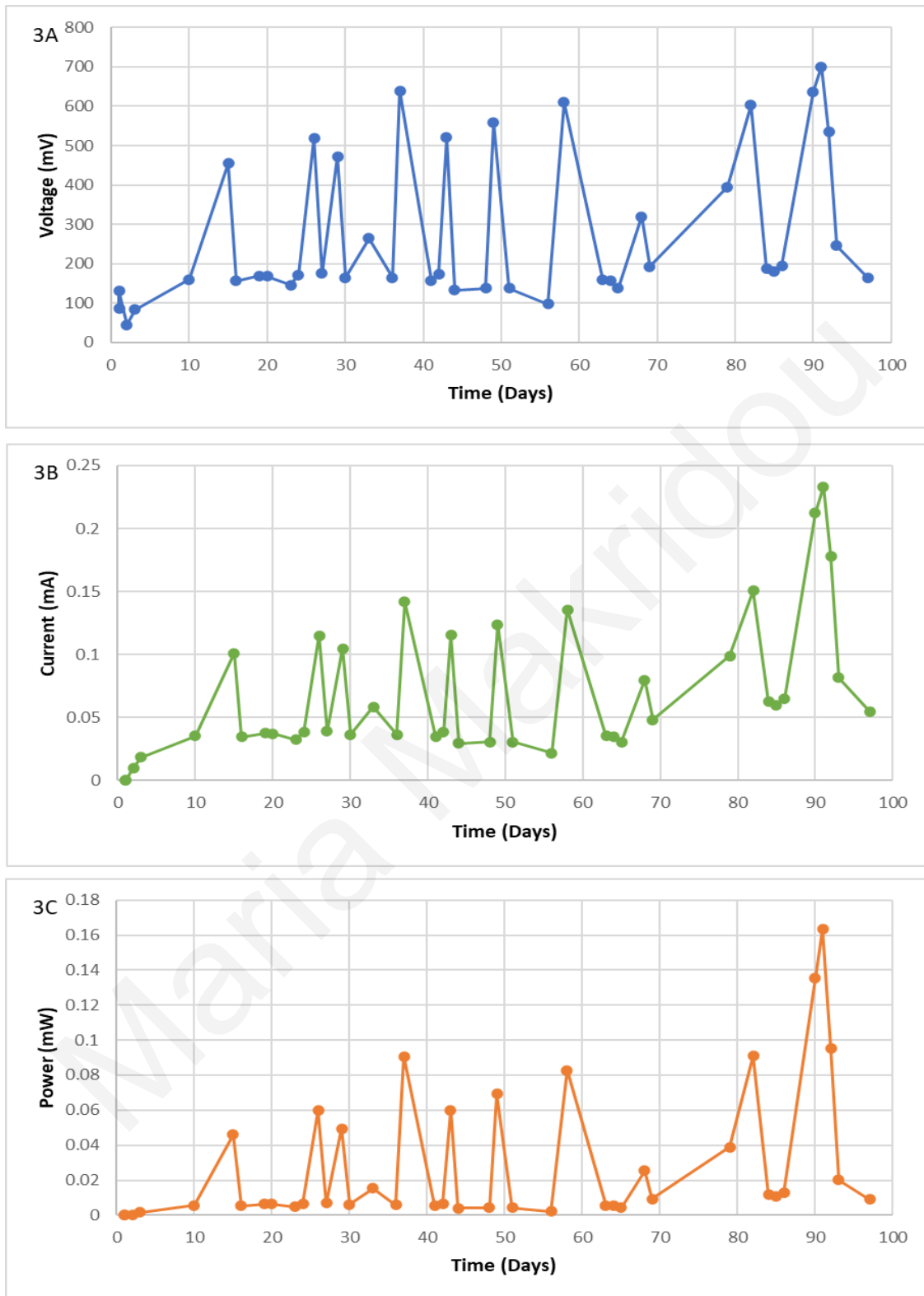
Figure 22. Voltage (mV), current (mA) and power (mW) of the double chambered
MFC 3 with mixed cultures and WCO.

5.4 Intracellular production/accumulation of FAMEs and PHAs in MFCs with mixed cultures and WCO

5.4.1 Intracellular production/accumulation of FAMEs in MFCs with mixed cultures and WCO

Fatty acids (FAs) were calculated on the 97th day of operation and 7 days after the last feed replacement of the anode with WCO. FAs accumulation ranging from C_5-C_{25} as shown in Table 8. Twenty-two FAs were detected in all MFCs at similar concentrations. Based on the quantitative analysis, the major intracellular FAs of the mixed cultures in the MFCs are methyl linoneate (12), methyl elaidate (13), methyl stearate (14), methyl palmitate (10) and methyl behenate (20). Even though the FAs mentioned above were detected in all MFCs, in MFC2 and MFC 3 most of them were found in relatively higher quantities.

Table 8. Qualitative and quantitative analysis FAMEs in MFCs with mixed cultures and WCO (intracellularly)

No.	Chemical (Empirical) Name	Molecular Formula	Molecular weight (g/mol)	Retention time (min)	MFC 1 Concentration (ppm)	MFC 2 Concentration (ppm)	MFC 3 Concentration (ppm)
	FAMEs in MFCs with mixed cultures and WCO (intracellularly)						
1	Butanoic acid, methyl ester – Methyl butyrate	$C_5H_{10}O_2$	102.13	2.913	912.72	389.42	607.33
2	Hexanoic acid, methyl ester – Methyl hexanoate	$C_7H_{14}O_2$	130.18	5.34	36.01	30.68	50.77
3	Trans-2-Octenoic acid, methyl ester	$C_9H_{16}O_2$	156.22	9.007	√	√	√
4	Octanoic acid, methyl ester – Methyl octanoate	$C_9H_{18}O_2$	158.24	8.317	68.55	52.47	47.08
5	2-Nonenoic acid, methyl ester (E)	$C_{10}H_{18}O_2$	170.25	14.343	√	√	√
6	Dodecanoic acid, methyl ester – Methyl dodecanoate	$C_{13}H_{26}O_2$	214.34	13.768	514.62	336.86	581.94
7	Tetradecanoic acid, methyl ester – Methyl tetradecanoate (myristate)	$C_{15}H_{30}O_2$	242.4	16.065	259.00	165.52	186.40
8	9-Methyltetradecanoic acid, methyl ester	$C_{16}H_{32}O_2$	256.42	16.933	√	√	√
9	13-Methyltetradecanoic acid, methyl ester	$C_{16}H_{32}O_2$	256.42	16.828	√	√	√
10	Hexadecanoic acid, methyl ester – Methyl palmitate	$C_{17}H_{34}O_2$	270.45	18.848	1947.00	1598.17	1428.38
11	Hexadecanoic acid 14-methyl-methyl ester	$C_{18}H_{36}O_2$	284.47	20.438	√	√	√
12	9,12-Octadecadienoic acid (Z,Z), methyl ester – Methyl linoneate	$C_{19}H_{34}O_2$	294.47	22.122	9152.81	8288.34	7556.25
13	9-Octadecenoic acid (E), methyl ester – Methyl elaidate	$C_{19}H_{36}O_2$	296.49	22.41	1553.92	7325.50	6283.80
14	Octadecanoic acid, methyl ester – Methyl stearate	$C_{19}H_{38}O_2$	298.5	22.593	337.13	6492.05	6745.84
15	9,12-Octadecadienoic acid (E,E), methyl ester – Methyl linolelaidate	$C_{19}H_{34}O_2$	294.47	23.598	191.66	514.48	407.93
16	Cis-13-Octadecenoic acid, methyl ester	$C_{19}H_{36}O_2$	296.48	22.347	√	√	√
17	Octadecanoic acid, 10-oxo-, methyl ester	$C_{19}H_{36}O_3$	312.5	26.224	√	√	√
18	Eicosanoic acid, methyl ester - Methyl arachidate	$C_{21}H_{42}O_2$	326.56	26.491	43.83	91.05	484.70
19	Heneicosanoic acid, methyl ester – Methyl heneicosanoate	$C_{22}H_{44}O_2$	340.58	28.745	83.86	76.14	94.60
20	Docosanoic acid, methyl ester – Methyl behenate	$C_{23}H_{46}O_2$	354.61	31.869	352.61	1241.41	1388.11
21	Tricosanoic acid, methyl ester – Methyl tricosanoate	$C_{24}H_{48}O_2$	368.64	35.651	200.91	230.74	234.87
22	Tetracosanoid acid, methyl ester – Methyl tetracosanoate	$C_{25}H_{50}O_2$	382.66	40.872	811.58	926.73	958.06

5.4.2 Intracellular production/accumulation of PHAs in MFCs with mixed cultures and WCO

A detailed analysis has been performed to identify the composition of PHAs in the MFCs with mixed cultures and WCO. In total, 6 medium chain length (mcl) PHAs were observed. The accumulation of the PHAs is shown in Table 9. Even though detailed quantitative analysis was not performed due to the lack of the appropriate calibration curve, a quantitative analysis based on the measurements of the GC area of the PHAs was done. The relative quantities of the PHAs in MFC 1 are presented in Figure 23. It is noticed that in MFC 1 the major PHAs were methyl 3-hydroxydodecanoate (3HDD), methyl 3-hydroxytetradecanoate (3HTD) and methyl 3-hydroxyundecanoate (3HUD), in this order. These specific PHAs were the most abundant in all MFCs with mixed cultures and WCO. However, methyl 3-hydroxyundecanoate (3HUD) was the major PHA produced in MFC 2 with an important difference (Fig. 24). Lastly, in MFC 3 the PHA which was produced in greater quantity was 3-hydroxydodecanoate (3HDD) and then methyl 3-hydroxyundecanoate (3HUD) (Fig. 25).

Table 9. Qualitative and quantitative analysis PHAs in MFCs with mixed cultures and WCO

No.	Chemical (Empirical) Name	Molecular Formula	HA methyl ester	Molecular weight (g/mol)	Retention time (min)	MFC 1	MFC 2	MFC 3
1	Methyl 3-hydroxypentanoate	$C_6H_{12}O_3$	3HP	132.1577	5.806	√	√	√
2	Methyl 3-hydroxyoctanoate	$C_9H_{18}O_3$	3HO	174.2374	7.26	√	√	√
3	Methyl 3-hydroxyundecanoate	$C_{12}H_{24}O_3$	3HUD	216.3	10.273	√	√	√
4	Methyl 3-hydroxydodecanoate	$C_{13}H_{26}O_3$	3HDD	230.34	13.015	√	√	√
5	Methyl 3-hydroxytetradecanoate	$C_{15}H_{30}O_3$	3HTD	258.4	15.453	√	√	√
6	Methyl 3-hydroxyoctadecanoate	$C_{19}H_{38}O_3$	3HOD	314.5	17.985	√	√	√
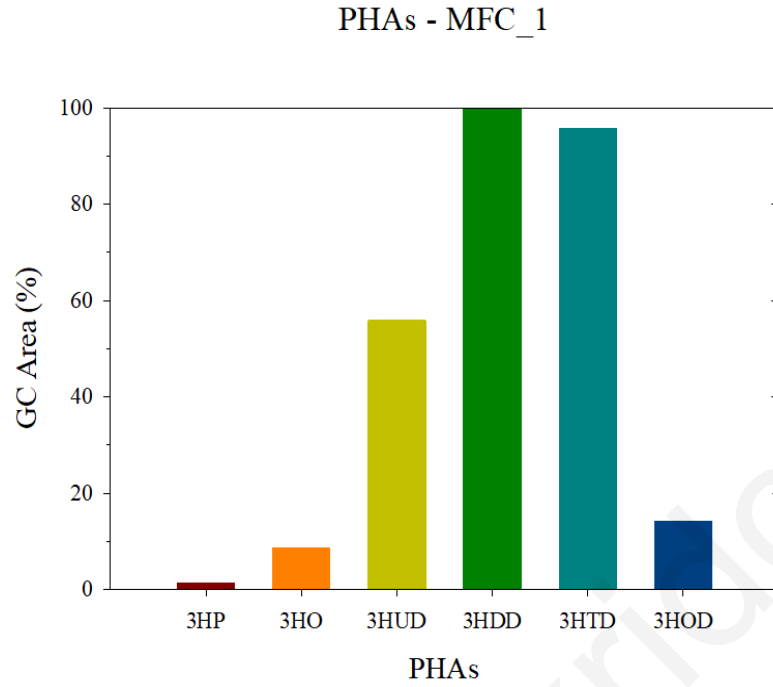
PHAs - MFC_1

Figure 23. Quantitative results of the PHAs in the MFC 1 with mixed culture and WCO
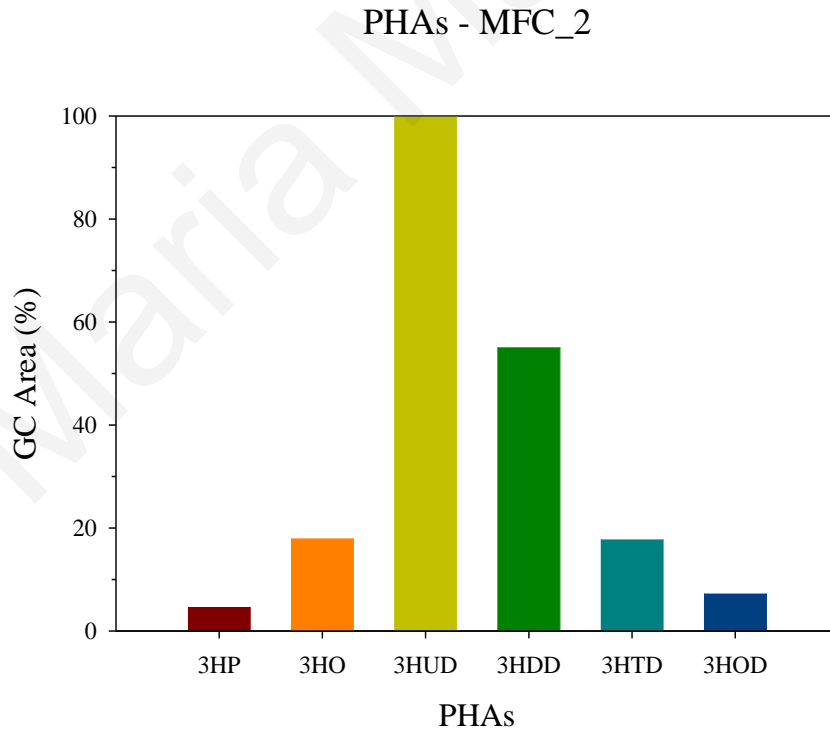
PHAs - MFC_2

Figure 24. Quantitative results of the PHAs in the MFC 2 with mixed culture and WCO

PHAs - MFC_3
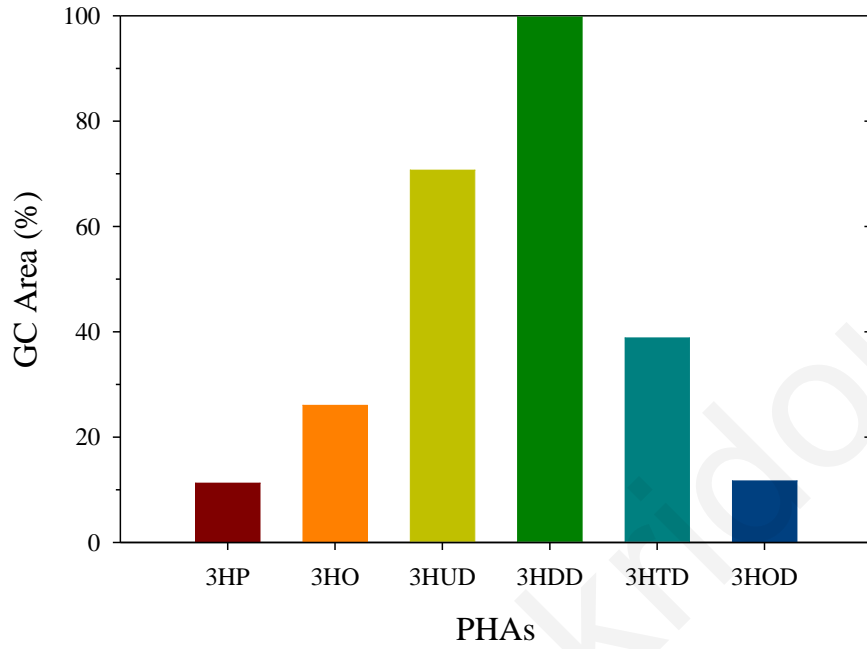
Figure 25. Quantitative results of the PHAs in the MFC 3 with mixed culture and WCO

5.5 Biodegradation of WCO in MFCs with mixed cultures and WCO

5.5.1 COD removal of MFCs with mixed cultures and WCO

The COD removal for each MFC with mixed cultures and WCO was measured at the last day (97th day), right before the weekly feed with WCO, in order to evaluate their biodegradation potential as well. The results for the % COD removal analysis are shown in Figure 26.
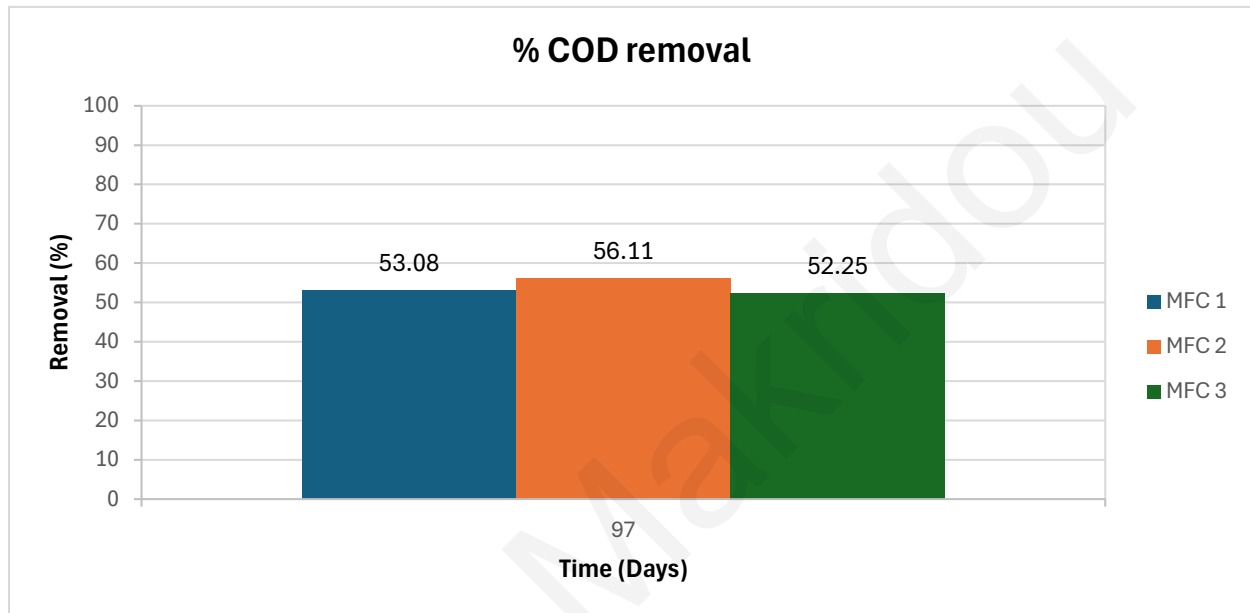
Figure 26. Indicative %COD removal from the three MFCs with mixed cultures and WCO

5.5.2 Total petroleum hydrocarbons (TPHs) and polycyclic aromatic hydrocarbons (PAHs)

TPHs were calculated on the 97th day of operation and 7 days after the last feed replacement of the anode with OW. GC coupled with MS was used to identify the TPHs contained in WCO. The analysis revealed that WCO consisted mainly of alkanes C_9 to C_{28}, with intermediate branched chain hydrocarbons, and other petroleum-based compounds, cyclic and aromatic. A set of 29 TPHs listed in Table 10.

The mixed cultures used appears to have degraded TPHs, under MFC operating conditions. Several TPHs were almost undetected by GC/MS. Table 9 presents the quantification results of GC/MS analysis, as well as the removal rate (%) of the TPHs in the MFCs. The mean hydrocarbons removal rate was 75.4%, with some of them, especially the n-alkanes, reaching removal rates > 60%. Both aromatic and aliphatic hydrocarbons were biodegraded.

PAHs were also calculated on the 97th day of operation and 7 days after the last feed replacement of the anode with WCO. GC/MS analysis did not detect PAHs in WCO and neither in the samples of MFCs anolytes.

Table 10. Quantification results of total petroleum and polycyclic aromatic hydrocarbons contained in the WCO of the MFCs

No.	Chemical (Empirical) Name	Molecular Formula	Molecular weight (g/mol)	Retention time (min)	Area				Removal rate (%)		
					WCO	MFC 1	MFC 2	MFC 3	MFC 1	MFC 2	MFC 3
1	5,6-dimethyl-Decane	$C_{12}H_{26}$	170.334	3.591	6036	1989	1021	1465	67.0	83.1	83.1
2	2,4-dimethyl heptane	C_9H_{20}	128.255	3.676	64749	2071	2066	2095	96.8	96.8	96.8
3	4-methyl octane	C_9H_{20}	128.255	4.241	12801	1918	1898	1920	85.0	85.2	85.2
4	(Z)-6-Methyl-2-undecene	$C_{12}H_{24}$	168.32	6.171	1299	0	158	317	100.0	87.8	87.8
5	3,5-dimethyl-octane	$C_{10}H_{22}$	142.281	6.433	5816	1927	1900	1928	66.9	67.3	67.3
6	Decane	$C_{10}H_{22}$	142.28	6.5	13000	251	724	1240	98.1	94.4	94.4
7	4-Methyltetradecane	$C_{15}H_{32}$	212.414	6.424	8122	1927	1900	1928	76.3	76.6	76.6
8	4-Methyl-5-propylnonane	$C_{13}H_{28}$	184.361	6.618	8430	4770	5890	8305	43.4	30.1	30.1
9	4-methyl-decane	$C_{11}H_{24}$	156.308	6.627	14822	1938	1922	1955	86.9	87.0	87.0
10	3,6-Dimethyldecane	$C_{12}H_{26}$	170.334	7.183	55368	1915	1888	1915	96.5	96.6	96.6
11	2,6,10-Trimethyltetradecane	$C_{17}H_{36}$	240.47	7.175	64583	0	0	162	100.0	100.0	100.0
12	2,6,10-Trimethyldodecane	$C_{15}H_{32}$	212.414	7.259	10942	1929	1902	1937	82.4	82.6	82.6
13	Tritetracontane	$C_{43}H_{88}$	605.158	7.942	19680	0	0	544	100.0	100.0	100.0
14	2,6,10-trimethyltridecane	$C_{16}H_{34}$	226.441	9.181	3271	1914	1890	1908	41.5	42.2	42.2
15	3-Methyldecane	$C_{11}H_{24}$	156.308	9.443	1967	1909	1878	1901	2.9	4.5	4.5
16	3,7-Dimethylundecane	$C_{13}H_{28}$	184.361	10.126	4742	463	382	776	90.2	91.9	91.9
17	11-(1-Ethylpropyl) heneicosane	$C_{26}H_{54}$	366.707	10.143	4620	702	563	1140	84.8	87.8	87.8
18	4-Ethyloctane	$C_{10}H_{22}$	142.281	10.353	7057	1916	1891	1906	72.8	73.2	73.2
19	1,4-Di-tert-butylbenzene	$C_{14}H_{22}$	190.324	11.45	129000	2814	2341	2909	97.8	98.2	98.2
20	2,7-Dimethylundecane	$C_{13}H_{28}$	184.361	11.643	10589	1969	1911	1943	81.4	82.0	82.0
21	Hexadecane	$C_{16}H_{34}$	226.441	13.431	17965	1923	1874	1908	89.3	89.6	89.6
22	Pentacosane	$C_{25}H_{52}$	352.68	18.937	5283	1931	1889	1929	63.4	64.2	64.2
23	2,3-Dimethylundecane	$C_{13}H_{28}$	184.361	20.547	7813	1998	1980	1988	74.4	74.7	74.7
24	Pentadecane	$C_{15}H_{32}$	212.414	23.827	3519	1902	1884	1875	46.0	46.5	46.5
25	7-Hexyleicosane	$C_{26}H_{54}$	366.707	25.581	2505	1993	1984	1961	20.4	20.8	20.8
26	Tetracosane	$C_{24}H_{50}$	338.653	26.407	21813	1984	1973	1964	90.9	91.0	91.0
27	Octacosane	$C_{28}H_{58}$	394.76	27.874	7190	1962	1938	1937	72.7	73.0	73.0
28	9-octyl-heptadecane	$C_{25}H_{52}$	352.68	33.481	12751	1986	1974	2000	84.4	84.5	84.5
29	2,6,10,15-tetramethyl-heptadecane	$C_{21}H_{44}$	296.574	34.847	7825	1970	1953	1974	74.8	75.0	75.0

5.5.3 Fatty acids methyl esters (FAMEs) degradation

Fatty acids (FAs) were calculated on the 97th day of operation and 7 days after the last feed replacement of the anode with WCO. FAs were subjected to methyl-esterification and the obtained FAMEs were analyzed by GC/MS.

In total, 7 FAMEs were detected in WCO. These are the methyl myristate (1), methyl palmitate (2), methyl linoleate (3), methyl elaidate (4), methyl stearate (5), methyl arachidate (6) and methyl behenate (7). Quantitative analysis revealed that the major FAMEs in WCO are linoleic, stearic, elaidic and palmitic, whereas methyl myristate, methyl arachidate and methyl behenate were identified in significantly lower concentrations (Table 11).

Mixed cultures in MFCs appear to have effectively diminished the unsaturated FAs of methyl elaidate and methyl linoleate, as well as methyl behenate. However, the concentrations of saturated ones to MFCs anolyte samples were significantly higher (Table 11). This outcome may be explained by the gradual growth of intra- and extracellular metabolites, such as polyhydroxyalkanoates (PHAs) and biosurfactants, in the anodic compartment.

Table 11. Quantification results of fatty acids methyl esters (FAMEs) contained in the WCO of the MFCs

No.	Chemical (Empirical) Name	Molecular Formula	Molecular weight (g/mol)	Retention time (min)	R^2	y_0	a	Concentration (ppm)			
								WCO	MFC 1	MFC 2	MFC 3
1	Tetradecanoic acid, methyl ester – Methyl tetradecanoate (myristate)	$C_{15}H_{30}O_2$	242.4	16.051	0.9975	1567.031	3169.238	14.6	16.3	200.4	87.6
2	Hexadecanoic acid, methyl ester – Methyl palmitate	$C_{17}H_{34}O_2$	270.45	18.729	0.9997	-10505.5	3400.087	564.4	422.7	1441.2	1391.2
3	9,12-Octadecadienoic acid (Z,Z), methyl ester – Methyl linoneate	$C_{19}H_{34}O_2$	294.47	22.122	0.9995	-8389.24	985.7395	4496.3	-	-	-
4	9-Octadecenoic acid (E), methyl ester – Methyl elaidate	$C_{19}H_{36}O_2$	296.49	22.41	0.9987	-9173.93	1100.179	2465.3	-	-	-
5	Octadecanoic acid, methyl ester – Methyl stearate	$C_{19}H_{38}O_2$	298.5	22.227	0.9963	-2720.08	668.06	2952.0	2606.6	7320.9	8008.0
6	Eicosanoic acid, methyl ester - Methyl arachidate	$C_{21}H_{42}O_2$	326.56	26.366	0.9998	-8976.24	1663.944	26.9	25.1	2118.1	87.2
7	Docosanoic acid, methyl ester – Methyl behenate	$C_{23}H_{46}O_2$	354.61	31.869	0.9999	-7155.25	880.5128	40.8	-	-	-

Emulsification Index (E24)
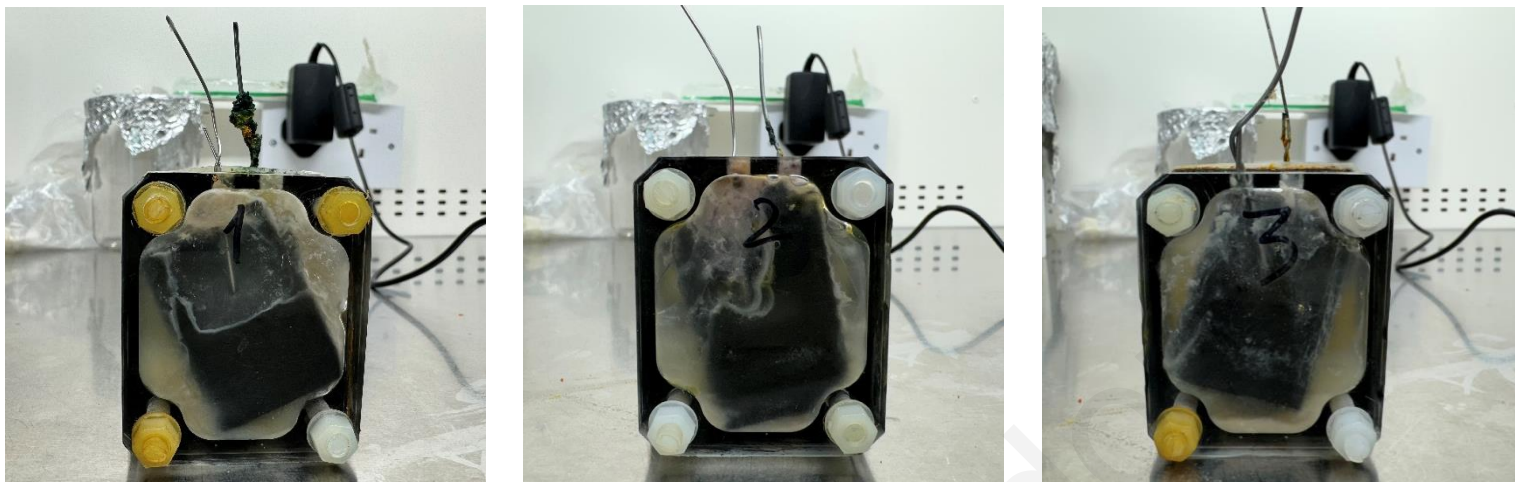
Figure 27. MFCs 1,2,3 with mixed cultures and WCO

An indication of the increased bioavailability is the emulsification index (E24) (Tsipa et al., 2021). The E24 using one solution of anode of the MFC 3 (MFCs with mixed cultures and WCO). The E24 results did not show high emulsification (13.33 %). This indicates that the organic molecules formed could be a low molecular weight molecule. In Figure 27, the observed biofilm of the MFCs is presented.

6. Comparison of the two different MFC set ups in terms of electricity generation: Mixed cultures vs activated sludge

From the MFC experimental set up that was based on addition of AS as inoculum and WCO as fuel, the best MFC performance, in terms of CCV and electricity generation was noted in MFC 3. That's because during the whole time that the experiment lasted, high and steady amounts of power and current were generated. Furthermore, the higher power production of the MFC 3 can perhaps be attributed to healthy biofilm formation over time on the anode electrode, as it was observed. Simultaneously, MFC 1 & MFC 3 from the MFC set up that was based on addition of mixed culture as inoculum and WCO as fuel performed very well. Even though electricity generation was relatively high and steady throughout the whole period for MFC 1, MFC 3 performed better especially during the last days of the experiment. Comparing all the MFCs, the maximum power generation was noticed in MFC 3 with mixed culture and WCO. In more detail, power was measured as high as 0.163 mW at the 91st day and current reached 0.233 mA at this point (Fig.15). Not comparable values were observed at the others MFCs performances. Even when this is

compared to MFC 3 with AS and WCO, that exhibited excellent performance in terms of electricity generation, but the maximum current was at 0.145 mA and power was measured at 0.105 mW which is lower when compared to MFC 3 with mixed culture and WCO.

Discussion

1. Microbial lipid production from Gram-positive bacteria

Numerous researchers have suggested different types of bacteria to convert waste cooking oil (WCO) into products with added value. Although bacterial cells can directly metabolize sugars, when WCO is the carbon source, an enzymatic hydrolysis is required. First, extracellular lipase hydrolyzes triglycerides, releasing glycerol and fatty acids (stearic, palmitic, oleic, and linoleic acids, depending on the WCO supply) into the culture medium. These fatty acids are carried across the membrane of the cell and converted to acetyl CoA by the b-oxidation pathway.

Numerous bacterial species, including *Burkholderia thailandensis*, *Alcaligenes*, and some *Pseudomonas* spp., are employed in the biotechnological conversion of WCO to produce compounds. Moreover, Gram-positive bacteria like *Propionibacterium freudenreichii* and *Bacillus* spp. Since these extracellular products play significant roles in the fatty acids' accessibility to the bacterial cells, biosurfactants and lipases are frequently produced by bacteria that break down oils (M. Lopes et al., 2020). Similarly, here, the gram-positive *Corynebacterium* species were able to produce several fatty acids which may be then used by the microorganism for different purposes.

2. MFCs

The anode's microbes oxidizing the substrate are the only source of electron generation in MFC systems. The anodic inoculations of MFCs employ both pure and mixed cultures. Pure cultures may convert substrates into electricity more effectively because they have distinct metabolic pathways. But it also has more stringent requirements for the purity and concentration of the substrate. As a result, pure cultures' preference for specific substrates may limit their capacity to generate energy using complex substrates like wastewater. Mixed cultures are useful for scaling up MFC systems because they are more tolerant of complex substrates. The synergistic effect of various strains in the mixed culture may lead to more efficient operation of MFC systems. Activated sludge is the most distinctive mixed culture utilized in MFC systems. The heated and acid-treated sludge has the potential to enhance energy output even more. Nevertheless, the microbial composition of activated sludge is very complex. It is difficult to pinpoint the precise substrate conversion process. As a result, the co-culture of chosen strains may increase the effectiveness of MFC systems based on their particular roles (J. Wang et al., 2022). Similarly, in

this thesis, a mixed culture dominated by Corynebacterium species was used for WCO synergistic electro-degradation showing promising results. The high-power production observed in this thesis in some MFCs can perhaps be attributed to healthy biofilm formation over time on the anode electrode.

The MFC technology has demonstrated potential as a combined waste treatment, biomass valuation, and sustainable energy recycling system. The key requirement for greater electricity generation has been satisfied by lab-scale MFC systems. Additionally, they have made significant strides in the fields of biosensor applications, value-added product manufacture, and COD removal. Nevertheless, scaling up and commercializing MFC systems still faces numerous obstacles.

One of the primary issues in this industry remains to be the MFC system's low output power. The metabolic activity of bacteria has a direct impact on the power generation of MFC systems. As a result, strain modification through genetic engineering and the screening of high-performance electrogenic strains are useful techniques for enhancing microbial electrogenicity. Future trends in strain selection for MFC systems may see modified strains gradually replacing wild-type strains as genetic engineering and synthetic biology technologies advance. Microbes require substrates in order for MFC systems to function. As a result, the choice of substrates must take into account how effectively a given strain uses a given substrate. More research is currently being done to assess the capabilities of MFC systems for treating wastewater and producing electricity utilizing synthetic wastewater. Further research on the adaptability of various strains to the complex environment of composition and concentrations in actual wastewater is still required, though.

Presently, one of the primary factors impeding the commercialization of MFC systems is the high cost of electrode materials. In the future, this issue will be resolved by producing high-performance electrode materials from waste and renewable natural feedstocks (J. Wang et al., 2022).

3. Added-value products (BSF/PHAs) in MFCs

Nowadays, because of the variety of strains and metabolic pathways, the application of microbial fuel cells further emphasizes the simultaneous generation of value-added products and electricity. Through the fermentation process utilized by MFCs to generate electricity, microbes can produce

a range of biofuels, volatile fatty acids, biopolymers, and other platform substances (J. Wang et al., 2022).

The synthesis of biosurfactants in BES was documented in 2008, and it was demonstrated that *Brevibacillus* sp. was able to carry out extracellular electron transfer through the interaction of rhamnolipids generated by *Pseudomonas* spp. with phenazines. These substances, when present in bioelectrochemical systems, could significantly improve the performance and efficiency of MFC by enhancing its power output. Biosurfactants can also be employed in microscale systems to address potential problems arising from low power output. Their presence enhances the hydrophilicity of the electrode surface and the bioavailability of hydrophobic substrates, which promotes better biofilm formation. Moreover, biosurfactants promote the enrichment of exoelectrogens in anodic bacterial communities by exerting a noteworthy influence on their diversity. These investigations demonstrate the significance of these amphiphilic substances for bioelectrochemical system starting and operation (Pasternak et al., 2023). Furthermore, some studies have shown that the generation of biosurfactants from frying waste oils was greater than that from pure oils. This is most likely because the waste oil contains more free fatty acids (M. Lopes et al., 2020). In this thesis, biosurfactant production was observed in both MFCs set ups. This suggests that the biosurfactants produced may enhance electron transfer and, thus, electricity generation.

In order biosurfactants to show potential in a number of industrial and environmental applications, they must possess good emulsification properties. The ability of an emulsifier to retain at least 50% of the initial emulsion volume 24 hours after creation is the criterion for assessing its emulsion-stabilizing abilities (E. M. Lopes et al., 2014). In the present thesis, the emulsification index was measured 13.33%. But this was after an operation of 97 days. During time the emulsification properties of biosurfactants may decrease.

Using traditional fermentation equipment, the production of value-added products from a variety of organic wastes has advanced significantly. Nonetheless, the utilization of MFC technology in this domain remains restricted. Microbes are unable to completely oxidize substrates to CO_2 in the anode chamber's anaerobic environment in order to produce electrons. Additionally, substrates may enter the fermentation pathway and produce anaerobic metabolites. Therefore, by combining

fermentation and electrochemical processes, the MFC system can achieve integrated production of value-added products and electricity (J. Wang et al., 2022). PHAs may be synthesized in microbial fuel cells as energy storage source inside microbial cells, allowing for the integration of bioelectricity and PHA synthesis in a MFC. PHAs are biosynthesized in bacteria using specific PHA polymerases using various monomers from the cellular metabolite pool. When, the fuel is depleted, microorganisms can then use PHAs as electron donors to continue the process of electron transfer which was also observed in this thesis. After 7 days with no feed where the WCO's components were significantly removed, PHAs were accumulated while electricity generation remained at high levels. On top, comparing PHAs accumulation at aerobic conditions (after enrichment) and PHAs under MFCs conditions, more PHAs, in terms of variety, were produced showing the capability of the microorganisms to survive and perform under adverse conditions (i.e. no WCO-fuel feed)

4. Actinobacteria

Actinobacteria (phylum Actinomycetota), which are present in every sample following the enrichment process and gradually increase in abundance going from S1 to S6, create a wide variety of bioactive compounds, many of which have the potential to be exploited in the future and are of commercial relevance. This includes the biosurfactants that numerous actinobacterial species produce. Some biosurfactant producers are members of the mycolic acid-containing (mycolate) genera *Rhodococcus, Corynebacterium, Dietzia, Gordonia* and *Tsukamurella* (Fiona M. Stainsby, 2016). The genus *Corynebacterium* is broad and includes some species with significant industrial, medicinal, or veterinary use. While many corynebacterial species are commensals, some are well-known pathogens, such as *Corynebacterium diphtheriae*, which is harmful to humans, and *Corynebacterium pseudotuberculosis*, which is predominantly harmful to sheep but can also infect other animals (Dover et al., 2021). In the present thesis, based on E24, the *Corynobacterium* dominated mixed culture can produce biosurfactants. However, it is worth mentioning that other species of this mixed culture may produce biosurfactants upon WCO biodegradation.

Based on 16S rRNA gene sequence analysis, the actinobacteria containing mycolic acid constitute a phylogenetically cohesive group that belongs to the order Mycobacteriales. In the present thesis, high abundance of Mycobacteriales are observed in S4, S5, S6. With a high guanine-plus-cytosine (G + C) content in their genomic DNA, the members are Gram-positive. As of right now, they are

divided into fifteen genera, including *Corynebacterium*. Together, these genera contain about 400 species. Members of this group produce mycolic acids almost universally, which is a synapomorphic feature exclusive to this evolutionary branch. However, over the course of evolution, certain members of this order—including some species of *Hoyosella* and *Corynebacterium*—appear to have lost the capacity to produce mycolic acids (Fiona M. Stainsby, 2016).

Therefore, Corynebacteria are Gram-positive bacteria that have a complex cell envelope architecture. The peptidoglycan cell wall core is covalently bound to the corynomycolates (short-chain α-branched, β-hydroxy fatty acids) via esterification, forming a mycolyl-arabinogalactan–peptidoglycan complex. These mycolic acids that are attached to cells serve as the foundation for the inner leaflet of a unique outer "mycomembrane," which is completed through intercalation with other free lipids and glycolipids based on trehalose that also include mycolic acid. Therefore, in both *Corynebacterium* and *Mycobacterium* strains, the presence of mycolic acids in the cell membrane is linked to stress resistance and pathogenicity (Dover et al., 2021). Mycolic acids are β-hydroxy FAs of C_{22}-C_{36}. In the present thesis, no such β-hydroxy FAs were observed as seen in Tables 8 & 11. Indicating that the present corynebacterium species in the mixed culture might not be that virulent.

5. PHAs and Corynebacterium

Naturally occurring polymers or macromolecule polyesters, polyhydroxyalkanoates (PHAs) are generated by numerous microorganism species. When there is an excess carbon source and nutrient limitation, PHAs build up as part of the carbon/energy, reducing-power storage granules within bacteria. Both terrestrial and marine settings can cause PHA to breakdown. Extracellular PHA depolymerases, which break down PHA to create oligomers and monomers that are then taken up by the cells, are released by microorganisms. Different PHAs can be stored by a number of bacteria, including both gram-positive and gram-negative species (Nwinyi & Owolabi, 2019).

Because it uses a waste stream as a source of microorganisms and lowers cultivation costs, using waste activated sludge (WAS) as inoculum offers a sustainable method for producing PHA. This is the reason, in this thesis, AS was used as inoculum in the enrichment process. The hydrolysate can be metabolized into PHA by the many bacteria present in the WAS. The microbial diversity,

oxygen condition adaptability, and cost-effectiveness of employing waste activated sludge as an inoculum for PHA production using hydrolysate as a substrate constitute advantages. When compared to pure bacterial strains, waste activated sludge is a more advantageous option due to these features, which also lead to increased productivity and efficiency in PHA generation from complex substrates.

According to Morya et al., 2023, certain microbial species—such as *Corynebacterium*, *Bacillus*, *Pseudomonas* sp., and others—that were more effective at producing PHAs, developed and became dominant due to the selective pressure that was placed on them during a cycle of feast and famine. The microbial community's total diversity dropped as a result. It's interesting to note that the highest PHA production occurred during a famine phase. This implied that, maybe as a result of the prevalence of particular PHA-producing microbial species, the conditions during this cycle were particularly suitable for high PHA generation, similarly to what is observed in the current thesis when MFCs were not fed. It's crucial to remember that a high PHA output doesn't always translate into a high level of microbial diversity because some species' dominance can actually lower overall diversity. For instance, certain microbial species may have been toxically affected by metabolites produced during PHA synthesis.

Catherine et al., 2022 reported that almost 100 % of the bacteria in the activated sludge used in their research, were PHA accumulating organisms. The most dominant phylum in the activated sludge was Beta-proteobacteria (59 %), followed by Bacteroidetes (16 %), Alpha-proteobacteria (4.6 %), Actinobacteria (4.37 %), Chloroflexi (3 %), Delta-proteobacteria (3.05 %), Verrucomicrobia (2.43 %) and 2.17 % of Gamma-proteobacteria. In the present thesis Actinobacteria and Bacteroidota were present in all the samples of mixed cultures following the enrichment thesis which is in agreement with literature. It is well known that the phylum Actinobacteria is extensively dispersed in soil, where it is essential to the breakdown of organic matter and the production of humus (Nwinyi & Owolabi, 2019).

Acetate has been reported by numerous researchers to be the only substrate used while enriching mixed cultures in order to produce PHA. This is the reason why, in the present thesis, acetate was used during the nrichment process. Furthermore, it has been shown by other researchers that lactate, propionate, and acetate can be combined to produce PHA. Combining the substrates

increased the likelihood of obtaining various PHA grades (Nwinyi & Owolabi, 2019). More spesific, it has been noticed that *Corynebacterium* produces PHA from biomass derived from lignocellulose. Additionally, it has been observed to use starch, fructose, and glucose to produce PHA. Some species of *Corynebacterium* exhibit good traits including powerful growth, high accumulation of PHA, and adaptability in using various carbon sources. Thus, utilizing their metabolic potential, *Corynebacterium* genus can provide a useful path for the long-term synthesis of PHAs (Morya et al., 2023).

6. MFCs and Corynebacterium

Microbial fuel cell (MFC) technology has emerged as one of the most significant bioenergy research hotspots in recent years. It is thought to be a viable option with the capacity to sustainably provide energy requirements (J. Wang et al., 2022). By using the biological ability of electrochemically active bacteria to donate electrons to conductive materials, a microbial fuel cell (MFC) is a bio-electrochemical system that provides an alternative power source by directly converting chemical energy in organic matter to electrical energy.

Extracellular Electron Transfer (EET)-capable microbial species are important participants in the global geochemical cycles of elements and possible partners of electronically linked microbial communities. Furthermore, because of their numerous potential biotechnological uses, including microbial fuel cells (MFCs), microbial electrosynthesis, and metal recovery and bioremediation, these bacteria are currently receiving a lot of interest (Pankratova et al., 2019). Electricigens are bacteria that can effectively connect to electrodes. These electricigens naturally transport electrons to an electrode in three ways: (i) through electron shuttles, which are redox-active molecules produced by bacteria; (ii) through short-range direct electron transport between the electrode and cytochromes on the outer membrane; and (iii) through long-range electron transport via conductive biofilms made up of motility apparatus (i.e., pili and filament) and extracellular matrix. Furthermore, the capacity of bacteria to move toward and colonize insoluble electron acceptors (electrodes) determines the efficacy of extracellular electron transfer (Lee et al., 2019).

In nature, electron transfer (ET) reactions are essential activities. EET is caused by the electronic connection of microbial metabolism to an external solid surface, such as minerals or electrodes. Direct ET (DET) and mediated ET (MET) were the primary classifications used in the past for ET

mechanisms that transcend the cell barrier (Fig.28). Without the use of any diffusible redox chemicals, DET can happen when a cell and an electrode come into direct physical contact. Redox
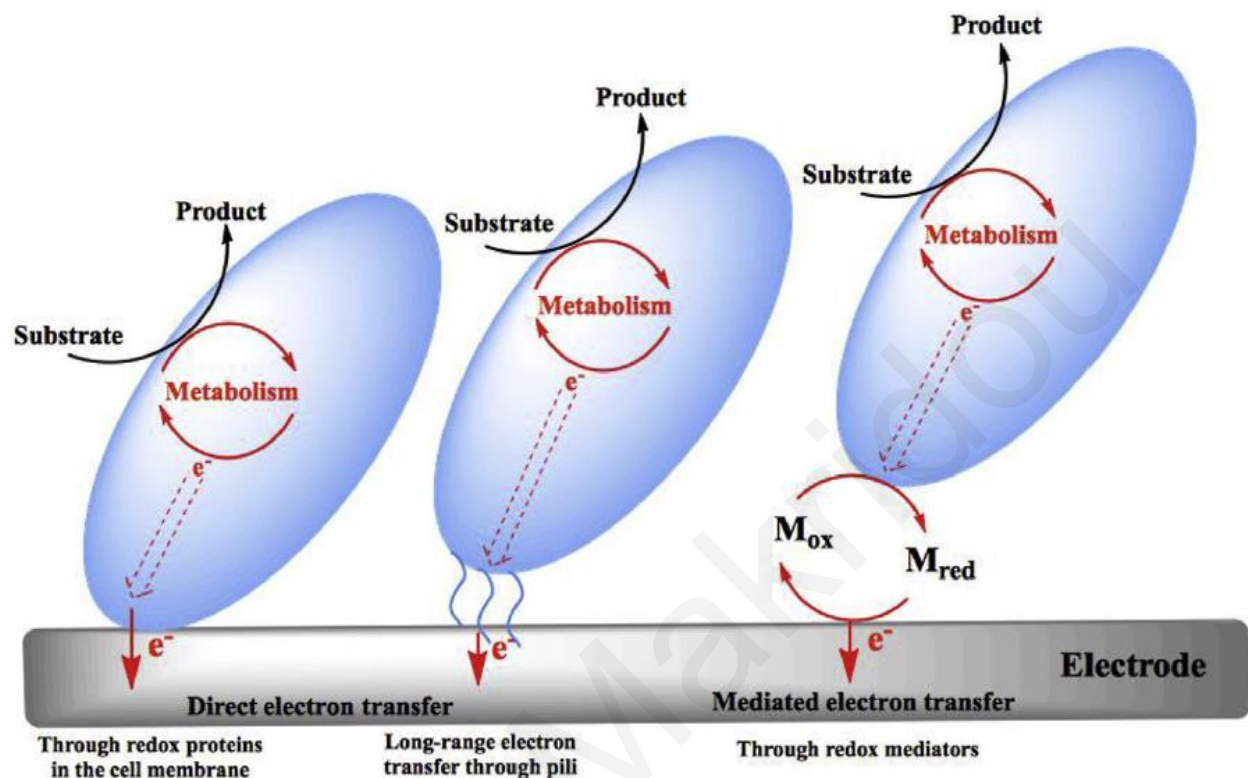
Figure 28. Microscopic Schematic representation of anodic EET mechanisms -direct and mediated electron transfer (Pankratova et al., 2019)

active mediating chemicals facilitate MET by moving electrons from an external donor/acceptor to a microbe. Depending on the type and origin of the mediating redox species—which may be metabolites released by a microorganism or an artificial mediator introduced to the system—MET can be achieved in a variety of ways. Numerous primary and secondary metabolites produced by bacteria have the potential to function as diffusible mediators in EET. Several reduced primary metabolites, such as H_2 and H_2S, are produced by some microbial species. These metabolites can be oxidized at the electrode surface to produce an electron flow. Phenazines produced by *Pseudomonas aeruginosa*, flavins produced by *Shewanella oniedensis*, and quinones produced by *Lactococcus lactis* are a few examples of low molecular weight secondary metabolites that function as redox mediators (Pankratova et al., 2019).

While both Gram-positive and Gram-negative bacteria are capable of producing electricity, Gram-positive bacteria, such as *Corynebacterium*, are far less electroactive due to their thicker, less conductive membrane, whereas favorable electricigens are Gram-negative (Fig.29). Gram-positive bacteria can therefore mediate electron transfer using exogenous mediators, which can be deliberately provided or present in the environment. An instance of Gram-positive electricigen that has been used in the presence of exogenously supplied mediators is Corynebacterium species (Lee et al., 2019). However, Liu et al., 2010 showed that, in alkaline conditions, a pure strain of Gram-positive *Corynebacterium* sp. could generate electricity in MFCs using a variety of substrates without the need for an external mediator. The cyclic voltammograms indicated that the strain itself produced dissolved components that may have contributed to the electron transfer. Therefore, *Corynobacterium* possess electroactive properties.
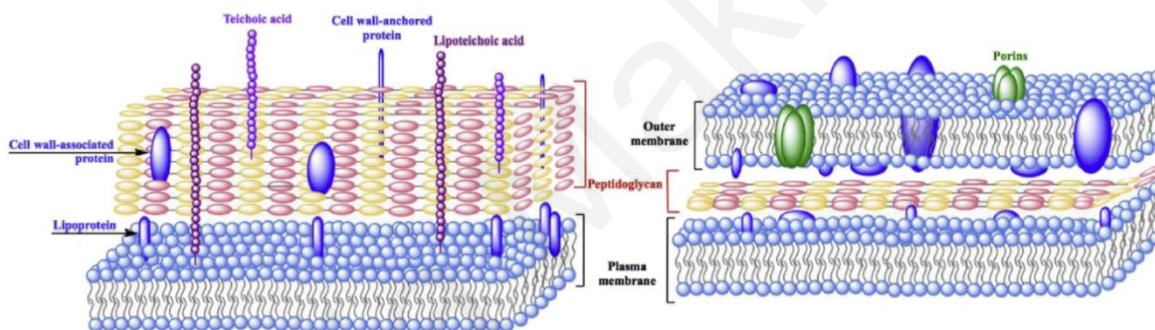
Figure 29. Model of a typical Gram-positive (left) and Gram-negative (right) cell envelope (Pankratova et al., 2019).

Several biotechnological applications using mixed consortia comprising Gram-positive species have reported a synergistic effect, i.e., a long-term power production and enhanced stability. In terms of practical applications, the adoption of mixed microbial communities is a more viable and sustainable method. In order to achieve a logical progression and enhancement of mixed microbial associations, consideration must be given to each member's EET characteristics (Pankratova et al., 2019).

Conclusions and future work

In this thesis, MFCs to remediate WCO were used as an alternative way of bioremediation to accelerate the process. Firstly, enrichment experiments, with activated sludge (AS) as inoculum and acetate, which is known to be favorable for PHAs production, as carbon source was used revealing that as acetate concentration was increased, an increased abundance of microorganisms belonging to the genus Corynebacterium of the family Corynebacteriaceae was present. In particular, the species *Corynebacterium sputi* was found in 8g/L and 10g/L acetate in high concentrations. Gas Chromatography-Mass spectrometry (GC/MS) intracellular analysis revealed that all samples had the same PHAs, at different abundance. In particular, 3-hydroxydecanoate, 3-hydroxydodecanoate and 3-hydroxytetradecanoate. Furthermore, the intracellular production of microbial lipids was observed. Two different MFC set-ups were compared, (1) with AS grown with WCO and (2) with mixed culture (10g/L acetate) grown with WCO. Both set-ups could produce electricity while effectively degrading WCO. In both set-ups, extracellular biosurfactants production was observed which can enhance electricity generation. In MFCs with AS, the specific biosurfactants' lipid profile indicates an enhanced degradation of hydrophobic substances, such as hydrocarbons and fats of WCO due to the many fatty acids detected in it. In the MFCs of mixed cultures and WCO, intracellularly, twenty-two FAs ranging from C_5-C_{25}, were detected in all MFCs at similar concentrations. In addition, in total, 6 medium chain length PHAs were observed which are the double amount compared to 24h-aerobic cultures. Comparing the MFCs found here and under 24h-aerobic conditions, the culture here shows itself to be in survival mode. On average 56% COD removal was observed. Extracellularly, removal of total petroleum hydrocarbons (TPHs) and FAs of WCO was 75.4%, the unsaturated FAs were completely depleted. However, the concentrations of saturated ones were significantly higher. This outcome may be explained by the gradual growth of intra- and extracellular metabolites, such as polyhydroxyalkanoates (PHAs) and biosurfactants, in the anodic compartment. In addition, the Emulsification Index test was performed indicating that this mixed culture possibly produces biosurfactants. Comparing the best MFCs from each condition (AS and mixed cultures), the MFC with AS and WCO reached maximum current at 0.145 mA and power was measured at 0.105 mW, while in the MFC with mixed culture and WCO power was measured as high as 0.163 mW and current reached 0.233 mA. In the latter MFC, it was noticed that when the fuel is depleted, microorganisms can then use PHAs as electron donors to continue the process of electron transfer which was also observed in

this thesis. After 7 days with no feed, where the WCO's components were significantly removed, PHAs were accumulated while electricity generation remained at high levels. Biosurfactants presence could potentially support this process. On top, comparing PHAs accumulation at aerobic conditions and PHAs under MFCs conditions, more PHAs, in terms of variety, were produced showing the capability of the microorganisms to survive and perform under adverse conditions (i.e. no WCO-fuel feed). This is a novel and promising circular-based approach for wastewater treatment with concurrent added-value products and renewable energy generation. These products are non-toxic, biodegradable, biocompatible with exceptional properties. Therefore, they could replace their synthetic counterparts compounds. While renewable energy by microbial activity could be an alternative to fossil-fuel based one.

In future work it is necessary to repeat the analysis of intracellular FAMEs and PHAs upon use of 8g/L during the enrichment process. In addition, the thesis showed that PHAs accumulation positively affects electricity generation under no fuel addition, therefore it is necessary to lower the external resistance of the MFCs in order to understand this effect under higher stress for the cells which is commonly used in the literature.

Bibliography

Behera, S., Priyadarshanee, M., Vandana, & Das, S. (2022). Polyhydroxyalkanoates, the bioplastics of microbial origin: Properties, biochemical synthesis, and their applications. *Chemosphere*, *294*. https://doi.org/10.1016/j.chemosphere.2022.133723

Catherine, M. C., Guwy, A., & Massanet-Nicolau, J. (2022). Effect of acetate concentration, temperature, pH and nutrient concentration on polyhydroxyalkanoates (PHA) production by glycogen accumulating organisms. *Bioresource Technology Reports*, *20*(July), 101226. https://doi.org/10.1016/j.biteb.2022.101226

Chaijak, P., Rakkan, T., Paichaid, N., Thipraksa, J., Michu, P., & Sangkharak, K. (2024). Exploring Potential Aspect of Microbial Fuel Cell (MFC) for Simultaneous Energy, Polyhydroxyalkanoate (PHA) Production and Textile Wastewater (TW) Treatment. *Journal of Polymers and the Environment*, *0123456789*. https://doi.org/10.1007/s10924-023-03141-0

Dover, L. G., Thompson, A. R., Sutcliffe, I. C., & Sangal, V. (2021). *Phylogenomic Reappraisal of Fatty Acid Biosynthesis , Mycolic Acid Biosynthesis and Clinical Relevance Among Members of the Genus Corynebacterium*. *12*(December). https://doi.org/10.3389/fmicb.2021.802532

Fiona M. Stainsby, J. H. and H. V. (2016). Biosurfactant Production by Mycolic Acid-Containing Actinobacteria. *Intech*, *5*(3), 38. http://dx.doi.org/10.1080/13504509.2016.1147502%0Ahttp://dx.doi.org/10.1039/C7RA00172J%0Ahttps://www.intechopen.com/books/advanced-biometric-technologies/liveness-detection-in-biometrics%0Ahttp://dx.doi.org/10.1016/j.colsurfa.2011.12.014%0Ahttp://search.p

Gajda, I., Greenman, J., Melhuish, C., Santoro, C., Li, B., Cristiani, P., & Ieropoulos, I. (2014). Water formation at the cathode and sodium recovery using Microbial Fuel Cells (MFCs). *Sustainable Energy Technologies and Assessments*, *7*, 187–194. https://doi.org/10.1016/j.seta.2014.05.001

Geng, Y. K., Yuan, L., Liu, T., Li, Z. H., Zheng, X., & Sheng, G. P. (2020). Thermal/alkaline pretreatment of waste activated sludge combined with a microbial fuel cell operated at alkaline pH for efficient energy recovery. *Applied Energy*, *275*(June), 115291. https://doi.org/10.1016/j.apenergy.2020.115291

Geng, Y. K., Yuan, L., Liu, T., Li, Z. H., Zheng, X., & Sheng, G. P. (2021). In-situ alkaline pretreatment of waste activated sludge in microbial fuel cell enhanced power production. *Journal of Power Sources*, *491*(October 2020), 229616. https://doi.org/10.1016/j.jpowsour.2021.229616

Goh, B. H. H., Chong, C. T., Ge, Y., Ong, H. C., Ng, J. H., Tian, B., Ashokkumar, V., Lim, S., Seljak, T., & Józsa, V. (2020). Progress in utilisation of waste cooking oil for sustainable biodiesel and biojet fuel production. *Energy Conversion and Management*, *223*(May). https://doi.org/10.1016/j.enconman.2020.113296

Greenman, J., Mendis, B. A., Gajda, I., & Ieropoulos, I. A. (2022). Microbial fuel cell compared to a chemostat. *Chemosphere*, *296*(January), 133967. https://doi.org/10.1016/j.chemosphere.2022.133967

Ieropoulos, I., Theodosiou, P., Taylor, B., Greenman, J., & Melhuish, C. (2017). Gelatin as a promising printable feedstock for microbial fuel cells (MFC). *International Journal of Hydrogen Energy*, *42*(3), 1783–1790. https://doi.org/10.1016/j.ijhydene.2016.11.083

Kensa, V. M. (2011). *BIOREMEDIATION - AN OVERVIEW*. *27*(2), 161–168.

Lee, S. Y., Min, J., Lee, S., Fitriana, H. N., Kim, M. S., Park, G. W., & Lee, J. S. (2019). Bioelectricity generation by Corynebacterium glutamicum with redox-hydrogel-modified carbon electrode. *Applied Sciences (Switzerland)*, *9*(20), 1–11. https://doi.org/10.3390/app9204251

Licciardello, G., Catara, A. F., & Catara, V. (2019). Production of polyhydroxyalkanoates and extracellular products using Pseudomonas corrugata and P. mediterranea: A review. In *Bioengineering* (Vol. 6, Issue 4). MDPI AG. https://doi.org/10.3390/bioengineering6040105

Liu, M., Yuan, Y., Zhang, L. X., Zhuang, L., Zhou, S. G., & Ni, J. R. (2010). Bioelectricity generation by a Gram-positive Corynebacterium sp. strain MFC03 under alkaline condition in microbial fuel cells. *Bioresource Technology*, *101*(6), 1807–1811. https://doi.org/10.1016/j.biortech.2009.10.003

Lopes, E. M., Cristina, T., Castellane, L., Moretto, C., Gertrudes, E., Lemos, D. M., & Jackson, A. (2014). *Bioremediation & Biodegradation Emulsification Properties of Bioemulsifiers Produced by Wild-Type and Mutant Bradyrhizobium elkanii Strains*. *5*(6). https://doi.org/10.4172/2155-6199.1000245

Lopes, M., Miranda, S. M., & Belo, I. (2020). Microbial valorization of waste cooking oils for valuable compounds production–a review. *Critical Reviews in Environmental Science and Technology*, *50*(24), 2583–2616. https://doi.org/10.1080/10643389.2019.1704602

Lu, J., Lu, Q., Hu, Q., & Qiu, B. (2024). Recovery of organic matters by activated sludge from municipal wastewater: Performance and characterization. *Environmental Research*, 118829. https://doi.org/10.1016/j.envres.2024.118829

Mohamed, H. O., Sayed, E. T., Obaid, M., Choi, Y. J., Park, S. G., Al-Qaradawi, S., & Chae, K. J. (2018). Transition metal nanoparticles doped carbon paper as a cost-effective anode in a microbial fuel cell powered by pure and mixed biocatalyst cultures. *International Journal of Hydrogen Energy*, *43*(46), 21560–21571. https://doi.org/10.1016/j.ijhydene.2018.09.199

Mohd Yusoff, M. Z., Hu, A., Feng, C., Maeda, T., Shirai, Y., Hassan, M. A., & Yu, C. P. (2013). Influence of pretreated activated sludge for electricity generation in microbial fuel cell application. *Bioresource Technology*, *145*, 90–96. https://doi.org/10.1016/j.biortech.2013.03.003

Morya, R., Andrianantenaina, F. H., Pandey, A. K., Yoon, Y. H., & Kim, S. H. (2023). Polyhydroxyalkanoate production from rice straw hydrolysate: Insights into feast-famine dynamics and microbial community shifts. *Chemosphere*, *341*(August), 139967. https://doi.org/10.1016/j.chemosphere.2023.139967

Nicolò, M. S., Franco, D., Camarda, V., Gullace, R., Rizzo, M. G., Fragalà, M., Licciardello, G., Catara, A. F., & Guglielmino, S. P. P. (2014). Integrated microbial process for bioconversion of crude glycerol from biodiesel into biosurfactants and phas. *Chemical Engineering Transactions*, *38*, 187–192. https://doi.org/10.3303/CET1438032

Nwinyi, O. C., & Owolabi, T. A. (2019). Scanning electron microscopy and Fourier transmission analysis of polyhydroxyalkanoates isolated from bacteria species from abattoir in Ota, Nigeria. *Journal of King Saud University - Science*, *31*(3), 285–298. https://doi.org/10.1016/j.jksus.2017.08.003

Obata, O., Greenman, J., Kurt, H., Chandran, K., & Ieropoulos, I. (2020). Resilience and limitations of MFC anodic community when exposed to antibacterial agents. *Bioelectrochemistry*, *134*, 107500. https://doi.org/10.1016/j.bioelechem.2020.107500

Pagliano, G., Galletti, P., Samorì, C., Zaghini, A., & Torri, C. (2021). Recovery of Polyhydroxyalkanoates From Single and Mixed Microbial Cultures: A Review. In *Frontiers in Bioengineering and Biotechnology* (Vol. 9). Frontiers Media S.A. https://doi.org/10.3389/fbioe.2021.624021

Pankratova, G., Hederstedt, L., & Gorton, L. (2019). Extracellular electron transfer features of Gram-positive bacteria. *Analytica Chimica Acta*, *1076*, 32–47. https://doi.org/10.1016/j.aca.2019.05.007

Pasternak, G., de Rosset, A., & Rutkowski, P. (2023). Horizontal microbial fuel cell system producing biosurfactants in response to current generation from waste cooking oil as a fuel. *Energy Conversion and Management*, *281*(March), 116807. https://doi.org/10.1016/j.enconman.2023.116807

Rashid, N., Cui, Y. F., Muhammad, S. U. R., & Han, J. I. (2013). Enhanced electricity generation by using algae biomass and activated sludge in microbial fuel cell. *Science of the Total Environment*, *456–457*, 91–94. https://doi.org/10.1016/j.scitotenv.2013.03.067

Raza, Z. A., Abid, S., & Banat, I. M. (2018). Polyhydroxyalkanoates: Characteristics, production, recent developments and applications. In *International Biodeterioration and Biodegradation* (Vol. 126, pp. 45–56). Elsevier Ltd. https://doi.org/10.1016/j.ibiod.2017.10.001

Sharma, S. C. D., Li, J., Hu, A., Chang, C. C., & Yu, C. P. (2021). Integration of pre-colonized and mediator immobilized mixed culture for the improvement of electricity production of microbial fuel cells. *Environmental Technology and Innovation*, *22*, 101514. https://doi.org/10.1016/j.eti.2021.101514

Sharma, S., Datta, P., Kumar, B., Tiwari, P., & Pandey, L. M. (2019). Production of novel rhamnolipids via biodegradation of waste cooking oil using Pseudomonas aeruginosa MTCC7815. *Biodegradation*, *30*(4), 301–312. https://doi.org/10.1007/s10532-019-09874-x

Sharma, V., Sehgal, R., & Gupta, R. (2021). Polyhydroxyalkanoate (PHA): Properties and Modifications. *Polymer*, *212*. https://doi.org/10.1016/j.polymer.2020.123161

Tomietto, P., Loulergue, P., Paugam, L., & Audic, J. L. (2020). Biobased polyhydroxyalkanoate (PHA) membranes: Structure/performances relationship. *Separation and Purification Technology*, *252*. https://doi.org/10.1016/j.seppur.2020.117419

Tsipa, A., Stylianou, K., Papalli, M., Papageorgiou, E., Kyriakou, L., Rigopoulos, I., Ioannou, I., & Pinakoulaki, E. (2021). Iron-stimulated production and antimicrobial potential of a novel biosurfactant produced by a drilling waste-degrading pseudomonas citronellolis strain. *Processes*, *9*(4). https://doi.org/10.3390/pr9040686

UNION, T. E. P. A. T. C. O. T. E. (2018). *DIRECTIVE (EU) 2018/850 OF THE EUROPEAN PARLIAMENT AND OF THE COUNCIL of 30 May 2018 amending Directive 1999/31/EC on the landfill of waste*.

Varnava, C. K., Persianis, P., Ieropoulos, I., & Tsipa, A. (2024). Electricity generation and real oily wastewater treatment by Pseudomonas citronellolis 620C in a microbial fuel cell: pyocyanin production as electron shuttle. *Bioprocess and Biosystems Engineering*. https://doi.org/10.1007/s00449-024-03016-1

Wang, H., Luo, H., Fallgren, P. H., Jin, S., & Ren, Z. J. (2015). Bioelectrochemical system platform for sustainable environmental remediation and energy generation. *Biotechnology Advances*, *33*(3–4), 317–334. https://doi.org/10.1016/j.biotechadv.2015.04.003

Wang, J., Ren, K., Zhu, Y., Huang, J., & Liu, S. (2022). A Review of Recent Advances in Microbial Fuel Cells: Preparation, Operation, and Application. *BioTech*, *11*(4).

https://doi.org/10.3390/biotech11040044

Wang, X., Aulenta, F., Puig, S., Esteve-Núñez, A., He, Y., Mu, Y., & Rabaey, K. (2020). Microbial electrochemistry for bioremediation. *Environmental Science and Ecotechnology*, *1*(December 2019). https://doi.org/10.1016/j.ese.2020.100013

Wang, X., Yi, K., Pang, H., Liu, Z., Li, X., Zhang, W., Zhang, C., Liu, S., Huang, J., & Zhang, C. (2024). An overview of quorum sensing in shaping activated sludge forms : Mechanisms , applications and challenges. *Science of the Total Environment*, *927*(February), 171886. https://doi.org/10.1016/j.scitotenv.2024.171886

You, J., Greenman, J., & Ieropoulos, I. A. (2021). Microbial fuel cells in the house: A study on real household wastewater samples for treatment and power. *Sustainable Energy Technologies and Assessments*, *48*, 101618. https://doi.org/10.1016/j.seta.2021.101618

Appendix

No.	Chemical – Empirical Name	Molecular Formula	Lipid Number	Molecular weight (g/mol)	Retention time (min)	R^2	y_0	a
	Appendix. FAMEs – Calibration results, Calibration curve: y = y0 + ax, where y = Area and x = Concentration (ppm)							
1	Butanoic acid, methyl ester – Methyl butyrate	$C_5H_{10}O_2$	C4:0	102.13	2.644	0.9997	18917.2041	200.7416
2	Hexanoic acid, methyl ester – Methyl hexanoate	$C_7H_{14}O_2$	C6:0	130.18	5.197	0.9999	-2380.7187	1148.7753
3	Octanoic acid, methyl ester – Methyl octanoate	$C_9H_{18}O_2$	C8:0	158.24	8.266	0.9998	-6281.6783	2086.4721
4	Decanoic acid, methyl ester – Methyl decanoate (carpate)	$C_{11}H_{22}O_2$	C10:0	186.29	11.141	0.9993	4625.5470	2484.7842
5	Undecanoic acid, methyl ester – Methyl undecanoate	$C_{12}H_{24}O_2$	C11:0	200.32	12.454	0.9974	2717.6387	847.1633
6	Dodecanoic acid, methyl ester – Methyl dodecanoate (laurate)	$C_{13}H_{26}O_2$	C12:0	214.34	13.719	0.9997	-7642.9121	3011.4547
7	Tridecanoic acid, methyl ester – Methyl tridecanoate	$C_{14}H_{28}O_2$	C13:0	228.37	14.902	0.9985	3335.8469	1419.6373
8	Methyl myristoleate	$C_{15}H_{28}O_2$	C14:1	240.38	15.904	0.9995	-5877.5082	1538.1160
9	Tetradecanoic acid, methyl ester – Methyl tetradecanoate (myristate)	$C_{15}H_{30}O_2$	C14:0	242.40	16.035	0.9975	1567.0308	3169.2381
10	*cis*-10-Pentadecenoic acid, methyl ester – Methyl *cis*-10-pentadecenoate	$C_{16}H_{30}O_2$	C15:1	254.41	17.117	0.9982	-17030.6961	1375.8269
11	Pentadecanoic acid, methyl ester – Methyl pentadecanoate	$C_{16}H_{32}O_2$	C15:0	256.42	17.253	0.9974	4149.6981	1131.8448
12	9-Hexadecenoic acid, methyl ester – Methyl palmitoleate	$C_{17}H_{32}O_2$	C16:1	268.43	18.400	0.9996	-11918.6003	1195.0292
13 (a)	Hexadecanoic acid, methyl ester – Methyl palmitate (5 – 100 ppm)	$C_{17}H_{34}O_2$	C16:0	270.45	18.693	0.9997	-10505.4959	3400.0867

13 (b)	Hexadecanoic acid, methyl ester – Methyl palmitate (250 – 1000 ppm) [2]				18.712	0.9992	277108.5000	2708.0849
14	*cis*-10-Heptadecenoic acid, methyl ester – Methyl *cis*-10-heptadecenoate	$C_{18}H_{34}O_2$	C17:1	282.46	19.989	0.9991	-11224.3366	1162.6887
15	Heptadecanoic acid, methyl ester – Methyl heptadecanoate	$C_{18}H_{36}O_2$	C17:0	284.48	20.322	0.9988	748.2107	976.1933
16 & 17	6,9,12-Octadecatrienoic acid, methyl ester – Methyl γ-linolenate & 9,12,15-Octadecatrienoic acid, methyl ester – Methyl α-linolenate	$C_{19}H_{32}O_2$	C18:3n6 & C18:3n3	292.46	21.291	0.9977	-3863.3040	907.8554
18	9,12-Octadecadienoic acid (Z,Z), methyl ester – Methyl linoneate	$C_{19}H_{34}O_2$	C18:2n6c	294.47	21.576	0.9995	-8389.2384	985.7395
19 & 20	9-Octadecenoic acid (Z), methyl ester – Methyl oleate & 9,12-Octadecadienoic acid (E,E), methyl ester – Methyl linolelaidate	$C_{19}H_{36}O_2$ & $C_{19}H_{34}O_2$	C18:1n9t & C18:2n6t	296.49 & 294.47	21.704	0.9999	-14945.9863	3094.2967
21	9-Octadecenoic acid (E), methyl ester – Methyl elaidate	$C_{19}H_{36}O_2$	C18:1n9t	296.49	21.803	0.9987	-9173.9298	1100.1792
22	Octadecanoic acid, methyl ester – Methyl stearate (5 – 1000 ppm) [2]	$C_{19}H_{38}O_2$	C18:0	298.50	22.164	1.0000	-7297.5593	1968.2920
23	*cis*-5,8,11,14-Eicosatetraenoic acid, methyl ester – Methyl arachidonate	$C_{21}H_{34}O_2$	C20:4n6	318.49	24.858	0.9998	-10816.0421	752.2348
24	*cis*-5,8,11,14,17-Eicosapentaenoic acid, methyl ester	$C_{21}H_{32}O_2$	C20:5n3	316.48	25.0030	0.9986	-6055.9784	715.5999
25	*cis*-8,11,14-Eicosatrienoic acid, methyl ester	$C_{21}H_{36}O_2$	C20:3n6	320.51	25.236	1.0000	-5845.5122	749.0011
26	*cis*-11,14-Eicosadienoic acid, methyl ester	$C_{21}H_{38}O_2$	C20:2	322.53	25.629	0.9998	-8430.6610	776.8425
27	Methyl *cis*-11-eicosenoate	$C_{21}H_{40}O_2$	C20:1n9	324.54	25.745	0.9999	-2996.4876	844.0545

28	*cis*-11,14,17-Eicosatrienoic acid, methyl ester	$C_{21}H_{36}O_2$	C20:3n3	320.51	25.783	0.9999	-6963.1297	889.6564
29	Eicosanoic acid, methyl ester – Methyl arachidate	$C_{21}H_{42}O_2$	C20:0	326.56	26.291	0.9998	-8976.2445	1663.9444
30	Heneicosanoic acid, methyl ester – Methyl heneicosanoate	$C_{22}H_{44}O_2$	C21:0	340.58	28.621	0.9999	-6797.3794	603.0064
31	*cis*-4,7,10,13,16,19-Docosahexaenoic acid, methyl ester	$C_{23}H_{34}O_2$	C22:6n3	342.51	29.263	0.9987	-10681.8285	428.7288
32	*cis*-13,16-Docosadienoic acid, methyl ester	$C_{23}H_{42}O_2$	C22:2	350.58	30.610	0.9997	-5189.8762	408.0545
33	Methyl *cis*-13-docosenoate – Methyl erucate	$C_{23}H_{44}O_2$	C22:1n9	352.59	30.742	0.9991	-4479.9231	487.0472
34	Docosanoic acid, methyl ester – Methyl behenate	$C_{23}H_{46}O_2$	C22:0	354.61	31.576	0.9999	-7155.2464	880.5128
35	Tricosanoic acid, methyl ester – Methyl tricosanoate	$C_{24}H_{48}O_2$	C23:0	368.64	35.413	0.9997	-4393.9871	268.1924
36	15-Tetracosenoic acid, methyl ester – Methyl *cis*-15-tetracosenoate	$C_{25}H_{48}O_2$	C24:1n9	380.65	39.050	0.9974	-8352.1428	193.6029
37	Tetracosanoid acid, methyl ester – Methyl tetracosanoate	$C_{25}H_{50}O_2$	C24:0	382.66	40.488	0.9998	-5249.7726	351.1534

[1] calibration curve: $y = y_0 + ax$, where y = Area and x = Concentration (5 – 500 ppm).
[2] calibration range: 5 – 1000 ppm.